Synthesis, Dyeing performance and Evaluation of Antimicrobial and Antioxidant Activities of Azo Dye derivatives Incorporated 1,3,4-thiadiazole combined with Molecular Modelling Studies

Kibrom Mezgebe Takele

A Thesis Submitted to the Department of Applied Chemistry
School of Applied Natural Science

Presented in Partial Fulfilment of the Requirement for the Degree of Master's in Applied Chemistry (Synthetic Organic Chemistry)

Office of Graduate Studies
Adama Science and Technology University

June, 2023
Adama, Ethiopia

Synthesis, Dyeing performance and Evaluation of Antimicrobial and Antioxidant Activities of Azo Dye derivatives Incorporated 1,3,4-thiadiazole combined Molecular Modelling Studies

Kibrom Mezgebe Takele

Advisor: Endale Mulugeta (PhD)

Co-Advisor: Yadessa Melaku (PhD)

A Thesis Submitted to the Department of Applied Chemistry

School of Applied Natural Science

Presented in Partial Fulfilment of the Requirement for the Degree of Master's in Applied Chemistry (Synthetic Organic Chemistry)

Office of Graduate Studies

Adama Science and Technology University

June, 2023

Adama, Ethiopia

Declaration

I hereby declare that this Master's thesis entitled **"Synthesis, Dyeing performance and Evaluation of Antimicrobial and Antioxidant Activities of Azo Dye derivatives Incorporated 1,3,4-thiadiazole combined with Molecular Modelling Studies "** is my original work. It has not been submitted for the award of any academic degree, diploma or certificate in any other university. All sources of materials that are used for this thesis have been duly acknowledged through citation.

Kibrom Mezgebe _____ _____

Name of student Signature Date

Recommendation

We, the advisors of this thesis, hereby certify that we have read the revised version of the thesis entitled **"Synthesis, Dyeing performance and Evaluation of Antimicrobial and Antioxidant Activities of Azo Dye derivatives Incorporated 1,3,4-thiadiazole combined with Molecular Modelling Studies"** prepared under our guidance by Kibrom Mezgebe submitted in Partial Fulfilment of the Requirement for the Degree of Master's in Applied Chemistry (Synthetic Organic Chemistry). Thus, we recommended the submission of revised version of the thesis to the department following the applicable procedures.

Endale Mulugeta (Phd)	_____	_____
Advisor	Signature	Date
Yadessa Melaku (Phd)	_____	_____
Co-advisor	Signature	Date

Approval Sheet

We, the advisors of the thesis entitled **"Synthesis, Dyeing performance and Evaluation of Antimicrobial and Antioxidant Activities of Azo Dye derivatives Incorporated 1,3,4-thiadiazole combined with Molecular Modelling Studies"** by Kibrom Mezgebe, hereby certify that the recommendation and suggestions made by the board of examiners are appropriately incorporated into the final version of the thesis.

Endale Mulugeta (Phd) Advisor	Signature	Date
Yadessa Melaku (Phd) Co-advisor	Signature	Date

We, the undersigned, members of the Board of Examiners of the thesis by Kibrom mezgebe have read and evaluated the thesis entitled "**Synthesis, Dyeing performance and Evaluation of Antimicrobial and Antioxidant Activities of Azo Dye derivatives Incorporated 1,3,4-thiadiazole combined with Molecular Modelling Studies**" and examined the candidate during open defense. This is, therefore, to certify that the thesis is accepted for partial fulfilment of the requirement of the degree of Master of Science in Applied Chemistry (Synthetic Organic Chemistry).

Chairman	Signature	Date
Internal Examiner	Signature	Date
Zelalem Abdissa (Phd) External Examiner	 Signature	15/07/2023 Date

Final approval and acceptance of the thesis is contingent upon submission of its final copy to the Office of Postgraduate Studies (OPGS) through the Department Graduate Council (DGC) and School Graduate Committee (SGC).

Department Head	Signature	Date
School Dean	Signature	Date
Office of Postgraduate Studies, Dean	Signature	Date

Acknowledgement

First and foremost, I would like to thank the almighty God for giving me great and lovely support, knowledge, ability and strength to carry out the preparation and writing of this thesis. Second I would like to express my gratitude to my advisor, Dr. Endale Mulugeta (PhD) for his professional advice, invaluable guidance and constructive comment during the whole writing up of this thesis work. In addition, I would like to thank co-advisor Dr. Yadessa Melaku (PhD) for his kindness, unreserved help and guidance. I am deeply grateful to acknowledge Department of Applied Chemistry and Adama Science and Technology University for offering me this scholarship opportunity to study my M.Sc. at the end, I would like to thank for my family, friends and partners' who give me help and strength to carry out everything as much as possible.

Table of Contents

List of Figures

List of Schemes

List of Tables

List of Abbreviation and Symbols

µ	Chemical potential
µl	Microliter
AA	Ascorbic acid
ABTS	2,2'-azinobis-(-ethyl-benzothiazoline-6- sulfonic acid)
ACD	Advanced chemistry development
AcOH	Acetic acid
ADMET	Absorption, distribution, metabolism, excretion, and toxicity
AIV	Avian influenza virus
ATCC	American Type Culture Collection
BHT	Butylated hydroxytoluene
C.albicans	Candida albicans
$CDCl_3$	Deuterated chloroform
CFU	colony-forming unit
CLSI	Clinical and Laboratory Standards Institute
CP	Ciprofloxacine
CQAPDN	4-({4-[(7-Chloroquinolin-4 yl)amino]phenyl}diazenyl) naphthalen-1-ol
Dept	Distortionless enhancement by proton transefer
DMSO-d_6	Dimethyl sulfoxide-d6
DNA	Deoxyribonucleic acid
DPPH	2,2-diphenyl-1-picrylhydrazyl
E.coli	Escherichia coli
E.faecalis	Enterococcus faecalis
ET/ISO-105-CO3	Ethiopia/International Organization for Standardization-*105-CO3*
FRAP	Ferric reducing ability of plasma
FTIR	Fourier transform infrared radiation
HCT-116	Colorectal Carcinoma -116
HOMO	Highest Occupied Molecular Orbital
K.pnemonia	Klebsiella pneumoniae
KC	Ketoconazole
LD_{50}	Lethal Dose 50%
LUMO	Lowest unoccupied molecular orbital
MeOH	Methanol

mg/kg	Milligram per kilogram
MHA	Muller Hinton Agar
MIC	Minimum Inhibitory Concentration
mL	Millilitres
MMP–2/9	Matrix metalloproteinase – 2/9
MOE	Molecular electrostatic potential
MR	Methyl Red
NDV	Newcastle disease virus
NMR	Nuclear magnetic resonance
NMR	Nuclear Magnetic
pH	Potential of hydrogen
PK	Pyruvate kinase
PRDX5	Human peroxiredoxin 5
R*f*	Retention factor
S	Softness
S.aureus	Staphylococcus aureus
S.epidermid	Staphylococcus epidermidis
S.typorumium	Staphylococcus typorumium
SDA	Sabouraud dextrose broth
T 80	Tween 80
T.mentographytes	Trichophyton
T.rumbrum	Trichophyton rubrum
TLC	Thin layer chromatography
TPSA	topological polar surface area
UV	Ultraviolet
UV-Vis	Ultra Violet and Visible
η	Hardness
χ	Electronegativity
ω	Electrophilicity

Abstract

*Nowadays, there is significant interest in the synthesis of azo dye derivatives incorporated with heterocyclic scaffolds as a potential scaffold in the pharmaceutical sector, since the incorporation of the heterocyclic moiety into the azo dye has enhanced the bioactive properties of the target derivatives. Herein, six novel azo dye derivatives incorporated with 1,3,4-thiadiazole scaffold were derived from 4-dimethylaminobezaldehyde/4-aminobenzoic acid, thiosemicarbaide and coupling agents (phenol, 1-naphthol, and 2-naphthol) through the conventional diazotization-coupling sequence. The structures of synthesized compounds were characterized and determined with the help of UV-visible, FTIR, ^{1}H NMR and ^{13}C NMR. The interaction, reactivity, physicochemical, pharmacokinetics and toxicity of the compounds were predicted by molecular modelling studies. The azo dyes were tested for their color fastness properties, and compound **136** and **137** displayed excellent fastnesses to washing and rubbing. The synthesized compounds were also evaluated for antimicrobial activity against six bacterial (S.aureus, S.epidermid, E.faecalis, E.coli, K.pnemonia, S.typorumium)* and three fungal *(C.albicans, T.mentographytes, T.rumbrum) strains by broth dilution method relative to ciprofloxacine and ketoconazole respectively. The antioxidant activity of the synthesized compounds was examined via the DPPH assay method compared to ascorbic acid. Among the tested, compound **136** and **137** showed moderate antimicrobial activities; especially compound **137** showed a good antimicrobial activity (MIC = 0.5 mg/mL) for both bacterial and fungal species compared to ciprofloxacin (0.0005 mg/mL) and ketoconazole (0.005 mg/mL) respectively. Compound **133**, displayed potential radical scavenging activity at IC_{50}= 10.7 µg/mL relative to ascorbic acid (IC_{50}= 9.6 µg/mL). In silico molecular interaction displayed that compound **136** exhibited highest binding affinity (-8.0 kcal/mol) to E.coli DNA gyrase B than that of ciprofloxacin (-7.3 kcal/mol). Similarly, the highest binding affinity was shown by compounds **134** and **137** (-6.1 kcal/mol) against S. aureus PK than the standard ciprofloxacin (-4.9 kcal/mole). Compound **137** showed highest binding affinity (-10.6 kcal/mol) with C. albican CYP51 than that of KC (-10.2 kcal/mol). Further, compound **137** showed highest binding affinity (-5.8 kcal/mole) with human peroxidoxins 5 than that of ascorbic acid (-4.2 kcal/mol). Compound **134** revealed lowermost chemical hardness (0.0453 eV) as well as the uppermost softness (22.0751 eV), due to lowest energy gap, which infer highest reactivity of the compound.*

Keyword: *Antibacterial, antifungal, antioxidant, azo dye, incorporated and thiadiazole.*

1. Introduction

1.1. Background

Azo dyes are the most versatile class of synthesized organic dyes having chromophoric azo group responsible as coloring agent (-N=N-) (Salimi and Mahdavi, 2018; Yousefi and Rassa, 2013). These dyes can be aliphatic or aromatic, and the aromatic azo compounds do not occur in nature, belong to the synthetic class of dyes, usually synthesized conventionally diazotization followed by coupling (Ali and Rashid, 2018). For decades these compounds largely applied in production of different materials, dye chemistry, pharmacological and medical applications (Albelwi *et al*., 2021; Ali *et al*., 2018; Mohammadi and Tahavor, 2015; Yousefi *et al*., 2013) even though some azo dyes were banned by the European union, since cleavage of the azo linkage results in the production of carcinogenic aromatic amine, and the indiscriminate disposal of these dyes become a threat to human, biota, and ecosystem health (Tropp *et al*., 2020).

1 R'—N═N—R R=R'= Aromatic arayl

Figure 1*:* Chemical structure of azo dyes.

Currently, azo dyes are synthesized through the incorporation of heterocyclic moiety containing hetero atoms such as sulphur, oxygen and nitrogen which display significant activity in the area of pharmacology and chemotherapy (Maliyappa and Pushpavathi, 2022). Moreover, they have the most easy two-step transformation, coupling of the diazonium salts which are usually produced from the reaction of aromatic amines with nitrites in the presence of strong acids at low temperatures to an electron-donating aromatic compound (Gaffer *et al*., 2019). As a result, the synthesis of these derivatives and investigation of their chemical and biological behaviour has attracted the attention of many researchers for biological and pharmaceutical reason (Harisha and Hoskeri, 2020).

Thiadiazoles are crucial five-membered classes of nitrogen-sulphur containing heterocyclic arrangements which are rarely found in nature (Serban and Bota, 2018). Nitrogen, sulphur and carbon atoms can be arranged in several different ways. Among the different isomers of thiadiazole,1,3,4-thiadiazole derivatives are most studied due to broad spectrum of pharmacological activities (Hu and Zhu, 2014; Serban *et al*., 2018). Due to the extreme instability of diazonium salts, they are used immediately after their formation in coupling reactions with phenols or amines, substituted with electron-donating groups (Kudelko *et al*., 2020).

Nowadays, much attention has been focused on 1,3,4-thiadiazole derivatives as a very important class of nitrogen-containing aromatic heterocyclic compounds because compounds containing such scaffold exhibit broad spectrum of biologic interactions and reported to have antifungal, antimicrobial, antioxidant, anti-inflammatory and anticancer activities(Altıntop *et al*., 2018; Gur *et al*., 2017; Hu *et al*., 2014; Karaburun *et al*., 2018; Kudelko *et al*., 2020; Li and Zhao *et al*., 2013; Ramprasad *et al*., 2015; Wu and Song, 2021).

2

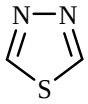

Figure 2: Chemical structure of 1,3,4-thiadiazole.

In reference of the above mentioned findings and our previous review on synthesis and pharmacological activities of azo dye derivatives incorporating heterocyclic scaffolds, herein planned to synthesis a bioactive compounds derived from 1,3,4-thiadiazole derivatives and electron-donating aromatics compounds. Finally, these compounds were assessed for dyeing performance and *in vitro* antimicrobial as well as antioxidant activities combined with *in silico* molecular docking, DFT, ADME and toxicity predictions of the compounds.

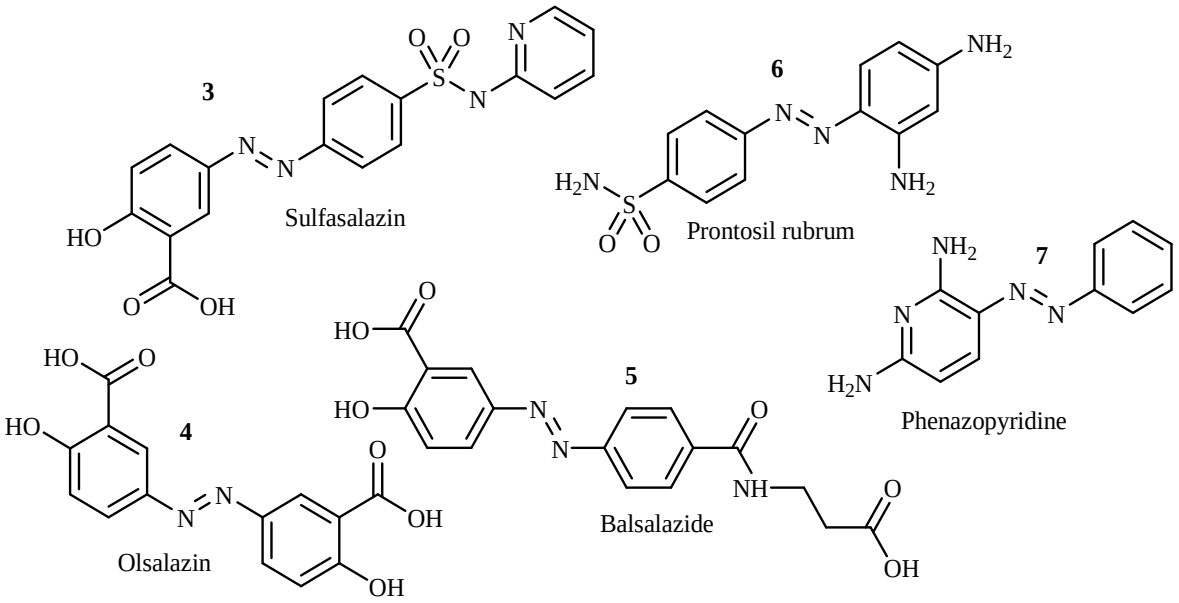

Figure 3: Chemical structure of drugs containing azo groups.

1.2. Statement of the Problem

According the world health organization reports the spread of infectious disease due to a variety of microbes including bacteria, virus, and fungi has been a serious challenge. This

is because of lack of synthetic drugs which target the disease completely and increase in resistance of microbes to different drugs (Talebi and Blatt, 2019).

Azo dyes are very important class of organic compounds applied broadly in dye chemistry, pharmacological and medicinal sectors; however, some azo-based drugs are not very much applied in medicine because they are easy and liable to cleave, and some of them exhibit sever side effect (Gicevic and Karacic, 2020). Furthermore, the cleavage of some azo dyes result in severs carcinogenic amines which are the sources of many cancer diseases. These azo dyes were banned by the European Union for such reason(Bruschweiler and Merlot, 2017). However, many heterocyclic azo dyes have been synthesized since they produce non carcinogenic amines which are biologically and pharmacologically potential compounds. Among the heterocyclic azo dyes, nitrogen containing azo dyes; especially 1,3,4-thiadiazole derivatives are responsible to broad spectrum biological application (Anthwal and Nain, 2022). So the intention of this work is to synthesis, and characterize azo dyes incorporated 1,3,4-thiadiazole which is the most biologically and pharmacologically active heterocyclic to enhance pharmacological application such as antibacterial, antifungal, and antioxidant activity of azo dyes in addition to dyeing performance.

1.3. Justification of the Study

Drug design and development is crucial to discover potential and novel drugs to treat and cure many diseases. Nowadays most researchers, pharmaceutical sectors and medical organizations invest their time, energy and money into drug design, development and discovery since the severity of infectious and pandemic diseases have been increasing from time to time. This helps to enhance knowledge, interest and development of different synthetic approaches to prepare different derivatives which are biologically and pharmacologically active.

This study provide information on the synthesis of novel azo dye derivatives incorporated 1,3,4-thiadiazole scaffold *via* conventional method diazotization followed by coupling which helps to look up useful lead drug candidates. Moreover, this study gives insight to grasp the interest and attention of researchers to this area, and to understand the potential of novel azo dyes on *in vitro* antimicrobial and antioxidant activities in addition to their dyeing performance combined with molecular modelling studies and predictions.

1.4. Objectives of the Study

1.4.1. General Objective

The objective is to synthesis, characterize and evaluate dyeing performance, *in vitro* antimicrobial and antioxidant activities of azo dyes incorporated 1,3,4-thiadiazole scaffold; combined with molecular modelling studies.

1.4.2. Specific Objectives

- To synthesis azo dye derivatives incorporated with 1,3,4-thiadiazole from 4-aminobenzoic acid/4-dimethylaminobanzaldahyde, thiosemicarbazide and coupling agents.
- To characterize structure of synthesized compounds using UV-Vis, FTIR, ^{1}H and ^{13}C NMR.
- To evaluate antibacterial activity of the synthesized compounds using broth dilution method against six bacterial stains, *S.aureus, S.epidermid, E.faecalis, E.coli, K.pnemonia, S.typorumium*.
- To evaluate antifungal activity of the synthesized compounds using broth dilution method against three fungal strains, *C.albicans, T.mentographytes and T.rumbrum*.
- To evaluate antioxidant activity of the synthesized compounds using DPPH assay method.
- To predict *in silico* modeling studies ADME, drug-likeness, toxicity, DFT and molecular docking analysis of the synthesized compounds.

1.5. Scope of the Study

The scope of this research work basically covered the synthesis of azo dye derivatives incorporated with 1,3,4-thiadiazole moiety though diazotization-coupling method. Accordingly, it explored the synthesis of six novel bioactive azo dye derivatives from 4-aminobenzoic acid/4-dimethylaminobanzaldahyde, thiosemicarbazide and coupling agents (phenol, 1-naphthole and 2-naphthole). The structures of the compounds were characterized by UV-Vis, FTIR, ^{1}H and ^{13}C NMR. Further, the interaction, reactivity, physicochemical, pharmacokinetics and toxicity of the compounds were predicted by molecular modelling studies namely; DFT, molecular docking, and online servers (SwissADME, PreADME and Pro-Tox II). The synthesized dyes were investigated for their washing and rubbing fastness using cotton fabric. The synthesized compounds were also evaluated for antimicrobial activity against six bacterial (*S.aureus, S.epidermid, E.faecalis, E.coli, K.pnemonia, S.typorumium*) and three fungal (*C.albicans, T.mentographytes, T.rumbrum*) strains by broth dilution method relative to standard drugs, ciprofloxacine and ketoconazole respectively. Further, the antioxidant activity of the

synthesized compounds was examined via the DPPH assay method using ascorbic acid as standard drug.

2. Literature review

2.1. Azo dye in industries

Azo dyes are coloring compounds which are chemically represented as R–N=N-R', where the R or R' can be either aryl or alkyl compounds (Chung *et al*, 2016;Gaffer *et al*., 2019; Shah *et al*., 2014). The word azo comes from *azote*, the French name for nitrogen that is derived from the Greek *a* (not) *zoe* (to live) (Chung *et al*., 2016). Aliphatic azo compounds are mostly colourless and relatively less stable than the aryl azo compounds. The C-N bond of an azo alkane cleaves at high temperature or upon irradiation, giving nitrogen gas and radicals. On the other hand, aromatic azo compounds are more common and highly stable. The presence of aryl groups on both sides of -N=N- group extend the delocalized system and make this class more stable (Ali *et al*., 2018). In addition to their use as colorants over 50% of all commercial dyes, they have been employed for many applications, such as in inkjet printing, thermal transfer printing, biomedical area, molecular recognition, light controlled polymers, liquid crystal industry, in the food, pharmaceutical, paper, cosmetics, textile and leather industries and others (Ali *et al*., 2018; Benkhaya and El Harfi, 2020; Crespi and Konig, 2019).

2.2. Toxicity and carcinogenicity of azo dyes

Azo dyes are colouring agents widely used in the textile, printing, cosmetic, and drug and food processing industries (Benkhaya *et al*., 2020; Gaffer *et al.*, 2019). The carcinogenic and mutagenic activity of many azo dyes is because of cleaved product, even though some azo dyes can be carcinogenic without being cleaved into aromatic amines (Chung *et al*., 2016; Gicevic and Karacic, 2019). Many azo dyes and their reductively cleaved products reported to affect human health, causing allergies and other human maladies (chung *et al*., 2016; Jadhav *et al*., 2016). Azo reduction can be accomplished by human intestinal microflora, skin microflora, environmental micro-organisms, to a lesser extent by human liver azo reductases, and other non-biological means. Some azo dyes reduced to carcinogenic aromatic amines such as 4-aminobiphenyl, 3,3´-dimethylbenzidine, benzidine, 4,4´-methylenedi-*o*-toluidine, 4-chloro-*o*-toluidine, *p*-cresidine, 2-napthylamine, 2,2´-dichloro-4,4´-methylenedianiline, o-aminoazotoluene, 4,4´-oxydianiline, 5-nitro-*o*-toluidine, 4,4´-thiodianiline, 4-chloroaniline, *o*-toluidine, 2,4-diaminoanisole, 2,4-diaminotoluene, 4,4´-methylenedianiline, 2,4,5-trimethylaniline, 3,3´-dichlorobenzidine,

2-methoxyaniline, 3,3´-dimethoxybenzidine and 4-aminoazobenzene are banned by the European Union and German Consumer Goods Ordinance (Bruschweiler and Merlot, 2017; Chakraborty and Chatterjee, 2017).

2.3. Synthesis of heterocyclic azo dyes

Currently, scholars have given much attention towards suitable preparation of the title compounds and their derivatives. So far, various analogous of heterocyclic containing azo dyes and their derivatives have been synthesized and reported *via* different methodologies. This section of the review mainly focuses on using the standard synthesis methodology towards various heterocyclic moiety containing azo dyes using the conventional method of diazotization and diazo-coupling reactions with one or more electron-rich nucleophiles segment.

2.3.1. Azo dyes containing thiophene and its derivatives

Wei and co-workers report the synthesis of pH-induced azo-keto and azo-enol tautomerism for 6-(3-methoxypropylamino)pyridin-2-one based thiophene azo dyes (Zhao and Huang, 2017). Through linking other functional group on azo dye scaffold with the post modification strategy, the bi-heterocyclic azo dye **12** was prepared. The diazotization reaction take place on 3-cyano-4-chloro-5-formylthiophene **8,** and 3-methoxypropylamino substituted pyridine derivatives **9** are used as coupling components **9** to produce **10**. The aldehyde of the formylthiophene moiety **10** further reacted with aniline **11** to afford Schiff base-azo dye **12** with thiophene as described in Scheme 1. Here, the azo dye is with stable pH no matter what the diazo components are used since no proton accepting sites are could be found in the pyridine ring; where both carbonyl groups are simultaneously replaced by 3-methoxypropan-1-amine.

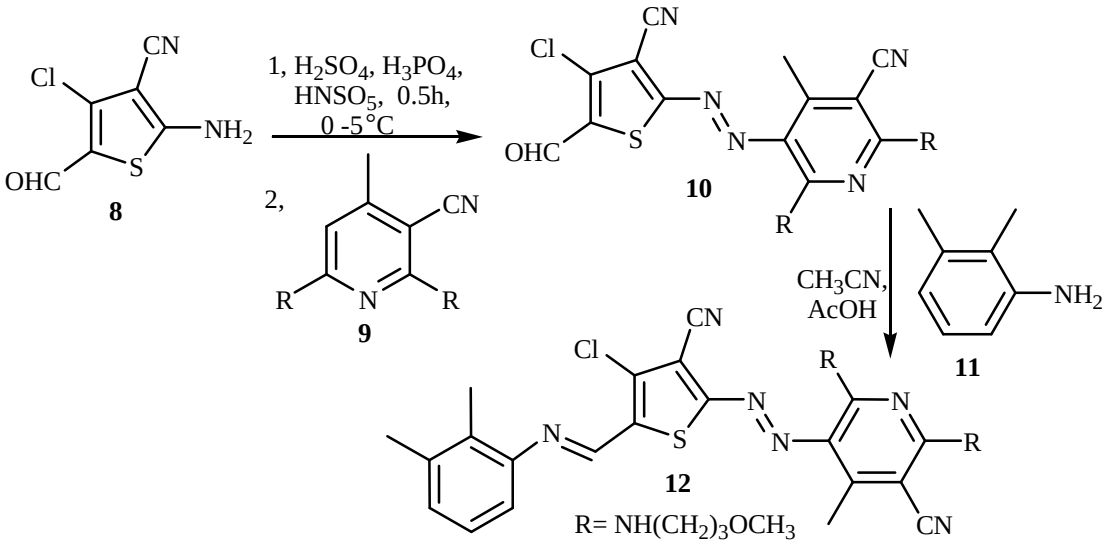

Scheme 1: General synthesis route of azo dye containing thiophene **12**.

As well, through modifying the terminal aldehyde radical into an imine version, 2-amino-3-cyano-4-chloro-5 formylthiophene provided the basis for blue colored heterocyclic azo dyes **15** with the enhanced π-conjugated system, solubility, and electronic spectrum properties of the synthesized compounds (Xu *et al*., 2016). Azo-azomethine compounds **15** were prepared through Schiff-base condensation between 2,3-dimethylaniline **14** and the formylthiophene unit of azo dye **13** with various derivatives of aniline coupling components. The general synthesis route of the dyes is shown in Scheme 2.

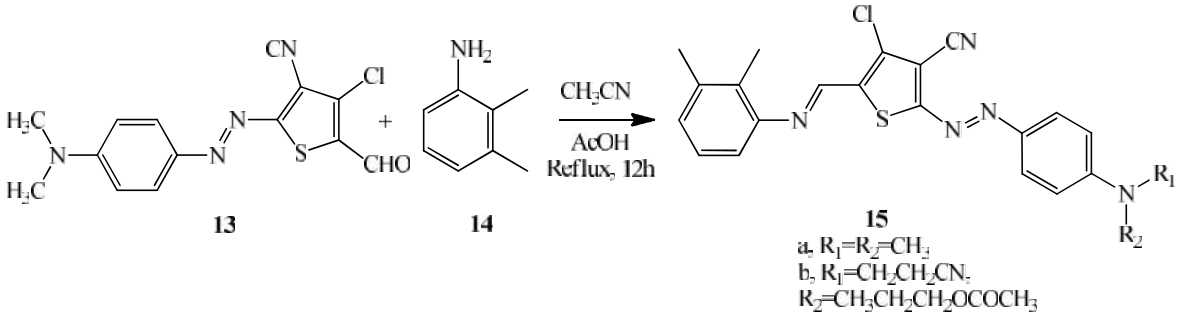

Scheme 2: General synthesis route towards Schiff base-azo dye derivative **15**.

2.3.2. Azo dyes containing pyrrole and its derivatives

Through the diazo coupling reaction, Maruszewska and Podsiadly synthesized and reported novel azo dye pyrrole derivatives **20** containing the azo-1*H*-pyrrole moiety (Maruszewska and Podsiadły, 2016). During the synthesis of azo dyes **20**, first aniline, 4-aminobenzoic acid, *N*,*N*-diethyl-*p*-phenylenediamine, *N*-ethyl-*N*-2-hydroxyethyl-*p*-phenylenediamine, and 5-aminoisophthalic acid, respectively, reacted with sodium nitrite/aqueous HCl at 0-5 °C to afford the substituted diazonium salt, and

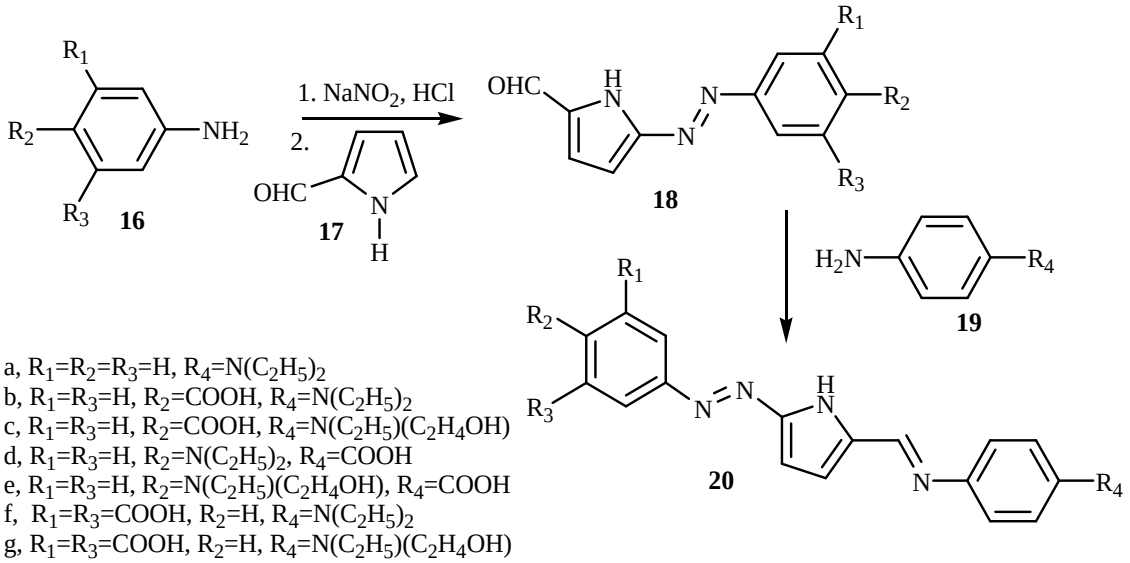

Scheme 3: General synthetic route towards azo dye derivatives incorporated pyrrole **20**.

the resulting salt reacted with 1*H*-pyrrole-2-carbaldehyde**17** in ethanol neutralised with pyridine to produce **18**. Finally, compound **18** condensed with appropriate aromatic amine **19** in ethanol gives dyes **20** (a-g) as described in Scheme 3. In these dyes, the electron-rich 1*H*-pyrrole moiety was assembled as *p*-bridges in donor-acceptor *p*-conjugated dye, and aminophenylimine fragments and the carboxyl group were used as donor and anchoring acceptor groups respectively.

Almeida and co-workers have also synthesized and reported pyrrole azo dye derivative **23** bearing 2-(4-dimethylaminophenylazo) benzoic acid **22**, also known as Methyl Red (Almeida *et al*., 2017). The monomer 3-(*N*-pyrrolyl)propyl-2-(4-dimethylaminophenylazo) benzoate (MRPy) **23** was obtained through a simple synthetic route, in mild conditions and with a good yield from 1-(3-Iodopropyl)pyrrole and methyl red in the presence of triethylamine which were added to dry CH_3CN. The reaction mixture was stirred at 80 °C for 3 h, and the reaction mixture was extracted with H_2O/CH_3Cl (1:1, v/v), and the crude product was purified after evaporation to give final product as shown in Scheme 4. The formation of MRPy successfully achieved with the addition of boron trifluoride diethyl etherate on to electrodes in $(C_4H_9)_4NBF_4/CH_3CN$ in the electrolyte system.

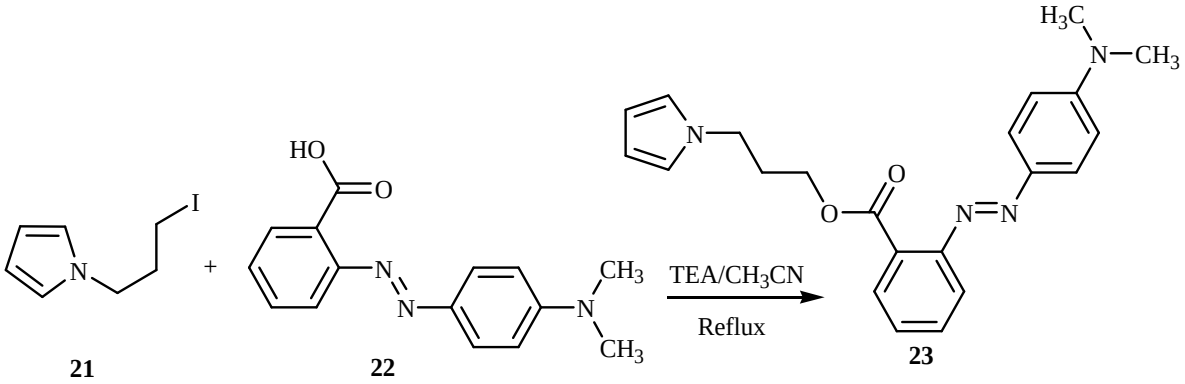

Scheme 4: General synthetic route towards azo dye derivatives containing pyrrole **23**.

2.3.3. Azo dyes containing imidazole and its derivatives

New red azo dye containing imidazole **27** was reported from previous works through diazo coupling reaction. The compound **27** was synthesized from the imidazole derivatives **24**, pass through the diazotization step in the presence of HCl and $NaNO_2$ to obtain the corresponding diazonium salts. The salt subjected to coupling with *N*-benzyl-*N*-ethyl-*m*-acetamide aniline **25** to afford compound **26** in good yields (Khattab and Rehan, 2018). Further compound **26** undergoes methylation reaction through alkylating agent to methylate the imidazole ring **27** as describe in Scheme 5.

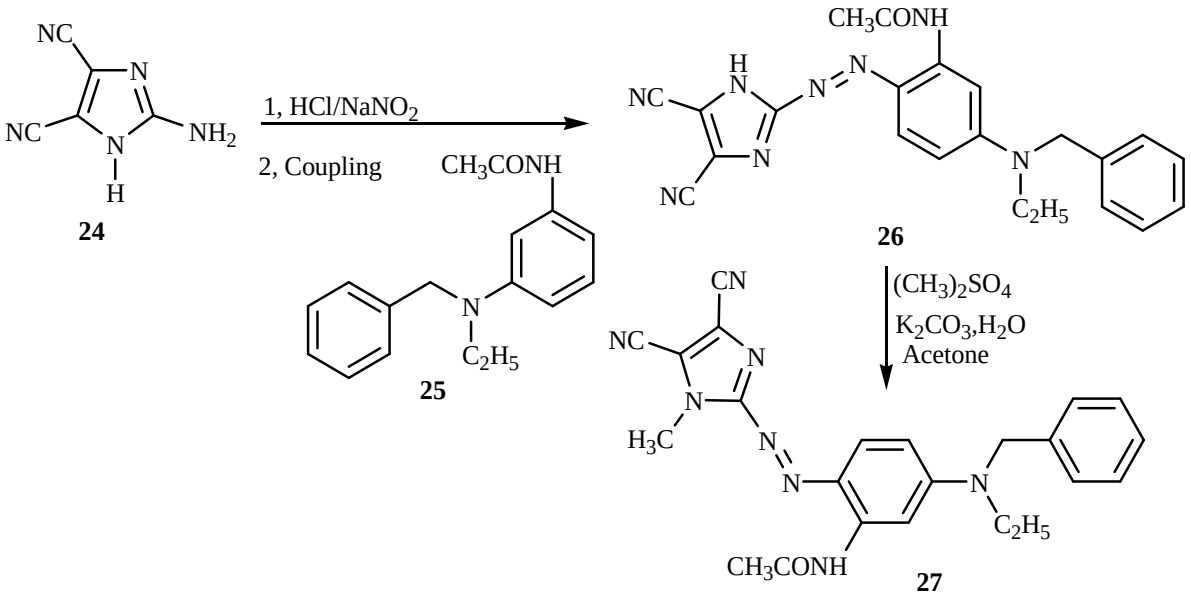

Scheme 5: General synthesis route towards azo dye derivative containing imidazole **27**.

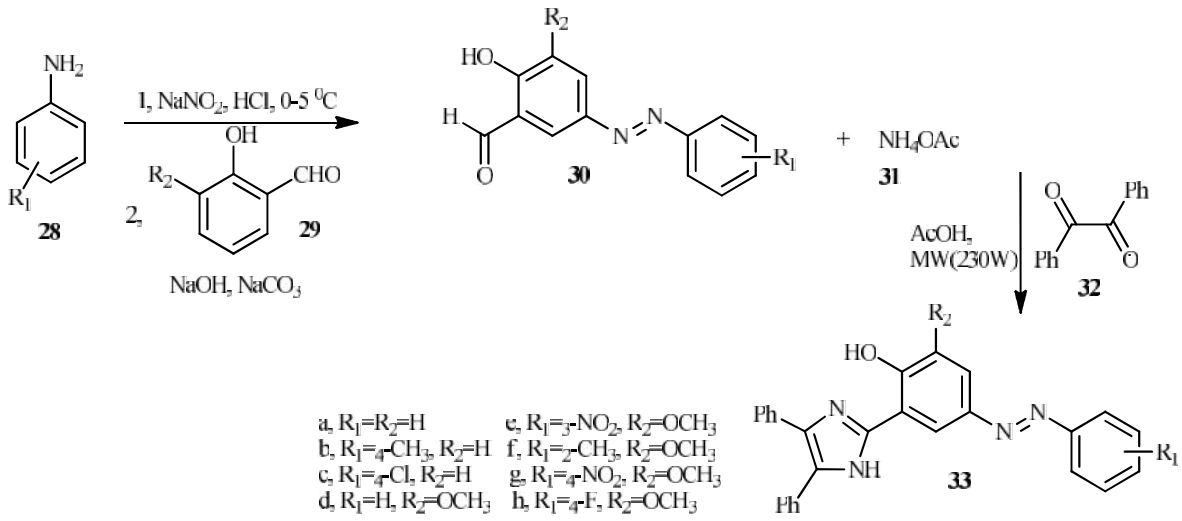

Scheme 6: General synthesis route towards azo-imidazole derivatives.

Similarly, through a convenient, one pot three-component synthesis methodology new azo-imidazole **33** (a-h) were reported by Mahmoodi and co-workers (Mahmoodi and Nadamani, 2017), with moderate to excellent yields from the corresponding azo dyes **30**, ammonium acetate **31** and benzyl **32** under microwave irradiation in the presence of glacial as solvent and organocatalyst in short reaction times. Glacial acetic acid mainly used to activate and enhance the nucleophilic attack of the carbonyl group by ammonia. Aniline derivatives **28** were diazotized in the presence of $NaNO_2$ and HCl at 0-5 °C temperature, and then coupled with the aldehyde derivatives **29** to give the precursor azo dye **30**.The resulting azo dyes **30** were subjected with ammonium acetate **31**, and followed

condensation reaction with the benzyl **32**, which in turn rearranges to the azo-imidazole **33** as outlined in Scheme 6.

2.3.4. Azo dyes containing pyrazole and its derivatives

Azo dyes derived from the pyrazole and pyrazolone derivatives have a potential broad spectrum biological properties such as, anti-bacterial, anti-cancer and antimicrobial activities, and they use in the pharmaceutical sector (Rizk and El-Borai, 2015). Demircali and co-workers reported the synthesis of five new azo dyes **41** containing pyrazole derivatives, which were derived from 5-amino-4-arylazo-3-methyl-1*H*-pyrazoles **38**, through diazotization followed by coupling reaction in the presence of hydrazine monohydrate **37**, as the general route for the synthesis of the dyes is depicted in Scheme 9 (Demircalı and Sari, 2021).

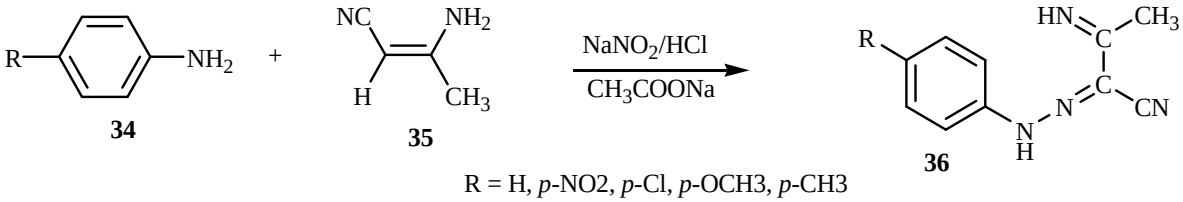

Scheme 7: Synthesis of the compounds **36**.

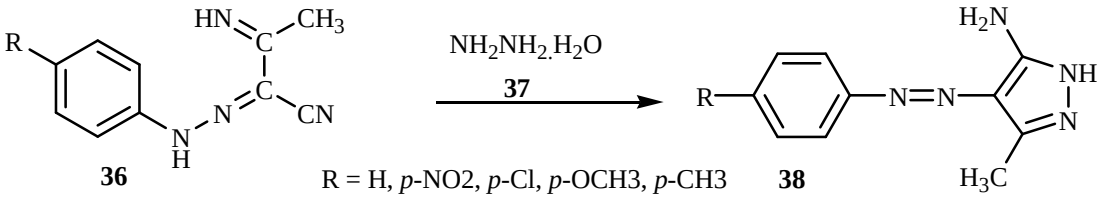

Scheme 8: Synthesis of the compounds **38**.

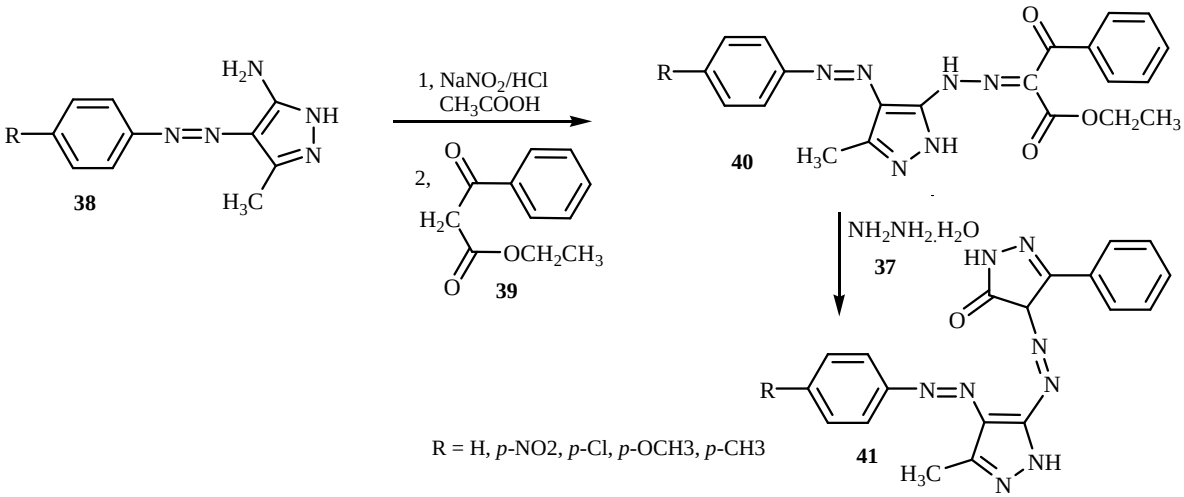

Scheme 9: General synthesis route of dis-azo dyes containing pyrazole and pyrazolone **41**.

Aniline derivatives **34** were diazotized in the presence of $NaNO_2$/HCl followed coupling with 3-aminocrotononitrile **35** to 2-arylhydrazo-3-ketiminobutyronitriles **36** as outlined in Scheme 7. 2-arylhydrazo-3-ketiminobutyronitriles **36** subjected with hydrazine monohydrate **37** to give 5- amino-4-arylazo-3-methyl-1*H*- pyrazoles **38** (Scheme 8). The electron withdrawing groups in the *p*-position results the azo dye to become more toxic, while the substitution of the electron donating groups caused the dye to be less toxic (Demircalı *et al*., 2021).

New series of dispersed disazo dyes **51** containing pyrazole and isoxazole groups were synthesized by a series of synthesis processes (Demircalı *et al*., 2019). These newly synthesized ten diazo disperse dyes, one was without auxochrome group and nine were with $-NO_2$, -Cl, $-CH_3$ auxochrome on *para*, *meta* and *ortho* positions. First, the different aniline derivatives **42** were diazotized and coupled with 3-aminocrotononitrile **43** and coupled to result in the corresponding 2-arylhydrazono-3-ketiminobutyronitriles **44**.

After cyclization process of 2-arylhydrazono-3-ketiminobutyronitriles, **44** with hydrazine monohydrate **45**, 5-amino-4-arylazo-3-methyl-1*H*-pyrazoles **46** which were diazotised and coupled with ethylacetoacetate and then produce a series of ethyl pyrazolyl hydrazonoacetoacetates **49**. Cyclization of **49** with hydroxylamine **50** afforded diazo dyes **51** (Scheme 10).

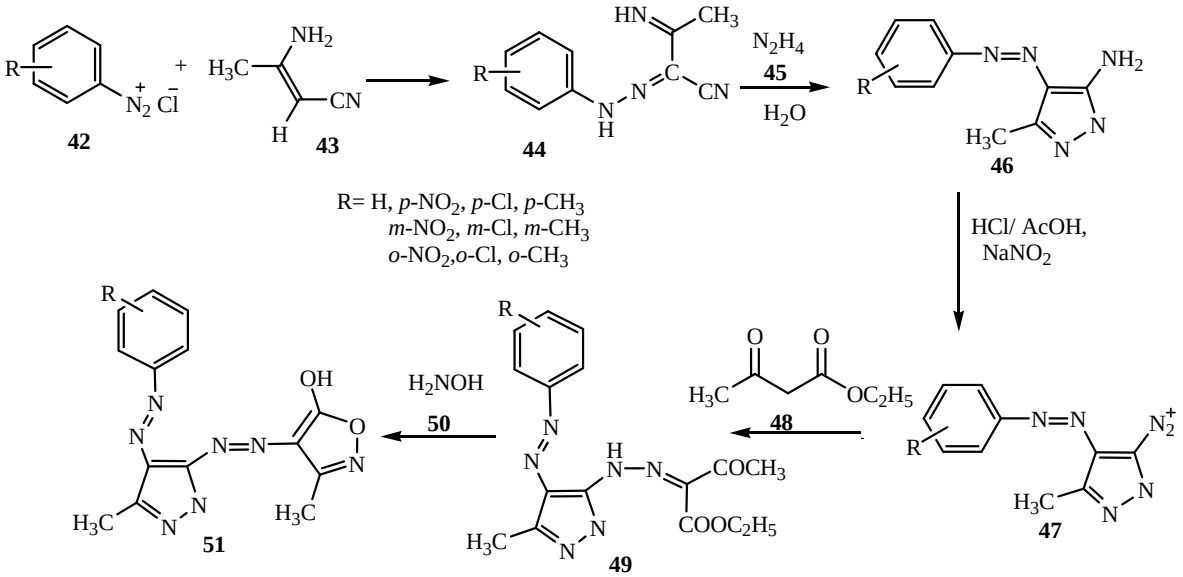

Scheme 10: General synthesis route of diazo dye containing pyrazole **51**.

2.3.5. Azo dyes containing thiazole and its derivatives

According to the reported literatures finding azo dyes containing thiazole fascinated the researchers because of their broad range of pharmacological activities such as anti-infectious, antioxidant, anticancer, antibacterial, antifungal, etc (Al-adilee and Hessoon,

2019; Mohamed and Fahmy, 2021; Prakash *et al*., 2021). Researchers have reported the synthesis of an azo dye containing a thiazole ring using various methods. Keshavayya and co-workers prolifically synthesized three potent anticancer active azo dyes possessing 2-amino-thiazole moiety *via* a simple, effective, economic, and conventional diazo-coupling reaction (Ravi and Zahara, 2021). During the reaction, 1,3-thiazole-2-amine **52** in acid mixture was reacted with nitrosylsulphuric acid at 0-5 °C to form diazonium salt. Azo dye **54** (a&b) formed, when diazonium salt solution added to the well cooled solution of coupling components **53** (a&b) in an aqueous KOH solution. The synthetic route for the preparation of azo dyes was represented in Scheme 11.

Similarly, Keshavayya and co-workers reported the synthesis of four new biologically active azo dyes **57** containing thiazole which was derived from 2-amino-5-nitrothiazole **55** by the conventional diazo-coupling method in an acid condition (Keshavayya and Ravi, 2020). 2-Amino-5-nitrothiazole **55** was diazotized in the presence of sodium nitrite in sulphuric acid, and rapidly cooled in an ice bath at 0-5 °C for 10 min.

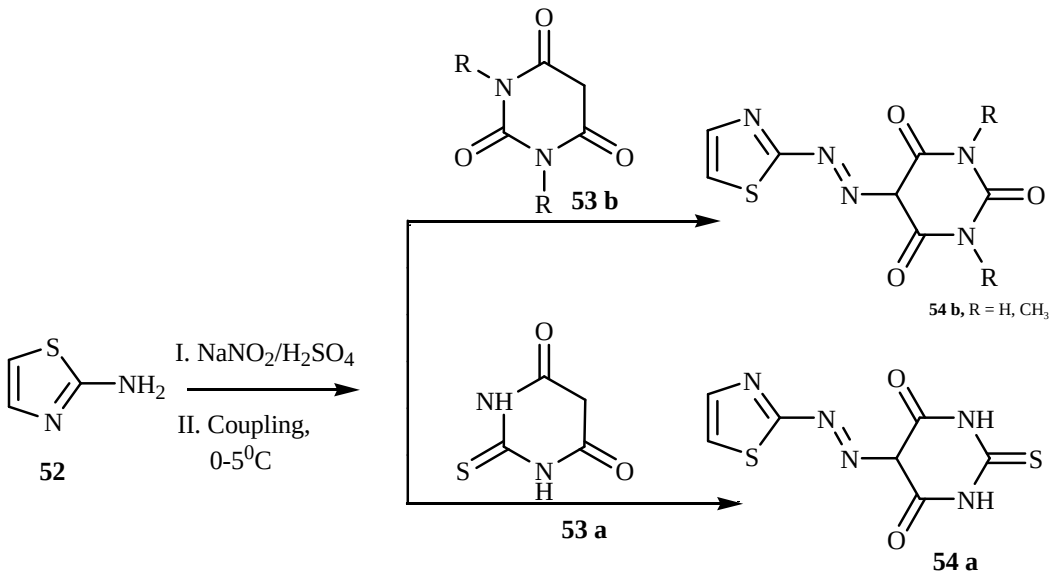

Scheme 11: General synthetic route towards azo dye derivatives containing thiazole.

Cold diazonium salt solution was added drop wise with vigorous stirring to the coupling compounds **56** (a-c) which were dissolved in acetic acid, and then the whole reaction mixture was stirred at 0-5 °C for 1 h to give the final azo dyes **57** (a-d) product, as described in Scheme 12. All the prepared azo dyes revealed promising growth inhibitory effect against selected antibacterial strains and also shown the potential antioxidant property.

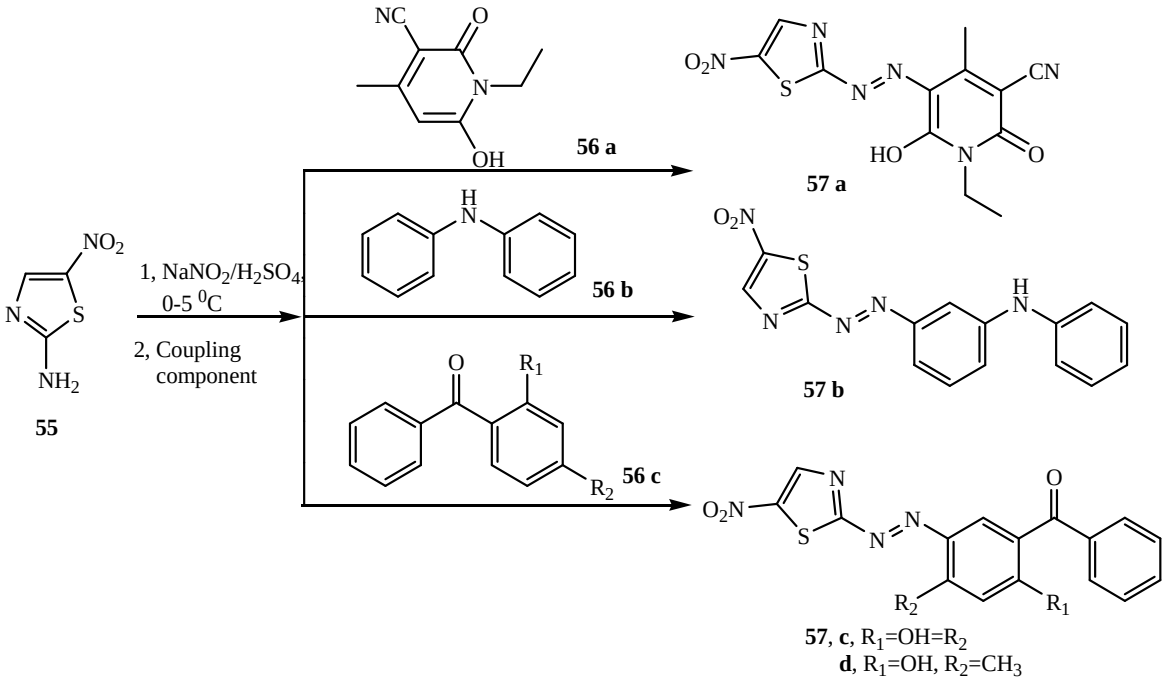

Scheme 12: General synthesis route of azo dye derivatives containing thiazole **57**(a-d).

2.3.6. Azo dyes containing oxazolone and its derivatives

According to, Albelwi and co-workers, novel azo dye-containing derivatives of the oxazolone compounds were obtained via the Erlenmeyer reaction of the azo dye precursors (Albelwi *et al*., 2021). The new 4-arylidene-5(4*H*)-oxazoloneazochromophore **63** was produced by condensation of 2-(4-(4-((2-hydroxyethyl)(methyl)amino)phenyl)diazenyl) acetic acid **61** with the corresponding benzaldehydes **62** in the presence of acetic anhydride and sodium acetate, as shown in Scheme 13. Compound **61** was formed from the diazotizotion of compound **58** followed by coupling of compound **60**.The formation of the unsaturated 5-[4*H*]-oxazolone has been elucidated via a two-step mechanism. The first step integrates the intermolecular condensation of the azochromophors **61** in the presence of acetic anhydride to yield intermediate. This intermediate has two acidic protons that can react with the benzaldehyde derivative **62** in the presence of sodium acetate under refluxing conditions to produce the oxazolone azo dyes **63** in good yields. The synthesized oxazolone based azo chromophores were exhibit strong potency of antifungal and antibacterial activities in comparison to the reference drug Amphotericin-B. Similarly, Hamidian and co-workers reported six new potent bioactive azo dyes **69** containing of 5(4*H*)-oxazolone ring (Hamidian *et al*., 2013), by diazotization of 4-aminohippuric acid **64** and coupling with aromatic derivatives **66** (*N*,*N*-dimethylaniline, 1-naphthol, and 2-naphthol) followed by condensation with benzaldehyde derivatives **68** as described in Scheme (14-16).

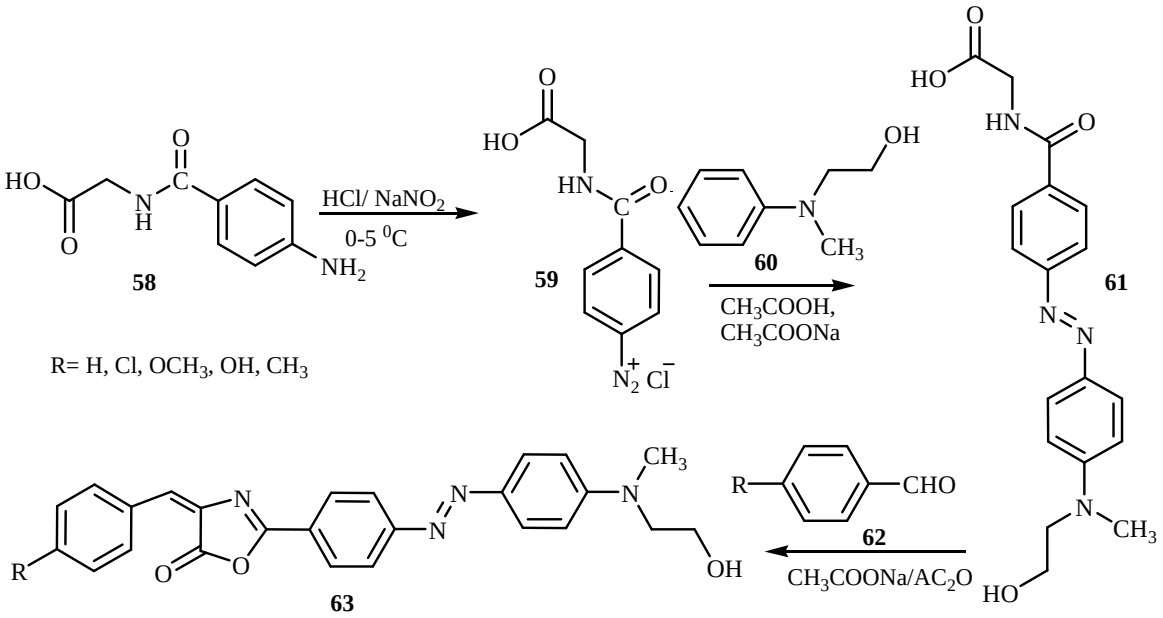

Scheme 13: General synthesis route towards azo dye derivatives containing oxazolone **63**.

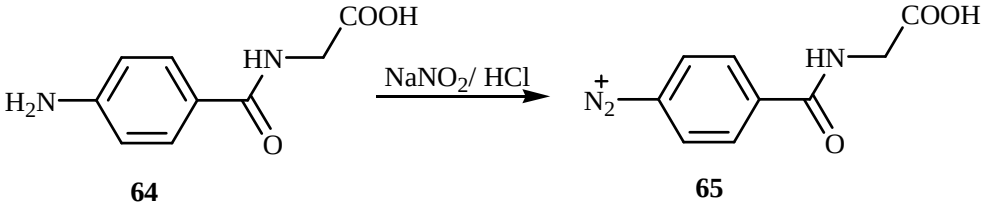

Scheme 14: Diazotization of 4-aminohippuric acid.

A mixture of anhydrous sodium acetate, 4-fluorobenzaldehyde or 4-trifluoromethoxy benzaldehyde, sodium salt of azo dye **67** and acetic anhydride was heated with stirring until the mixture is transformed from an orange semi-solid mass to a deep red liquid. After cooling, the precipitated product was filtered and recrystallized in toluene to obtain the final azo dyes **69** product. All synthesized compounds exhibited high tyrosine's inhibitory behaviour.

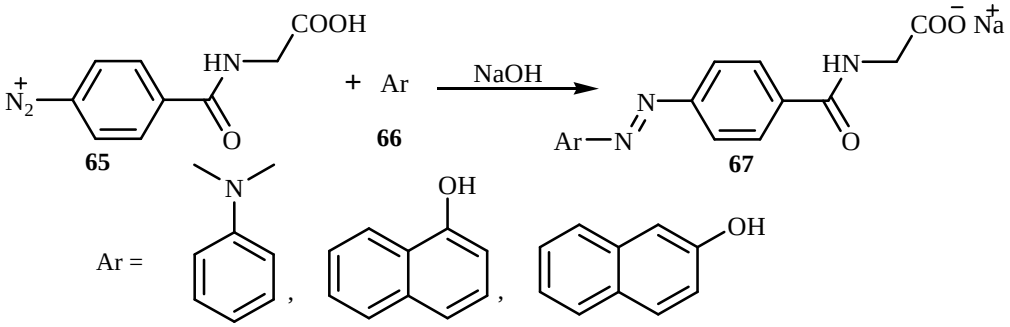

Scheme 15: Coupling of diazonium salt with aromatic compounds.

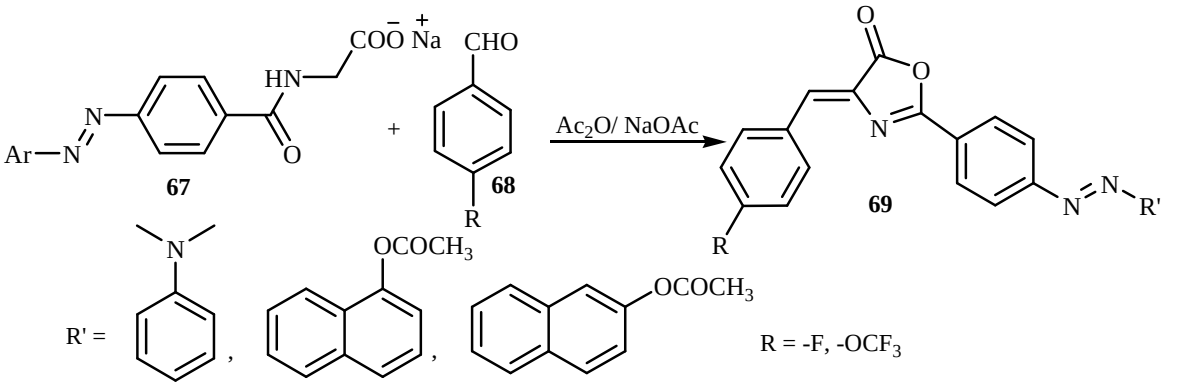

Scheme 16: General synthesis route towards azo dye derivatives containing oxazolone **69**.

2.3.7 Azo dyes containing thiadiazole and its derivatives

Thiadiazoles are five membered heterocyclic rings associated with diverse biological activity, especially studies reported that 1,3,4-thiadiazoles become biologically more potential than all other isomers of thiadiazole (Anthwal *et al*., 2022; Hu *et al*., 2014). Recently, Gur reported an antimicrobial active azo dyes containing 1,3,4-thiadiazole via diazotization followed coupling (Gur *et al*., 2019). Compound **72** (a-e) were prepared when thiosemicarbazide was subjected with ester group derived from 2-aminobenzothiazole and the ester **71** at 150 °C under reflux for 3h. These compounds were treated with diazotized aniline derivatives as coupling agent to furnish the azo dyes **74** (a-e).

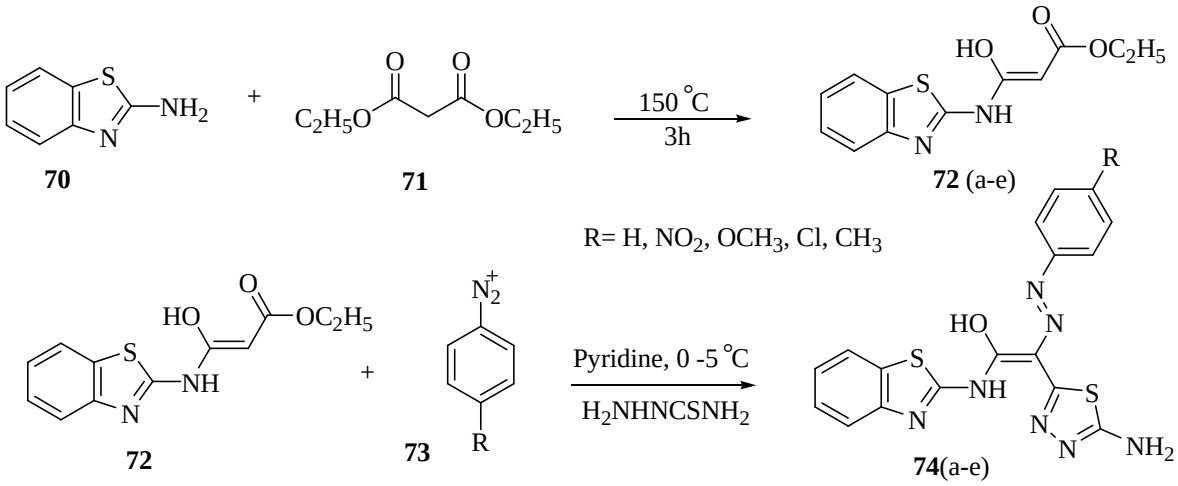

Scheme 17: General synthesis route of azo dye derivatives incorporated thiadiazole.

On previous work, the synthesis of three series azo dyes derived from 2-amino-5-aryl-1,3,4-thiadiazoles with coupling agents were reported by Kudelko and co-workers (Kudelko *et al.*, 2020). During the reaction, benzoic acid derivatives were subjected with thionyl chloride followed with thiosemicarbazide in the presence of conc. H_2SO_4 for cyclization at room temperature under reflux to give compound **77**. These compounds were

diazotized in the presence of $NaNO_2$ and conc. H_2SO_4 at 0-5 °C temperature followed coupling with aniline, N,N-dimethylaniline and phenol dissolved in H_2O at 0-5 °C and then neutralization with aqueous $NaCO_3$. The final azo dyes series **80** (a-c) were obtained from the filtration, washing and recrystallization of the mixture with appropriate solvent.

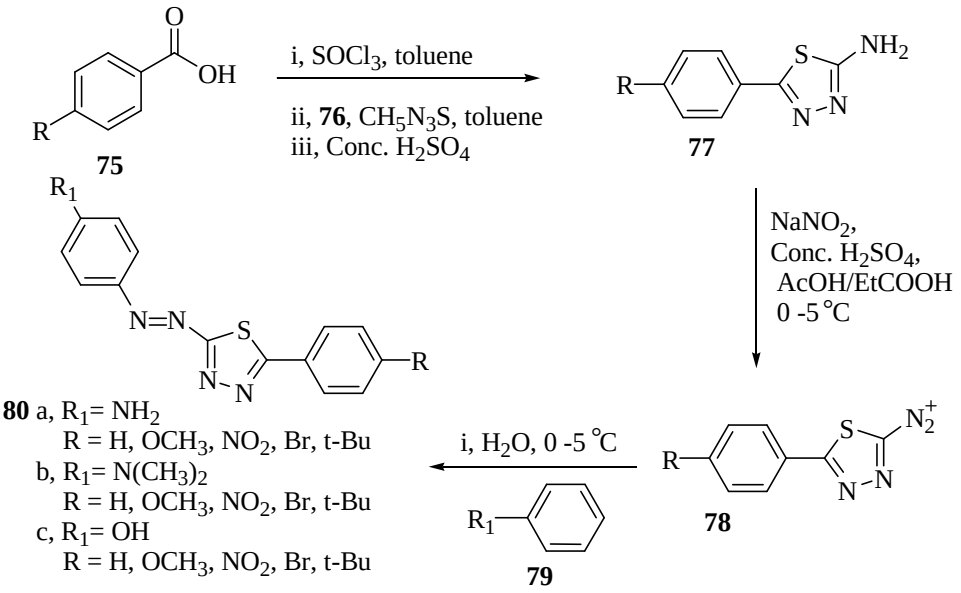

Scheme 18: General synthesis route of azo dye derivatives incorporated thiadiazole.

2.3.8. Azo dyes containing benzothiazole and its derivatives

Song and co-workers reported new bi-heterocyclic dyes **83** which contain *N*-ethyl-3-cyano-4-methyl-6-hydroxy-2-pyridine groups from substituted benzothiazoles (Song and Hu, 2020).

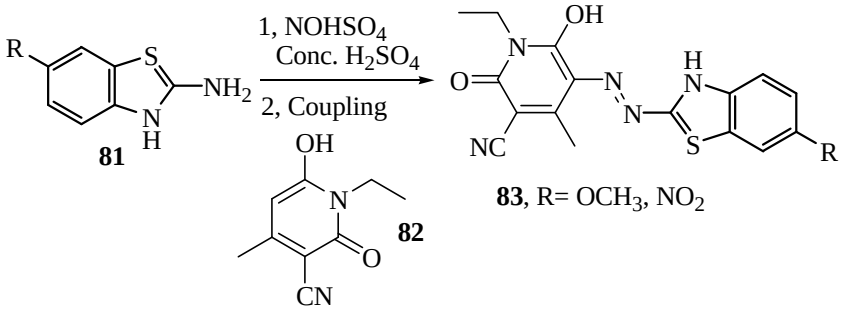

Scheme 19: General synthesis route of azo dye derivatives containing benzothiazole **83**.

Under vigorous mechanical stirring at 40 °C, the substituted benzothiazole **81** was mixed with concentrated phosphoric acid, concentrated sulfuric acid, and glacial acetic acid to form diazonium salt. When diazonium salt was added drop wise to pyridine derivatives **82** under vigorous mechanical stirring, azo dye **83** was formed. The synthesis route of designed bi-heterocyclic disperse dyes is shown in Scheme 19.

Malayappa and co-workers reported the synthesis of four benzothiazole-based dispersed azo dyes **87** derived from 2-phenyl-2,4-dihydro-3*H*-pyrazole-3-one **75** by diazo coupling

electrophilic substitution at 0-5 °C (Maliyappa and Basavarajappa, 2020). 2-Amino-6-substituted benzothiazoles **84** were dissolved in a mixture of glacial acetic acid and propionic acid (2:1), and this solution was added drop wise to a well-cooled solution of nitrosylsulfuric acid ($NaNO_2$ in H_2SO_4) at 0-5 °C, to form diazonium salt **85**. The resulting diazonium salt **85** coupled with 5-methyl-2-phenyl-2,4-dihydro-3*H*-pyr-azol-3-one **86** in acetic acid at 0-5 °C. The precipitated colored product was filtered off, washed several times with distilled water, dried and recrystallized from ethanol. The general route for the synthesis of azo dyes **87** is outlined in Scheme 20.

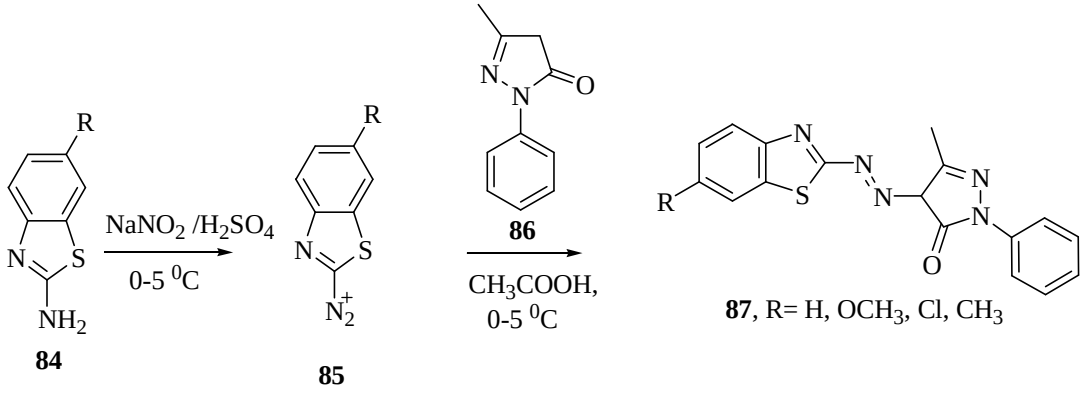

Scheme 20: General synthesis route of azo dye derivatives containing benzothiazole.

2.3.9. Azo dyes containing quinolone and its derivatives

Shinde and Sekar have reported synthesis of novel heterocyclic acid dyes **91** by diazotizing various sulphonic acid based amines and coupling with 4-hyrdoxyl-1-methyl-2(1*H*)-quinolone (Shinde and Sekar, 2019).

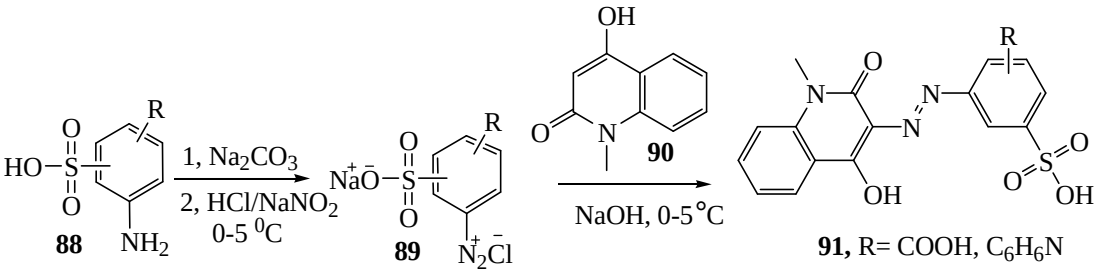

Scheme 21: General synthetic route towards azo dyes derivatives containing quinolone.

The dye intermediates, aminosulphonic acids **88** was dissolved in Na_2CO_3, cooled to 0-5 °C, and then diazotized in the presence of sodium nitrite and conc. HCl to form **89** by reverse diazotization and combined with 4-hydroxyl-1methyl-2(1*H*)-quinolone **90** to give azo dye **91**. A general synthetic route towards the preparation of azo dyes is shown in Scheme 21.

Recently, Rufchahi and co-workers reported novel antibacterial active azo disperse dyes **97** which synthesized by linking diazotized *p*-substituted aniline derivatives **96** with 8-methyl-

4-hydroxyl-2-quinolone **95** (Rufchahi *et al*., 2013). Compound **95** was synthesized from the reaction of *N,N'*-di-(2-methylphenyl)malonamide **94** with polyphosphoric acid. Compound **94** was synthesized by reacting 2-methyl aniline **92** and diethyl malonate **93** in a microwave oven at 320 W for 5 min. The general Synthetic routes for the preparation of azo dyes **97** described in Scheme 22. The dyes exhibited significant antibacterial activity against, *S.enterica, P.aeruginosa, B.subtilis* and *M.luteus*.

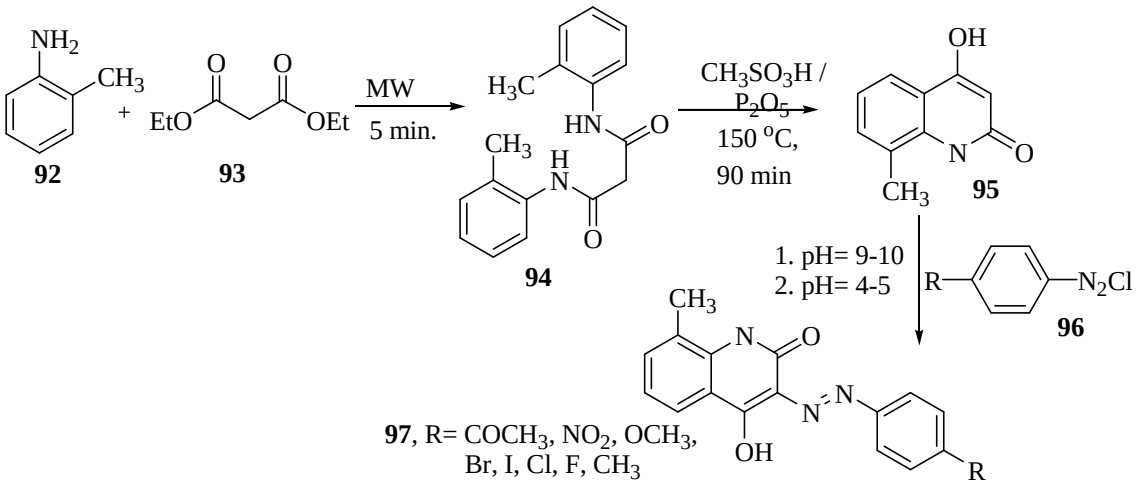

Scheme 22: General synthesis route azo dye derivatives containing quinolone.

2.4. Biological activity

A variety of biological and pharmacological applications are explored by azo dyes that contain heterocycles (Gaffer and Khattab, 2017; Keerthi and Shoukat, 2013). Heterocycle is an important component of the azo dye and plays an important role in increasing its pharmacological and medicinal properties, such as antibacterial activity (Gaffer and Khattab, 2017; Olomola and Olasunkanmi, 2018), antioxidant activity , anticancer and antitumor activity , anti-inflammatory activity (Canan and Benay, 2017; Gouda and Berghot, 2016; Keerthi Kumar *et al*., 2013).

2.4.1. Antibacterial activity

Banpurkar and co-workers reported the synthesis of 3-methyl-4*H*-isoxazol-5-one at room temperature by simple stirring method from ethyl acetoacetate and hydroxylamine hydrochloride in aqueous medium and coupled with diazotized substituted amine to form series of 4-(substituted-phenylazo)-3-methyl-4*H*-isoxazol-5-ones through green chemistry (Banpurkar and Perdih, 2018). Antibacterial activity of the synthesized azo dyes was screened against *E.coli, P.aeruginosa, S.aureus,* and *S.pyogenus*. All the synthesized compounds exhibit good antibacterial activity against Staphylococcus aureus close to that of reference drug ampicillin. Moreover, compounds **98** and **99** (Figure 4) show

antibacterial activity at (62.5 µg/mL) and (100 µg/mL) respectively, against *E.coli* close to that of ampicillin (100 µg/ mL).

In a recent study, novel disazo dyes containing imidazole and pyrazole cycles were synthesized through diazotization-coupling (Karabacak *et al*., 2017). The antimicrobial activity of synthetic dyes was tested against a number of pathogenic bacteria (*S.aureus, B.cereus, E.coli, S.typhimurium, S.enteritidis* and *L.monocytogenes*) and the synthetic dyes **100**, **101** and **102** (Figure 4) showed good antimicrobial activity against *B.cereus*, *S.aureus* and *L.monocytogenes* at 4000 µg/mL with inhibition zone of (18, 16 and 22 mm respectively) compared to tetracycline (28, 26 and 34 mm respectively) at 10 mg/mL.

In addition to the synthesis, Gur evaluated the antimicrobial activity of the synthesized azo dyes against Gram-negative bacteria (*S. enteritidis, S. typhimurium, E. aerogenes,* and *S. infantis*) and gram-positive bacteria (*S. aureus, S. epidermidis, E. durans,* and *E. faecium*) (Gur *et al*., 2019). Among the tested, compound **103** displays appreciable antimicrobial activity with inhibition zones 8 mm at 60 mL against *E.aerogenes.*

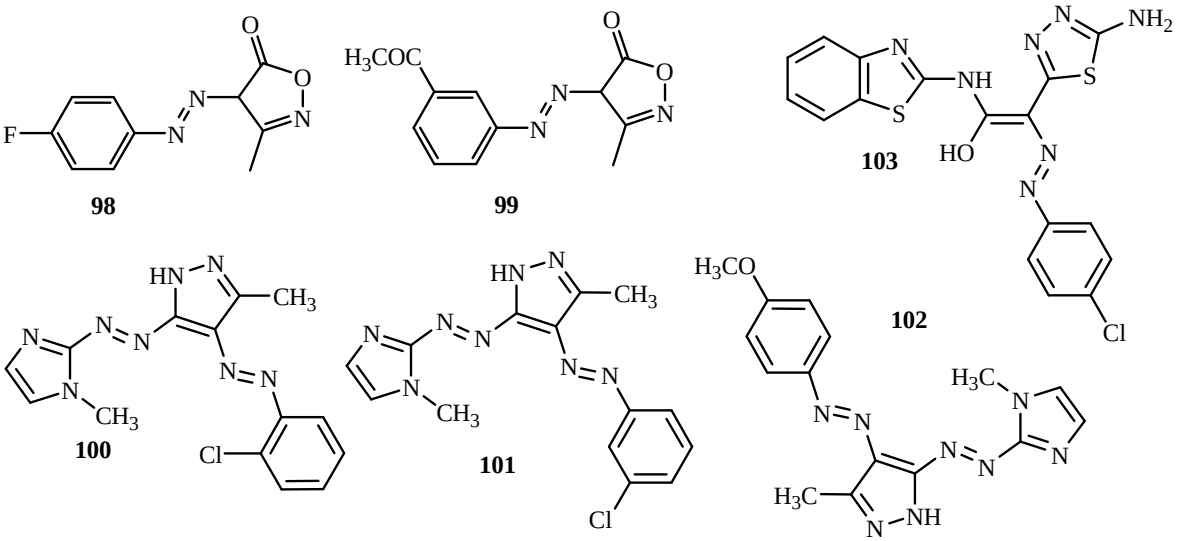

Figure 4: Chemical structures of antibacterial active azo dye derivatives incorporated heterocyclic moieties.

2.4.2. Antifungal activity

Recently, Matada and colleagues reported new S-heterocyclic azo dyes synthesized from 1, 3-benzothiazole-2-thiol with various amines via diazo-coupling (Matada *et al*., 2020). The azo molecules derived from benzothiazole were screened for their microbial inhibition by modified tube dilution assay against two fungal strains *C.albican*, and *A.flavus* with reference drug fluconazole. The antifungal activities of **104**, **105** and **106** (Figure 5) showed good results (MIC = 25 mg/mL) against *C.albican* and *A.flavus* compared to fluconazole (MIC = 0.4 mg/mL). The structure contributes to the enhancement of

antifungal activity, as described in (Abou Elmaaty and Sofan, 2022; Barros *et al*., 2018; Raman and Pravin, 2014).

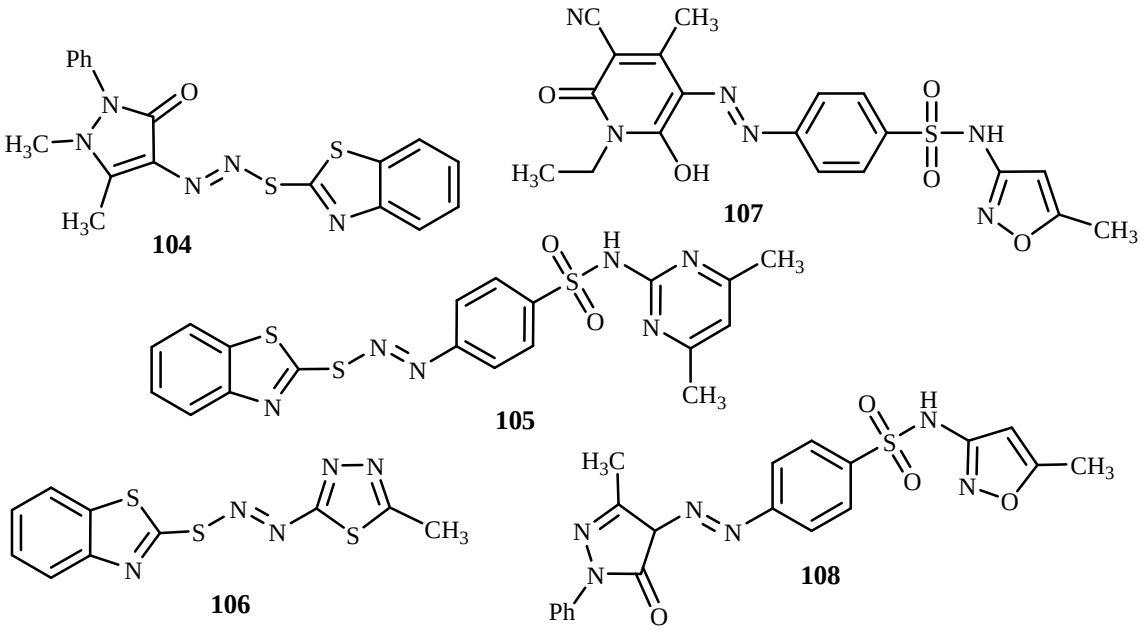

Figure 5: Chemical structures of antifungal active azo dye derivatives containing heterocyclic scaffolds.

Mallikarjuna and Keshavayya synthesized and reported bright coloured heterocyclic azo dyes from sulfamethoxazole with various coupling compounds (Mallikarjuna and Keshavayya, 2020). The antifungal activity of these target compounds was studied against *A.flavus* and *C.albican*, with reference drug fluconazole, and synthesized azo dyes **107** and **108** (Figure 5) were proven to have antifungal properties ((70 and 74) and (64 and 78) mm) respectively against *A.flavus* and *C.albican* compared to fluconazole (78 and 81 mm respectively) at 50 mg/mL. Further, these azo dyes has shown promising antibacterial, anti-mycobacterial, and anticancer activity which indicate that the compounds have proved to be efficient in inhibiting multiple diseases.

2.4.3. Anti-tuberculosis activity

In the recent years, tuberculosis has become one of the most dangerous infectious diseases and a leading cause of death worldwide (Correia *et al*., 2014). Still, it is a challenge for the chemists and researchers to design effective anti-TB drugs. An azo dye based on coumarin-benzothiazole was synthesized by Bodke and co-workers (Manjunatha and Sridhar, 2021). The effectiveness of the synthesised dyes was tested against mycobacterium tuberculosis (H37 RV strain) and compared to the standard drugs using the microplate Alamar Blue Assay method. Among the azo dyes **109** and **110** (Figure 6) exhibited excellent and similar sensitivity (MIC=1.6µg/mL) relative to standard streptomycin (MIC= 6.24 µg/mL).

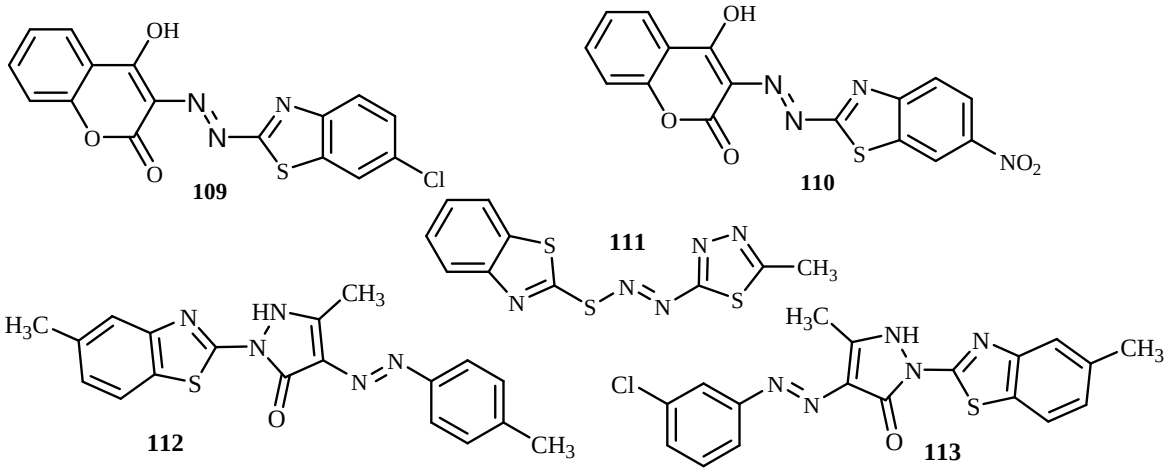

Figure 6: Chemical structures of an anti-mycobacterial active azo dye derivatives containing benzothiazole moiety.

In addition to their synthesis route, the synthesized compounds were evaluated for their antitubercular activity against *M. tuberculosis* by microplate blue Almar assay (Matada *et al*., 2020). Among the tested, compound **111** exert significant activity with MIC= 3.12 µg/mL in the presence of streptomycin as reference drug.

Maliyappa, and co-workers evaluated antimycobacterial activity of the synthesized compounds against *M.tuberculosis* via microplate Alamar Blue Assay method (Maliyappa and Pushpavathi, 2020). Among the tested compounds, **112** and **113** showed the highest activity with MIC = 1.6 µg/mL better than the standard drug, streptomycin (MIC = 6.25 µg/mL).

2.4.4. Anticancer activity

An anticancer active novel heterocyclic azo dye were synthesized and reported by Maliyappa and co-workers through conventional diazo coupling reaction (Maliyappa *et al*., 2020). The anticancer activity of the compounds was studied against human cancer cell lines, colon cell line (HCT116), lung carcinoma cell line (A549), T-lymphocyte cell line (Jurkat) and chronic myeloid leukemia cell line (K562), and the compounds **114** and **115** (Figure 7) exhibit good activity towards human colon cell line (HCT116) to inhibit the growth of the cancerous cells with IC_{50} value (34.65 ± 0.35 and 48.19 ± 0.31 µM) respectively. All the synthesized azo compounds in the lung carcinoma cell line (A549), T-lymphocyte cell line (Jurkat) and chronic myeloid leukemia cell line (K562) showed moderate results IC_{50} (>50 µM).

Additionally, Keshavayya and colleagues reported powerful anti-cancer active heterocyclic azo dyes, **116** and **117**, derived from 2-amino-5-methyl-thiazole by diazo coupling reaction

(Ravi and Santhosh, 2020). The azo dyes were screened *in vitro* against A-549 and K-562 cell lines, and both the compounds exhibit potent anticancer activity with IC_{50} values (5.39 and 3.16 µg/mL) for A-549 and (17.30 and 10.75 µg/mL) for K-562 cell lines respectively, compared to cisplatin which has the IC_{50} 10.70 and 7.36 µg/mL for A-549 and K-562 respectively.

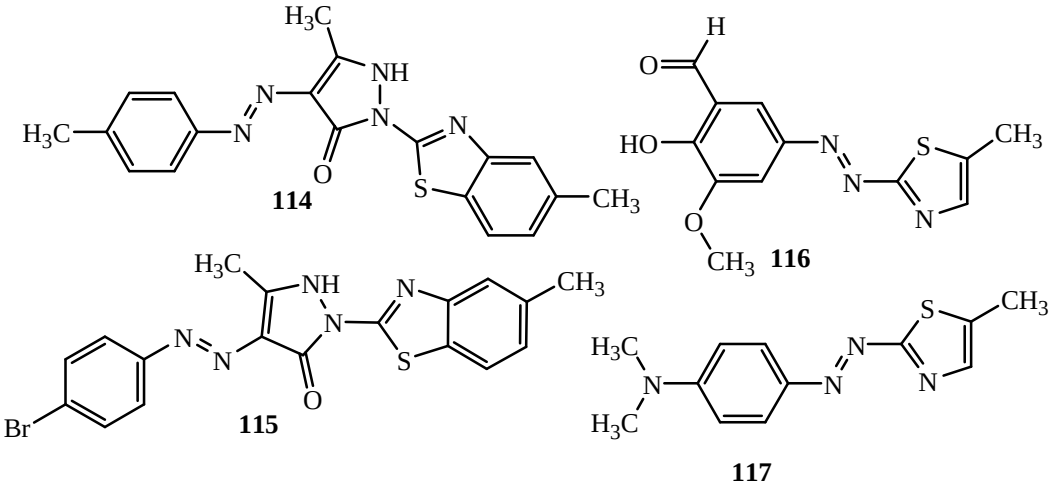

Figure 7: Chemical structures of anticancer active azo dye derivatives incorporated hetero-cyclic scaffolds.

2.4.5. Anti-inflammatory activity

In a conventional diazo coupling reaction, Bodke and co-workers synthesized novel anti-mycobacterial isoxazolone-thiazole based azo dyes (Manjunatha and Bodke, 2021). Further, it was evaluated anti-inflammatory activity of the synthesized azo dyes against matrix metalloproteinase-2 (MMP-2) and matrix metalloproteinase-9 (MMP-9) using gelatin zymography. The azo dye **118** exhibit significant anti-inflammation activity against MMP-2 and MMP-9 with % inhibition of (85 and 50 %) respectively compared with tetracycline hydrochloride (100 and 95 %) respectively.

In a recent paper, Unnisa and co-workers reported and synthesized pyrimidine azo dyes by coupling diphenylpyrimidine-2-amine with different aromatic amines (Unnisa *et al*., 2020). The synthesized compounds were screened for their anti-inflammatory activities through the heat-induced hemolysis method. Most of the synthesized compounds exhibit a membrane stabilization effect by inhibiting the lysis of the erythrocyte membrane. Compounds **119** and **120** (Figure 8) have maximum inhibitory activities of 71.08%, and 71.91%, respectively, which are closer to the standard aspirin 72.91%.

Harisha and co-workers evaluated in-vitro anti-inflammatory activity of the synthesized compounds via inhibition of bovine serum albumin denaturation method (Harisha *et al*.,

2020). Out of the tested compounds for anti-inflammatory activity, compound **121** and **122** have exhibited an excellent anti-inflammatory activity having 48.74 and 50.13 % compared to the standard aspirin 85% at (200 µg/mL).

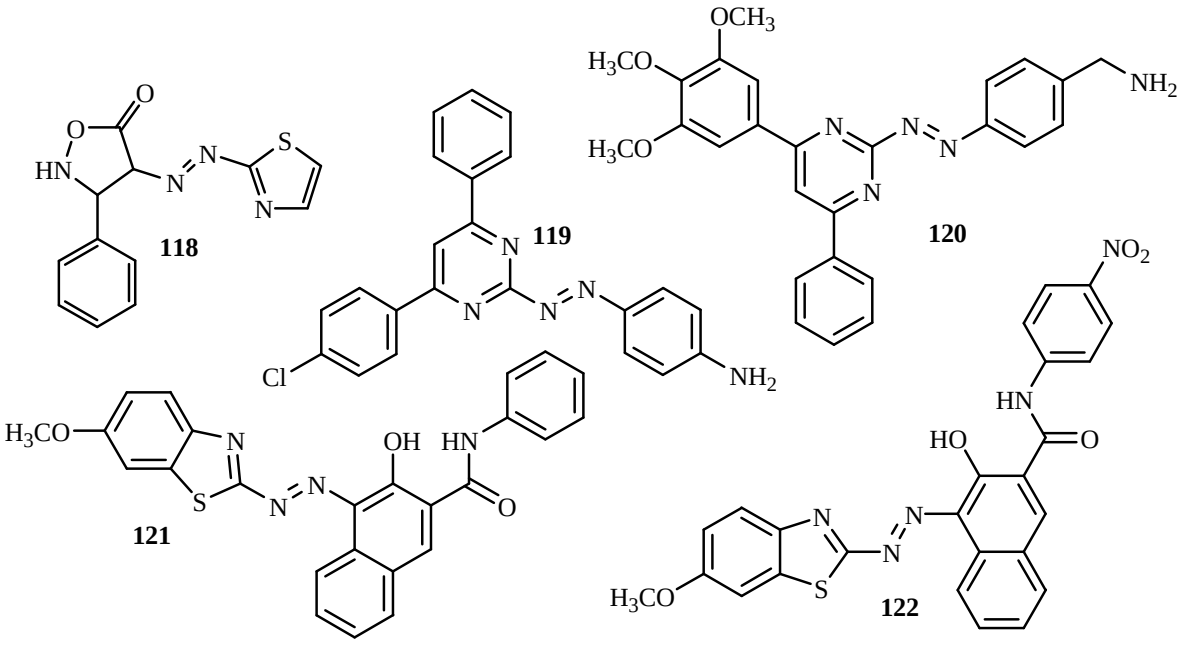

Figure 8: Chemical structures of anti-inflammatory active azo dye derivatives incorporated heterocyclic scaffolds.

2.4.6. Antioxidant activity

A series of novel bioactive disperse dyes (Figure 9) consisting of thiazolyl and piperazine moieties was reported by Mohammadi and co-workers via azo coupling reactions (Mohammadi *et al*., 2015).

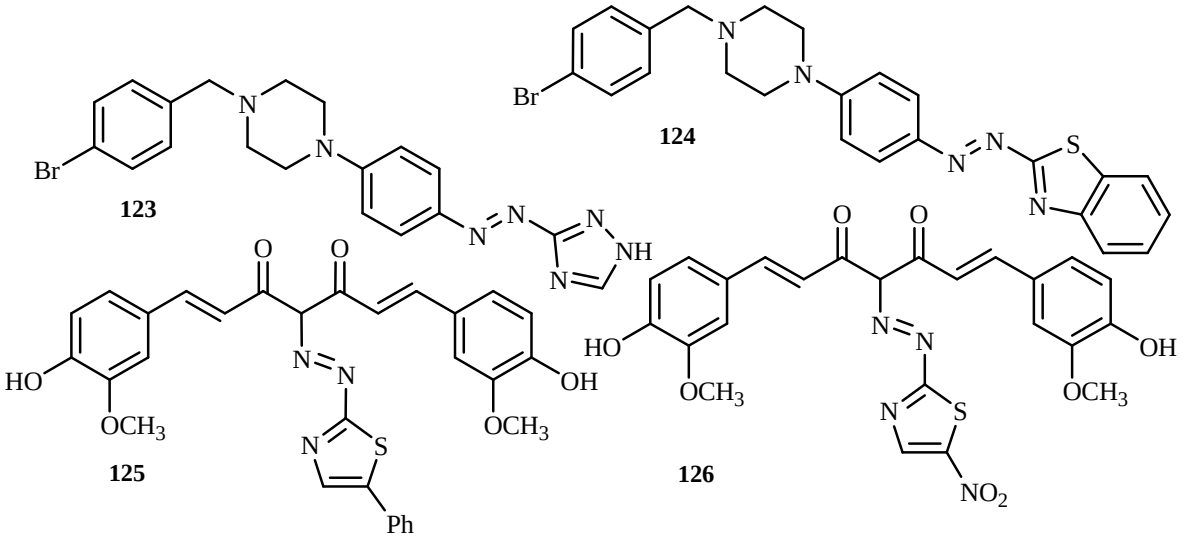

Figure 9: Chemical structure of antioxidant active heterocyclic incorporated azo dye derivatives.

The antioxidant activity of newly synthesized compounds was evaluated by FRAP. All of the compounds displayed significant antioxidant activity; especially, azo dyes **123** and **124** exhibit good radical scavenging activity (140 and 160 µM) respectively. The activity of these compounds was attributed for the presence of thiazolyl derivatives and piperazine moiety as bioactive components in the structures of synthesized dyes (Mohammadi *et al*., 2015).

Abu-Melha and co-workers reported the synthesis of novel bioactive thiazolyl-curcumin azo dyes in which curcumin become coupled with different aromatic diazonium salts of 2-a minothiazole derivatives, such as 2-aminobenzothiazole, 2-amino-5-phenylthiazole, 2-amino-5-methylthiazole and 2-amino-5-nitrothiazole (Abu-Melha *et al*., 2019). All synthesized compounds were tested alongside antioxidant activity reflected the ability to inhibit oxidation. Antioxidant activity of the synthesized compounds were examined by ABTS inhibition, and compounds **125** and **126** showed higher antioxidant activity with % inhibition (84.5 and 87.25 %), comparable to ascorbic acid (87.38 %) as standard. Furthermore, the synthesized thiazolyl-curcumin derivatives exhibited respectable antimicrobial, anticancer and antioxidant activity (Figure 9).

2.4.7. Antiviral activity

A yellow colored heterocyclic azo dye **127** and **128** which is antiviral in nature was synthesized and reported by author Mohammad Ashfaq (Ashfaq and Tabassum, 2020).

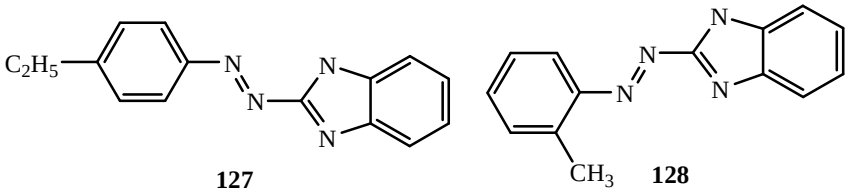

127 **128**

Figure 10: Chemical structures of antiviral active azo dye derivatives containing benzimidazole scaffold.

The compounds were tested in vivo against viruses in developing chick embryos. Labels were applied to nine-day-old embryonated chicken eggs based on the compound used. As a result of the hemagglutination test in case of anti-NDV potential of compounds for 100% at 0.1 mg/100 µl, both compounds inhibit 50% of NDV and AIV (H9N2) viral growth (Figure 10).

3. Materials and Methodology

3.1. Chemicals and reagents

This study was carried out in the presence of chemicals and reagents including; distilled water, petroleum ether, n-hexane, methanol, DMSO, acetone, ethyl acetate, ciprofloxacin, ascorbic acid, ketoconazole, ferric chloride ($FeCl_3$), DPPH, ethanol (96 and 97 %), 4-dimethylaminobenzaldhyde, 2,3,5-triphenyltetrazolium chloride, MHA, SDA, tween 80 (5%), 4-aminobenzoic acid, acetic acid, sodium acetate, thiosemicarbazide, $NaNO_2$, H_2SO_4 (98 %), HCl (37 %), NaCl, NaOH, KOH, phenol, 1-naphthol and 2-naphthol. All the chemicals and reagents were purchased from commercial sources and used without further purification.

3.2. Equipments and Apparatus

The necessary apparatus and instruments to be used are beakers, electronic balance, dropper, capillary tube, whatman number 1 filter paper, funnel, TLC chamber, measuring cylinders, oil bath, water bath, round bottom flasks, condenser, forceps, scissor, vial, refrigerator, Crock meter, washing fastness tester, dyeing pot, petri-dishes, oven, gray scal, bio-safety cabinet, incubator, cotton swap, autoclave and other equipments. Furthermore, there were also different instruments and techniques which help to identify, determine, separate and characterize synthesized compounds such as, TLC, UV-light at 254 and 366 nm, IR (cm^{-1}) recorded on KBr disk, UV visible (nm) (P9 double beam UV-Visble sepectrophotometer), NMR (ppm) using $CDCl_3$ and DMSO-d_6 as solvent and TMS as standard.

3.3. Methods of Synthesis

3.3.1. General Synthesis rout of 2-Amino-1,3,4-thiadiazole Derivatives (131)

4-(dimethylamino)benzaldhyde **129a**/4-(amino)benzoic acid **129b** (0.01mol) and thiosemicarbazide **130** (0.01mol) refluxed for 2-4h in the presence of conc. H_2SO_4 (0.5 mL) and EtOH (10 mL) at 50-60 °C temperature under continuous stirring. The solution was cooled to room temperature followed with addition of 5% sodium hydroxide to alkalize. The solution was transferred to crushed-ice. The precipitated product was filtered and washed with EtOH, dried and recrystallized from EtOH to give 2-amino-1,3,4-thiadiazoles derivatives **131b**, but the purified aldehyde derivatives (0.005 mol) further treated with 0.01 mol of ferric chloride in the presence of distilled water 2-3 h to furnish 2-amino-1,3,4-thiadiazoles derivatives **131a** (Kudelko *et al*., 2020) as in Scheme 21.

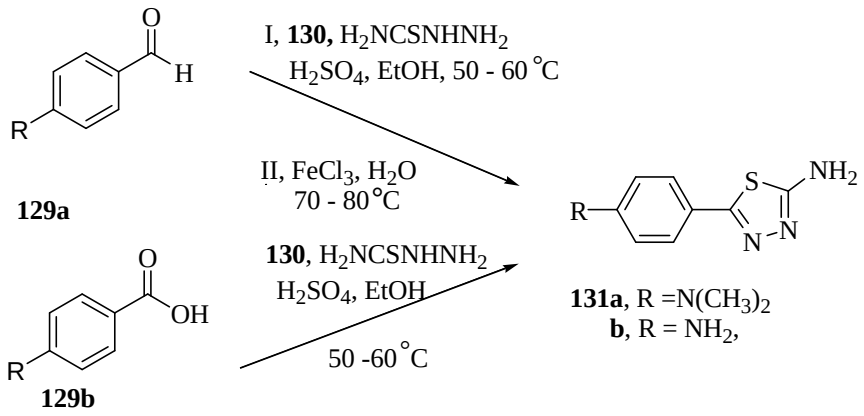

Scheme 23: General synthesis route of 2-amino-1,3,4-thiadiazole derivatives.

3.3.2. General procedure for the synthesis of azo dye derivatives

Compound **131a/131b** (0.005 mol) was dissolved separately in 10 mL H_2O followed by addition of 0.01 mol of sodium nitrite dissolved in 1 mL of aqueous HCl. The resulting diazonium salt was added slowly to vigorously stirred solution of 0.005 mol of coupling component in 10 mL of 5% potassium hydroxide under continuous stirring for 2h at 0-5 °C.

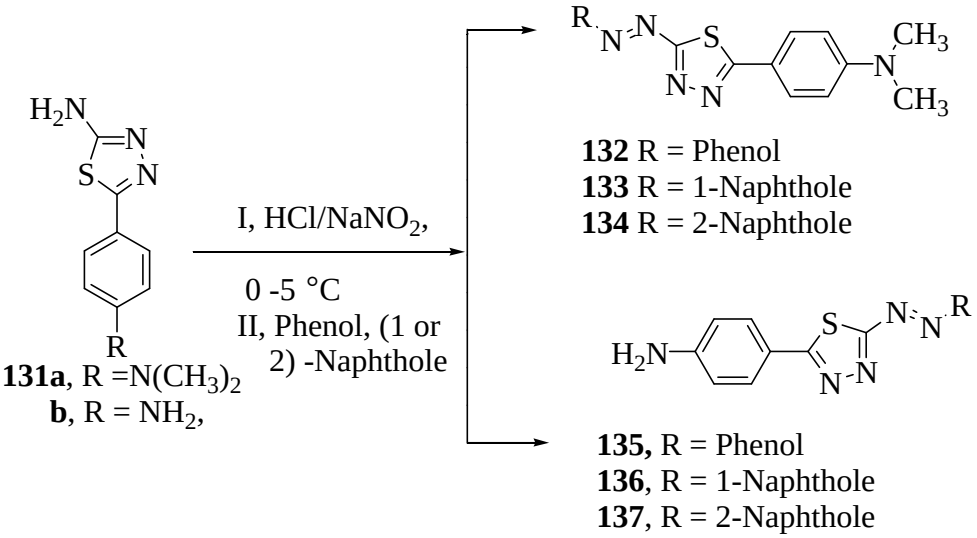

Scheme 24: General synthesis route of azo dye derivatives incorporated 1,3,4-thiadiazole.

After that, the pH of the reaction mixture was maintained by the simultaneous addition of saturated solution of sodium carbonate. The solid was filtered and washed with distilled water, and recrystallized in EtOH to give pure azo dye derivatives **132-134** and **135-137** as shown in Scheme 23 (Kumar *et al.*, 2013; Sahu and Routray, 2013).

3.4. Purification and characterization

The synthesized compounds were separated and purified by washing and recrystallization with the help of the TLC profile, visualised under UV lamp with short and long

wavelength. The purified compounds were characterized by as UV-visible, FTIR, ^{1}H NMR and ^{13}C NMR to confirm their structure.

3.5 Dyeing Performance

3.5.1 Dyeing Procedure

Cotton fabrics (5g) were weighed and added to six dye pots containing 30mL of each dye and 2 g of sodium chloride for exhaustion. Samples were placed in dyeing machine at 30 °C, after 20 min the temperature was raised to 60 °C. Next, after 20 min 1.5 g of sodium carbonate was added to each pot for fixation, and the dyeing was continued for 1h at pH of 5. Finally, the dyed samples were removed, after washed (hot, cold) followed by soap washing (0.5 g/L), then hot and cold wash.

3.5.2 Color Fastness

Color fastness of the dyed samples were evaluated according the standard method (Dyers and Colourists *et al*., 1990). Washing fastness of dyed samples was evaluated on washing fastness tester by ET/ISO-105-CO3. Color fastness to rubbing was carried out on Crock meter by ET/ISO 105-X12. The staining and color change of cotton for both fastnesses were measured with gray scale under suitable illumination.

3.6. Antimicrobial Activity

3.6.1 Media and Inoculums' Preparation

First of all, 38g of MHA and SDA were weighed separately and dissolved in 1 mL of distilled water with frequent agitation separately, and then followed by autoclaving at 121 °C for 15 minutes. MHA (bacteria) and SDA (fungus) were utilized to subculture the microorganisms. 3-5 well isolated colonies of the same morphological type from the refreshed agar plate culture were selected. The cultured colonies of bacteria and fungi were transferred to the broth MHB (bacteria) and SDB (fungi) using inoculating loop. During this time, UV spectrophotometer was used to adjust the bacterial or fungal suspension by measuring its absorbance with 1 cm path length at the wavelength of 625 nm. So, the absorbance was in the range of 0.08 to 0.1 which is proportional to $1*10^{8}$ CFU/mL bacteria and $1*10^{7}$ spores/mL fungi (Degu and Bitew, 2021). This inoculums suspension was further diluted to get $5*10^{5}$ CFU/mL for bacteria and 5*CFU/mL for fungi to determine MIC (Eloff *et al*., 1998).

3.6.2 Determination of Minimum Inhibitory Concentration

The MIC of the synthesized compounds were evaluated against six bacterial (*S.aureus, S.epidermid, E.faecalis, E.coli, K.pnemonia, S.typorumium)* and three fungal *(C.albicans,*

T.mentographytes, T.rumbrum) stains using broth dilution method according to Clinical and Laboratory Standards Institute (Eloff *et al.*, 1998; Humphries and Schuetz, 2021). The tests were employed by using MHB and SDB for bacteria and fungi respectively. First, 32 mg/ml of stock was prepared for each the synthesized compound in 5% tween 80. 100 µL of the compound, positive control and negative controls was added on the first row followed two-fold serial dilutions were made down from row A to H. Samples with different concentrations of the compounds, ciprofloxacin and ketoconazole were prepared respectively starting from 16-0.125 mg/mL, 4-0.0325 µg/mL and 50-0.3906 µg/mL. Then, the bacterial and fungal suspension containing approximately $5*10^5$ and $5*10^4$ CFU/ml respectively was prepared from a refreshed culture. From this suspension, 100 µL was inoculated into each well. The plates were incubated at 37 °C for 18-24 h for bacterial pathogens and at 25 °C up to 7 days for fungal pathogens. After incubation, 40 µL of 0.4 mg/mL solution of 2,3,5-triphenyltetrazolium chloride was added to each as an indicator of microbial growth and incubated at 37 °C for 30 minutes. The MIC values were made in triplicate and visually determined by observing the presence of purple color. The lowest concentration of each compound displaying no visible purple color was record as the MIC. Additionally, during the above all antimicrobial assay negative controls, sterility controls and growth controls were run parallel to the experimental tests. (Eloff *et al*., 1998).

3.7. Antioxidant activity

Scavenging activity of all synthesized compounds were measured by DPPH method according to Brand-Williams *et al* described in (Shridhar and Hoskeri, 2016). Samples were prepared by dissolving 4 mg of DPPH in 100 mL of MeOH. All synthetic compounds were separately dissolved in methanol and serially diluted using methanolic solution of DPPH to furnish 62.5, 125, 250, 500 and 1000 µg/mL. The mixture was shaken vigorously and allowed to stand at 37 °C for 30 min. Then the absorbance of the compounds were measured compared to that of ascorbic acid by using UV-Vis spectrophotometer (517 nm). The DPPH radical scavenging rate of each sample will be calculated as described in (Sahu *et al*., 2013).

$$\text{Inhibition } \% = \frac{(A0 - A1)}{A0} * 100$$

Where, A_0 is the absorbance of the control and A_1 is the absorbance of the sample.

3.8. *In silico* molecular docking studies

A molecular docking study was performed to investigate the binding mode of the synthesized compounds against target proteins. The chemical structures of the test

compounds were drawn using ACD/ChemSketch, then optimized by the DFT/B3LYP method with 6–31G(d,p) basis sets using Gaussian09 software (Frisch *et al*., 2009). The energy-minimized ligands were then input into the docking procedure. The targets, *E. coli* DNA gyrase (PDB ID: 6F86), *S. aureus pyruvate kinase* (PDB ID: 3T07), *C. albican* CYP51 (PDB ID: 5V5Z) and Human peroxiredoxin 5 (PDB ID: 1HD2) were retrieved from the Protein Data Bank (https://www.rcsb.org/). Biovia Discovery Studio 2020 was used to prepare the targets (Pawar and Rohane, 2021). The protein complex's water molecules were removed, and the bound ligand was chosen to determine the characteristics of the binding site before being removed from the complex (Trott and Olson, 2010). Re-docking of bound ligand with the target protein was carried out to validate the binding sites (Ramachandran and Rajappan, 2022). The target was augmented with polar hydrogen atoms and the necessary charges. Using Auto Doc Vina (MGLTools-1.5.6), the target and ligand were generated in the necessary format (pdbqt) for docking, and docking was performed (Trott and Olson, 2010). Nine conformers and their associated binding energies were generated for each ligand during the docking procedure (Nguyen *et al*., 2019). Using Biovia Discovery Studio 2020, the conformation with the lowest binding energy was chosen to determine the interactions between the receptor and ligand.

3.9. *In silico* pharmacokinetics and drug likeness prediction

The *in silico* based design and prediction of compounds is crucial way for low cost and efficient synthesis of molecules (Breznik *et al*., 2023; Gokalp and Atay, 2020). The *in silico* ADMET and drug likeness prediction help to understand whether a drug has preferable properties for being an orally active drug, based on the established concept of the Lipinski rule of five and the Veber rule (Daina and Zoete, 2017; Nagasundaram *et al*., 2022; Veber *et al*., 2002). The structure of the synthesized compounds was submitted to SwissADME tools so as to arrange into canonical simplified molecular input line entry system (SMILE). This helps to estimate in silico pharmacokinetics, toxicities and other properties of the compounds (Naz and Ul-Haq, 2020). The physicochemical properties, pharmacokinetics and drug likeness of the synthesized azo dyes were estimated using ADME descriptors by SwissADME (http://www.swissadme.ch) and PreADMET (https://preadmet.webservice.bmdrc.org/adme/) online servers. The organ toxicities and toxicological endpoints of the ligands and their LD_{50} were predicted using ProTox-II (https://tox-new.charite.de/protox_II).

3.10. DFT Studies

The Gaussian 09W with GaussView 6.0 programme was used to perform geometry optimisation. Incorporating density functional theory (DFT) and the B3LYP 6-31G(d, p) basis set was employed to generate optimised structure, molecular orbitals (MOs) and molecular electrostatic potential map (MEP) as per the reported method (Uzzaman *et al*., 2021). Global chemical reactivity has been calculated by analyzing molecular orbital features using following equations (Uzzaman *et al*., 2021);

$$\text{Gap } (\Delta E) = [\varepsilon LUMO - \varepsilon HOMO]; \eta = \frac{[\varepsilon LUMO - \varepsilon HOMO]}{2}; \; S = \frac{1}{\eta}; \mu = \frac{[\varepsilon LUMO + \varepsilon HOMO]}{2};$$

$$\chi = -\frac{[\varepsilon LUMO + \varepsilon HOMO]}{2}; \quad \omega = \frac{\mu^2}{2\eta}$$

4. Result and Discussion

4.1 Synthesis of the compounds

As shown in Scheme 24, heterocyclic dye derivatives incorporated with 1,3,4-thiadiazole moiety were fruit fully synthesized through the conventional diazotization followed coupling reaction. On one hand, 5-(4-dimethylamino-phenyl)-1,3,4,-thiadiazole-2-amine was prepared from 4-dimethylaminobenzaldehyde and thiosemicarbazide in the the presence of 0.5 mL HCl in EtOH followed treatment with ferric chloride in distilled water. The precipitated solid was washed and recrystallized from ethanol followed coupling with phenol, 1-napnthol and 2-napnthol at 0-5 °C to give compounds **132-134**. On the other hand, 5-phenyl-1,3,4-thiadiazole-2-amine derivative was prepared from 4-aminobenzoic acid in the presence of 0.5 mL of concentrated sulphuric acid in ethanol under reflux with continuous stirring at 50-60 °C for 5-8h. The purified solid was treated with coupling agent's phenol, 1-naphthol and 2-naphthol at 0-5 °C, to afford compound **135-137**. The physical parameter and percentage yield of the synthesized compounds was depicted in Table 1.

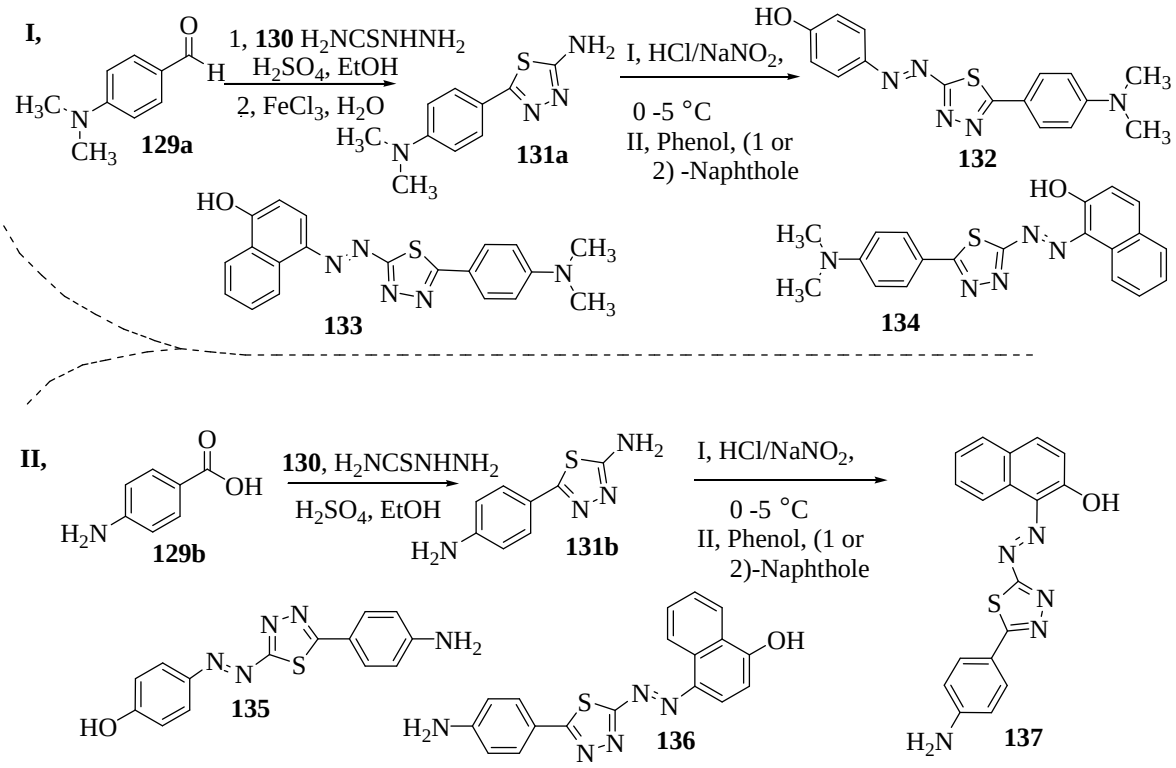

Scheme 25: General synthesis route of compounds **132-137**.

Table 1: Physical properties and yield of the compounds.

Compound	Molecular formula	Observed color	Retention factor PE: EtOAc	Melting point (°C)	Percentage yield %
131a	$C_{10}H_{12}N_4S$	Yellow	0.49	150-151	90
131b	$C_8H_8N_4S$	White	0.54	168-169	89
132	$C_{16}H_{15}N_5OS$	Orange	0.51	178-179	67
133	$C_{20}H_{17}N_5OS$	Olive	0.54	89-90	73
134	$C_{20}H_{17}N_5OS$	golden	0.62	93-94	69
135	$C_{14}H_{11}N_5OS$	Pecan brown	0.71	135-136	56
136	$C_{18}H_{13}N_5OS$	Cherry red	0.65	119-120	71
137	$C_{18}H_{13}N_5OS$	Candy apple red	0.78	92-93	82

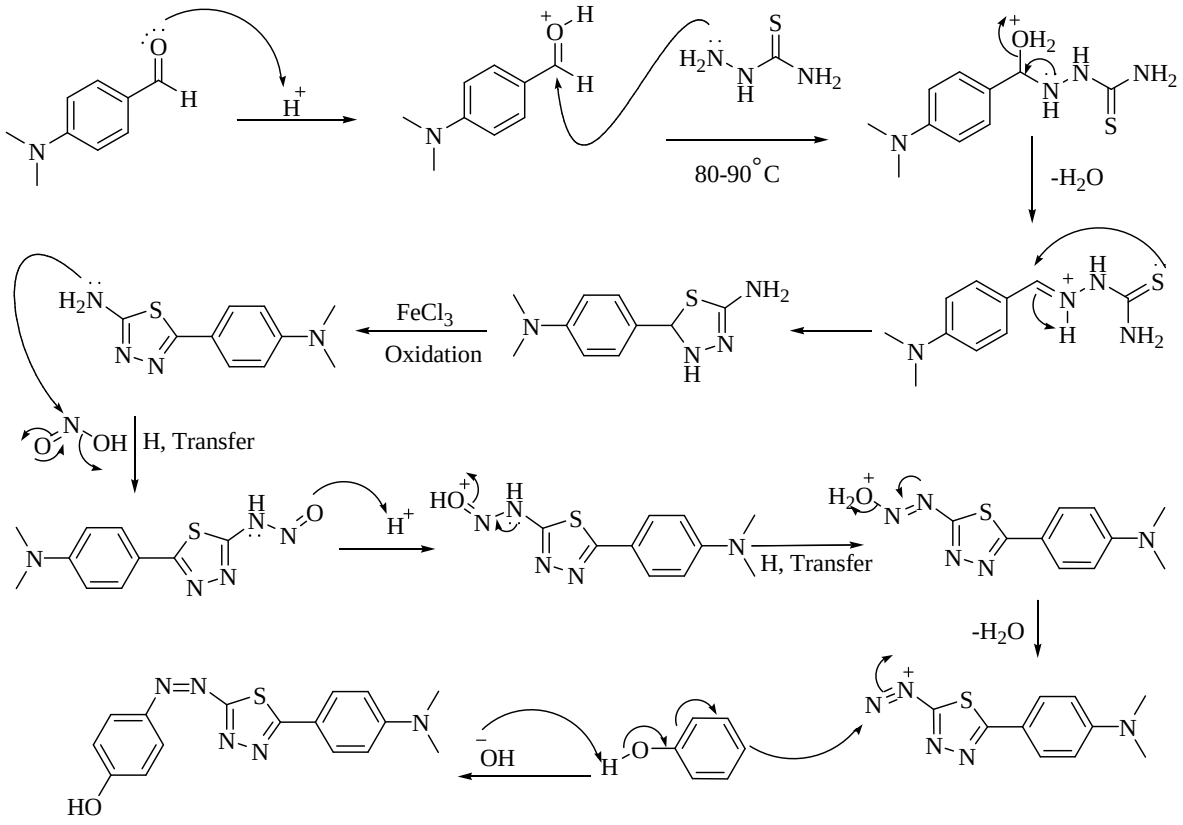

Scheme 26: A plausible mechanism of the synthesis of azo dye derivatives using phenol (**132-137**).

4.2 Characterization of the synthesized compounds

4.2.1 Characterization of compound 131a

Compound **131a** was obtained as a yellow solid with melting point of 150-151 °C and 90 % yield. TLC showed a spot at R*f* = 0.49 using petroleum ether: ethyl acetate (7:3), visualized under UV lamp at 254 and 365 nm. The IR spectrum ((KBr) υ_{max}/cm^{-1}) (Appendix 1) of compound **131a** displayed a fermi doublet (-NH_2) at 3370-3272 cm^{-1} and an intense band of aromatic carbon (-CH) at 3137 cm^{-1} along with sharp band (C=N) at 1615 and 1525 cm^{-1}. The ^{1}H-NMR (DMSO-d_6, 400 MHz) (Appendix 2) of compound **131a** showed the presence of AA'XX' spin system of *para*-substituted phenyl ring at δ 7.66 (1H, d, *J* = 8 Hz, H-1, 5) and 6.91 (1H, d, *J* = 8 Hz, H-2, 4). The singlet peaks at δ 8.0 (2H, s, NH_2) and 2.99 (6H, s, H-9, 10) confirms the presence of amine protons and methyl protons respectively. The ^{13}C-NMR (DMSO-d_6, 100 MHz) (Appendix 3) displayed the presence of seven types of carbons at δ_C 177.7 (C-8), 150.0 (C-3), 128.8 (C-7), 130.0(C-1, 5), 125.0 (C-2, 4), 115.0 (C-6) and 41.7 (C-9, 10). The ^{13}C NMR spectrum with the aid of Dept-135 (Appendix 4) of the compound confirmed the presence of three carbons with one

impurity that have proton. Thus, according to the above result and explanations the proposed compound is in agreement with the spectral data.

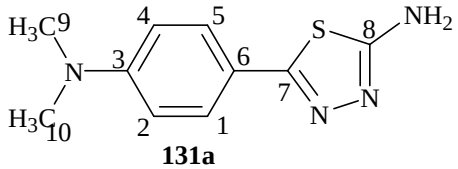

131a

4.2.2 Characterization of compound 131b

Compound **131b** was obtained as a white solid with melting point of 168-169 °C and 89 % yield. TLC showed a spot at R*f* = 0.54 using petroleum ether: ethyl acetate (7:3), visualized under UV lamp at 254 nm. The IR spectrum ((KBr) υ_{max}/cm^{-1}) (Appendix 5) of compound **131b** displayed two fermi doublets (-NH_2) at 3417-3371 and 3268-3236 cm^{-1} with sharp band of aromatic carbon (-CH) at 3133 cm^{-1} together with two sharp bands (C=N) at 1591 and 1507 cm^{-1}. The ^{1}H-NMR (DMSO-d_6, 400 MHz) (Appendix 6) of compound **131b** showed the presence of AA'XX' spin system of *para*-substituted phenyl ring at δ 8.12 (1H, m, H-1, 5) and 7.05 (1H, m, H-2, 4). Moreover, the singlet peaks at δ 6.45 (2H, s, NH_2) and 4.65 (2H, s, NH_2) confirms the presence of amine protons connected with C-8 and C-3 respectively. The ^{13}C-NMR (DMSO-d_6, 100 MHz) (Appendix 7) displayed the presence of six types of carbons at δ_C 166.4 (C-8), 153.9 (C-3), 131.5 (C-1, 5), 116.5 (C-7), 113.1 (C-2, 4) and 113.4 (C-6). The ^{13}C NMR spectrum with the aid of Dept-135 (Appendix 8) of the compound confirmed the presence of two carbons which have proton. Thus, according to the above result and explanations the proposed compound is in agreement with the spectral data.

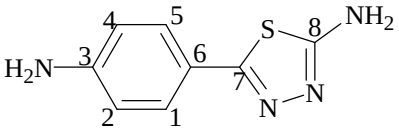

131b

4.2.3 Characterization of compound 132

Compound **132** was obtained as an orange solid with melting point of 178-179 °C and 67 % yield. TLC showed a spot at R*f* = 0.51 using petroleum ether: ethyl acetate (7:3), visualized under UV lamp at 254 nm. The UV-Vis spectrum (MeOH) (Appendix 9) of the compound **132** displayed an absorption band with λ_{max} at 362 nm which results excitation of stable electrons to higher energy state, π-π* transition level. The ^{1}H-NMR (DMSO-d_6, 400 MHz) (Appendix 10) of compound **132** showed the presence of two AA'XX' spin system of the *para*-substituted phenyl rings at δ 7.58 (1H, d, *J* = 8 Hz, H-1, 5), 6.75 (1H, d, *J* = 8 Hz, H-12, 16), 7.99 (1H, m, H-2, 4) and 7.78 (1H, m, H-13, 15). Moreover, the

singlet peak at δ 8.95 (1H, s, OH) and 3.79 (6H, s, H-9, 10) confirm presence of hydroxyl and methyl protons. The ^{13}C-NMR (DMSO-d_6, 100 MHz) (Appendix 11) displayed the presence of carbon at δ_C 180.1 (C-8) , 157.4 (C-14), 153.9 (C-3), 145.6 (C-12, 16), 131.9 (C-1, 5), 137.1 (C-11), 127.6 (C-7),125.6 (C-6), 115.7 (C-2, 4), 114.2 (C-13, 15) and 43.5 (C-9, 10). The ^{13}C NMR spectrum with the aid of Dept-135 (Appendix 12) of the compound confirmed the presence of five carbons which have proton. Thus, according to the above result and explanations the proposed compound **132** is in agreement with the spectral data.

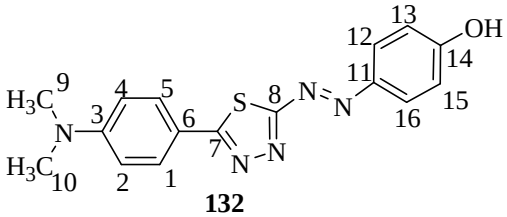

132

4.2.4 Characterization of compound 133

Compound **133** was obtained as olive solid with melting point of 89-90 °C and 73 % yield. TLC showed a spot at R*f* = 0.54 using petroleum ether: ethyl acetate (7:3), visualized under UV lamp at 254 nm. The UV-Vis spectrum (MeOH) (Appendix 13) of the compound displayed an absorption band with λ_{max} at 355 nm that causes excitation of stable electrons to higher energy from π-π* transition level. The ^{1}H-NMR (DMSO-d_6, 400 MHz) (Appendix 14) of compound **133** showed the presence of AA'XX' spin system of the *para* substituted phenyl ring at δ 8.37 (1H, d, *J* = 8 Hz, H-1, 5) and 7.48 (1H, d, *J* = 8 Hz, H-2, 4) together with the presence of six methyl protons at δ 3.74 (6H, s, H-9, 10). In addition the presence of AA'BB' spin system fused with substituted benzene clearly indicated at δ 8.78 (1H, dd, H-19), 8.73 (1H, dd, H-16), 8.55 (1H, ddd, H-18), 8.06 (1H, d, *J* = 7 Hz, H-12) and 7.87 (1H, d, *J* = 6 Hz, H-13). The peak at δ 8.21 (1H, s) displayed the hydroxyl proton. The ^{13}C NMR (DMSO, 100 MHz)(Appendix 15) displayed the presence of carbon at δ_C 177.4 (C-8), 151.8 (C-3), 143.9 (C-19), 129.1 (C-1, 5), 127.9 (16), 127.4 (C-7), 124.4 (C-20, 121.8 (C-20), 112.5 (C-15), 112.4 (C-12), 112.1 (C-2, 4), 111.5 (C-13) and 40.2 (C-9, 10). The ^{13}C NMR spectrum with the aid of Dept-135 (Appendix 16) of the compound confirmed the presence of nine carbons which have proton. Thus, according to the above result and explanations the proposed compound **133** is in agreement with the spectral data.

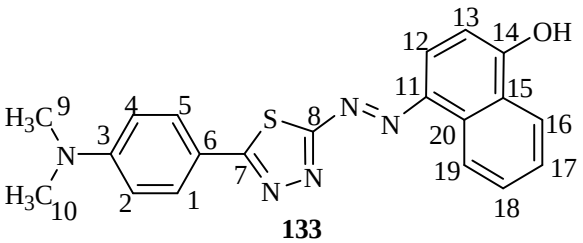

133

4.2.5 Characterization of compound 134

Compound **134** was obtained as a golden solid with melting point of 92-93 °C and 69 % yield. TLC showed a spot at R*f* = 0.62 using petroleum ether: ethyl acetate (7:3), visualized under UV lamp at 254nm. The UV-Vis spectrum (MeOH) (Appendix 17) of the compound displayed an absorption band with λ_{max} at 356 nm which results excitation of stable electrons to higher energy from π-π* transition level. The ^{1}H-NMR (DMSO-d_6, 400 MHz) (Appendix 18) of compound **134** showed the presence of AA'XX' spin system of the *para* substituted phenyl ring at δ 7.79 (1H, dd, *J* = 6, 12 Hz, H-1, 5) and 6.89 (1H, d, *J* = 6 Hz, 2, 4) with singlet peak at δ 3.71 (6H, s, H-9, 10) which confirm the presence of six methyl protons. Further, the presence of AA'BB' spin system fused with substituted benzene is displayed at δ 8.22 (1H, dd, H-19), 7.98 (1H, dd, H-16), 7.83 (1H, ddd, H-18), 6.96 (1H, d, H-12) and 6.93 (1H, d, H-13). The singlet peak at δ 8.16 (1H, s) is evident for the presence of hydroxyl proton. The ^{13}C NMR (DMSO-d_6, 400 MHz) (Appendix 19) of the compound showed the presence of carbon at δ_C 177.4 (C-8), 157.5 (C-12), 151.8 (C-3), 143.9 (C-19), 129.8 (C-1,5), 129.1(C-14), 128.0 (C-20), 127.5 (C-16), 126.4 (C-18), 123.0 (C-15) , 121.8 (C-7), 114.8 (C-11), 112.7 (C-6), 112.4 (C-17), 112.1 (C-2, 4), 111.4 (C-13) and 40.2 (C-9, 10). The ^{13}C NMR spectrum with the aid of Dept-135 (Appendix 20) confirmed the presence of nine carbons that have proton. Thus, the proposed structure of compound **134** is in agreement with the spectral data.

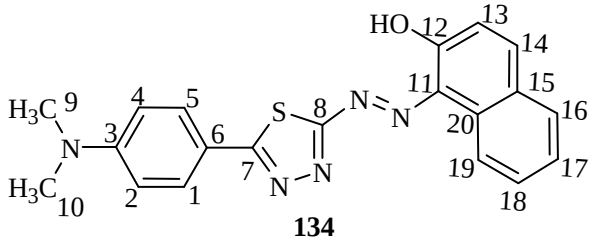

134

4.2.6 Characterization of compound 135

Compound **135** was obtained as a pecan brown solid with melting point of 219-220 °C and 56 % yield. TLC showed a spot at R*f* = 0.71 using petroleum ether: ethyl acetate (7:3), visualized under UV lamp at 254 nm. The UV-Vis spectrum (MeOH) (Appendix 21) of compound **135** displayed an absorption band with λ_{max} at 362 nm which results excitation

of stable electrons to higher energy from π-π* and n-π* transition level. The ^{1}H-NMR ($CDCl_3$, 400 MHz) (Appendix 22) of the compound showed the absence of proton peak from δ 9.5 to 12 indicate that the complete conversion of the 4-aminobenzoic acid. The peaks at δ 8.20 (1H, m, H-1, 5) and 7.01 (1H, m, H-10, 14), 7.92 (1H, d, *J*= 8 Hz, H-2, 4) and 7.91 (1H, d, *J* = 8 Hz, H-11, 13) confirm presence of two AA'XX' spin system of the *para*-substituted phenyl ring. The singlet peak at δ 8.0 (1H, s) and 4.7 (2H, s) confirms the presence of hydroxyl and amine protons respectively. The ^{13}C-NMR ($CDCl_3$, 100 MHz) (Appendix 23) displayed the presence of carbon at δ_C 166.6 (C-8), 159.5 (C-12), 155.3 (C-3), 147.0 (C-9), 131.4 (C-7), 130.6 (C-1, 5), 125.5 (C-10, 14), 122.4 (C-11, 13) and 116.0 (C-2,4). The ^{13}C NMR spectrum with the aid of Dept-135 (Appendix 24) displayed the compound has four aromatic carbons (CH). Thus, the proposed structure of compound **135** is in agreement with the spectral data.

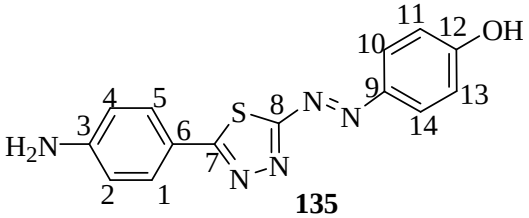

135

4.2.7 Characterization of compound 136

Compound **136** was obtained as a cherry red solid with melting point of 219-220 °C and 80 % yield. TLC showed a spot at R*f* = 0.65 using petroleum ether: ethyl acetate (7:3), visualized under UV lamp at 254 nm. The UV-Vis spectrum (MeOH) (Appendix 25) of the compound displayed an absorption band with λ_{max} at 463 nm which results excitation of stable electrons to higher energy from π-π* and n-π* transition level. The ^{1}H NMR ($CDCl_3$, 400 MHz) (Appendix 26) of the compound showed presence of AA'XX' spin system of the *para* substituted phenyl ring at δ 8.21 (1H, m, H-1, 5), 6.41 (1H, dd, *J* = 6, 12 Hz, H-2, 4). The presence of AA'BB' spin system fused with substituted benzene is confirmed at δ 7.88 (1H, m, H-17), 7.78 (1H, m, H-14) and 7.42 (1H, d, H-16). The singlet peaks at δ 4.15 (2H, s) confirmed the presence of amine proton connected to C-3. Thus, according to the above the proposed structure of compound **136** is in agreement with the spectral data.

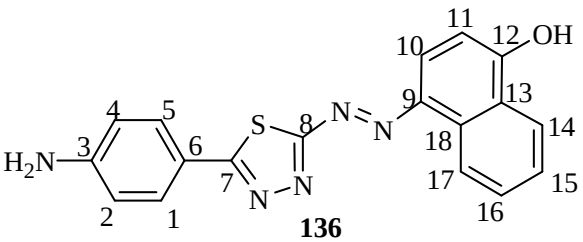

136

4.2.8 Characterization of compound 137

Compound **137** was obtained as a candy apple red solid with melting point of 92-93 °C and 82 % yield. TLC showed a spot at R*f* = 0.78 using petroleum ether: ethyl acetate (7:3), visualized under UV lamp at 254 nm. The UV-Vis spectrum (MeOH) (Appendix 27) of the compound showed an absorption band with λ_{max} at 481 nm that causes excitation of stable electrons to higher energy, π-π* and n-π* transition level. The 1H-NMR ($CDCl_3$, 400 MHz) (Appendix 28) of compound **137** displayed the presence of AA'XX' spin system of para-substituted of the phenyl ring at δ 8.43 (1H, d, *J* = 8 Hz, H-1, 5) and 7.64 (1H, m, H-2, 4). The presence of AA'BB' spin system fused with sustituted benzene ring is diplayed at δ 8.13 (1H,dd, H-17), 8.12 (1H, dd, H-14), 7.56 (1H, ddd, H-16) 7.54 (1H, ddd, H-15), 7.51 (1H, d, H-12) and 7.41 (1H, d, H-11). The singlet peaks at δ 7.55 (1H, s) and 6.74 (2H, s) showed the presence of aromatic hydroxyl and amine protons connected to C-10 and C-3 respectively. The ^{13}C NMR ($CDCl_3$, 100 MHz) (Appendix 29) showed the presence of different types of carbon at δ 178.0 (C-10), 166.0 (C-8), 146.6 (C-3), 142.3 (C-12), 133.3 (C-18), 131.3 (C-1, 5), 131.0 (C-13), 129.42 (C-2, 4), 128.91 (C-17), 128.3 (C-6), 127.6 (C-7), 126.7 (C-11), 126.1 (C-14), 122.1 (C-16) and 116.8 (C-15). The ^{13}C NMR spectrum with the aid of Dept-135 (Appendix 30) of the compound confirm for the presence of only eight carbons which have proton. Thus, the proposed structure of compound **137** is in agreement with the spectral data.

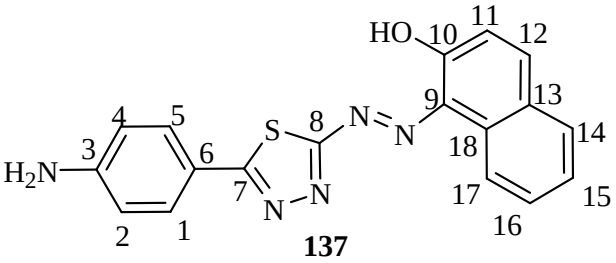

137

4.3 Color Fastness

As shown in Table 2, washing fastness of the dyed cotton fabrics were revealed that all the dyes have poor to excellent fastness in the range of 2-5 gray scale. All the tasted compounds were revealed excellent staining against acrylic, wool and polyester. This indicate that, absence of color staining effect while washing of cotton fabric dyed with these dyes in the presence of acrylic, wool and polyester fabrics. Compound **132, 136** and **137** were shown excellent color staining. However, the rating for change in shade shown that, all the compounds were exhibited poor to good fastness to washing ranges 2-4 gray scale. On the other hand, all the tested dyes except compound **132** were revealed excellent dry and wet fastness to rubbing. This infers, absence of color staining while rubbing the dyed cotton fabric with other cloths. Thus, color staining of washing fastness indicate, that

these dyes are fruit full to apply on nylon fabric. The result is in agreement with the absorption spectra of the synthesized compounds which infer compound **136** and **137** are responsible as potential coloring compounds.

Table 2: Washing and rubbing fastness rating for dyed cotton fabric.

Samples	Washing fastness							Rubbing fastness	
	Change in shade	Color staining						Staining	
		DA	C	N	P	A	W	Dry	Wet
132	4	4/5	4/5	4/5	5	5	4/5	5	5
133	3	4/5	5	4	5	5	4/5	4	4
134	2	4	4/5	3	5	5	4/5	5	4/5
135	2	4/5	4	3/4	5	5	4/5	5	5
136	5	5	5	5	5	5	4/5	5	5
137	4/5	4/5	5	5	5	5	4/5	5	5

Notice: DA-diacetate, C-cotton, N-nylon, P-polyester, A-acrylic, W-wool

Figure 11: The washing fastness test of the compounds (**132-137**).

4.4 Antimicrobial Activity

The antimicrobial activity of the newly synthesized compounds were reported as minimum inhibitory concentration (Tropp *et al.*, 2020) against six bacterial strains *(S.aureus, S.epidermid, E.faecalis, Ecoli, K.pnemonia, S.typorumium)* and three fungal stains *(C.albicans, T.mentographytes, T.rumbrum)* along with the reference drug ciprofloxacin and ketoconazole respectively (Table 3). Among the tested compounds, compound **136**

and **137** exhibited good antimicrobial activities against all bacterial and fungal strains, but compound **133** and **134** have the lowest antibacterial and antifungal activities against all strains. Compound **137** has displayed a good antibacterial activity against *E.faecalis and E.coli* with MIC (0.5 mg/ml) relative to reference drug ciprofloxacin MIC (0.0005, 0.000125 mg/ml respectively) while compound **132, 136** and **137** were exhibited moderate to good antifungal activity against all species, especially to *T.rubrum* with MIC (0.5 mg/ml) relative to the MIC of the reference drug, ketoconazole 0.005 mg/ml. This, study showed that incorporation of phenol and naphthol as coupling agent enhances the activity of the synthesized compounds as described in (Govender *et al*., 2016).

Table 3: The antimicrobial activities (MIC in mg/ml) of the synthesized compounds.

Compounds	Antibacterial Activity						Antifungal Activity		
	S.aureus	*S. epidermids*	*E.faecalis*	*E.coli*	*K. pneumonae*	*S. typorumium*	*C. albicans*	*T.mento graphytes*	*T.rubrum*
132	8	4	4	8	8	8	8	2	2
133	4	4	2	4	4	4	1	2	0.5
134	4	4	4	4	4	4	16	16	4
135	8	8	8	8	8	16	8	8	4
136	4	2	1	0.5	1	4	2	1	0.5
137	2	2	0.5	0.5	1	2	2	2	0.5
CP	0.00025	0.000125	0.0005	0.000125	0.000125	0.0005	-	-	-
KC	-	-	-	-	-	-	0.00125	0.0005	0.005
5 % T 80	-	-	-	-	-	-	-	-	-

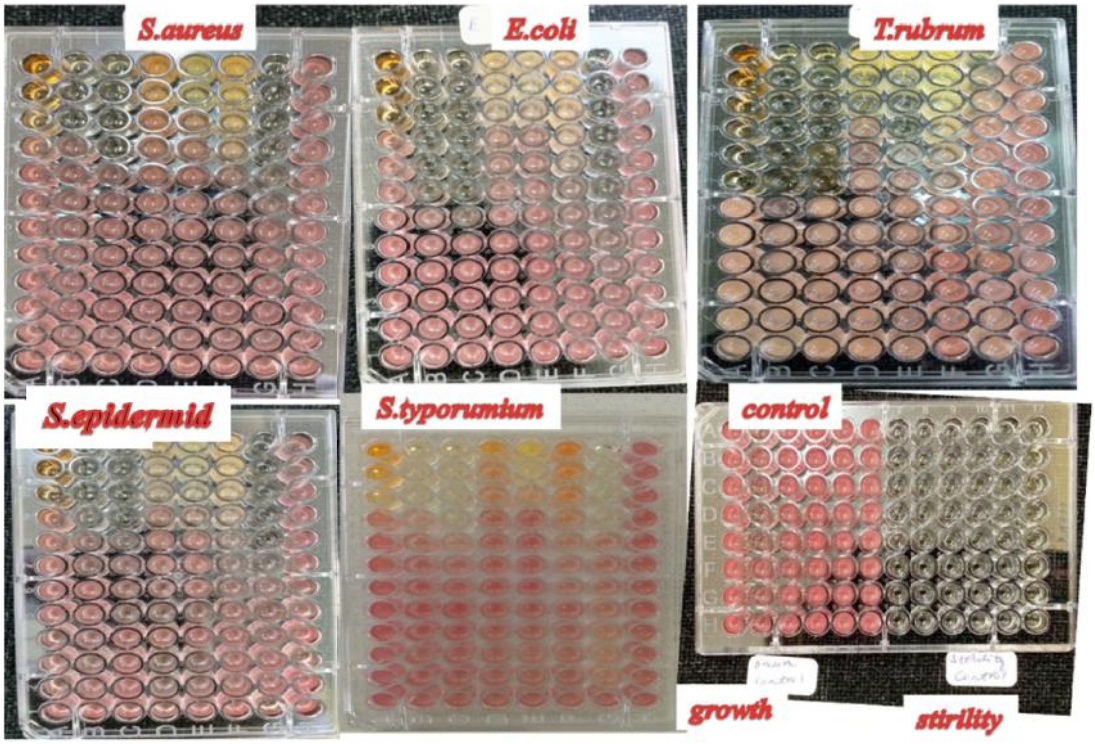

Figure 12: Antimicrobial activities of the compounds (**132-137**).

4.5 Antioxidant Activity

DPPH assay was employed to determine radical scavenging activity of the synthesized compounds (**132-137**) relative to the reference drug ascorbic acid. The radical scavenging activity of the synthesized compounds was recorded as per their potential to react with the stable DPPH radical species (Zeb *et al*., 2020). The DPPH scavenging activity of the compounds was linearly increased along with the concentration of each compound. Among of all tested, most of the compounds were exhibited significant percentage of radical scavenging activity at all concentration, especially at 1000 µg/ml. Compound **132** and **133** exhibited excellent radical scavenging activity at 1000 µg/ml together with IC_{50} (14.7 and 10.7 µg/ml), respectively compared to the radical scavenging activity (98.72±0.17) ascorbic acid along with IC_{50} (9.6 µg/ml), even though the rest of the compounds have poor to moderate activities (Table 4). So, compound **132** and **133** explored promising antioxidant activity, of all the synthesized compounds. The significant and potential activity of the compounds could be due to the presence of hydroxyl group that displays the ability to eliminate the free radical species (Zeb *et al*, 2020).

Table 4: The radical scavenging activity (%) of the synthesized compounds.

Conc. (µg/ml)	**132**	**133**	**134**	**135**	**136**	**137**	A.A

62.5	43.21± 0.01	44.31± 0.03	44.34± 0.32	35.11± 0.12	28.82± 0.45	35.22± 0.12	37.97± 0.15
125	49.11± 0.11	48.51± 0.12	55.30± 0.14	55.12± 0.01	45.44± 0.56	40.21± 0.14	56.±0.32
250	77.23± 0.13	76.31± 0.15	65.41± 0.21	70.14± 0.31	60.54± 0.02	55.34± 0.11	77.55± 0.18
500	86.22± 0.22	87.51± 0.05	87.35± 0.22	80.67± 0.22	65.17± 0.17	65.1± 0.03	88.31± 0.2
1000	97.50± 0.30	97.56± 0.11	97.41± 0.21	93.83± 0.16	85.34± 0.18	75.53± 0.13	98.72± 0.17
IC_{50}	14.7	10.7	21.4	82.9	260.4	289.6	9.6

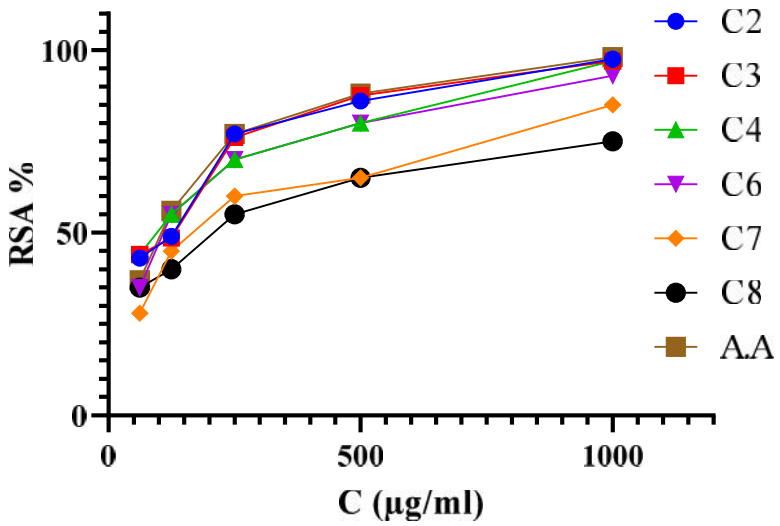

Figure 13: Radical scavenging activity (%) of the synthesized compounds.

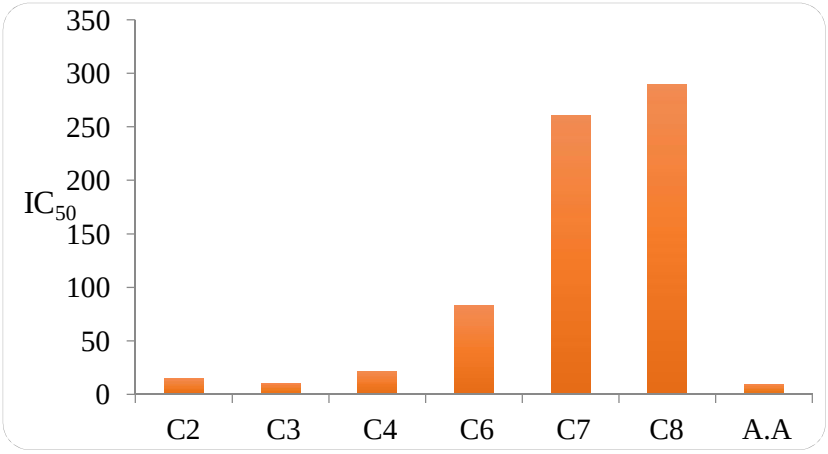

Figure 14: IC_{50} of the synthesized compounds (**132-137**).

4.6 *In silico* Molecular Docking Analysis

4.6.1 Molecular Docking with DNA gyrase B

DNA gyrase is a topoisomerase type enzyme that is required during bacterial DNA replication and transcription to maintain topology and integrity. It consists of four subunits (two A subunits and two B subunits) attached together to form a tetrameric holoenzyme (Janupally *et al*., 2015). Currently, DNA gyrase is considered one of the primary targets and has been clinically validated in most pathogenic bacteria (Narramore and Fishwick, 2019).

In this study *E. coli* DNA gyrase B (PDB ID: 6F86) was used as a target and a fluroquinolone class of antibacterials, ciprofloxacin was used as a reference control for docking with the target. Binding affinity and interactions with different amino acids are presented in the Table 4, and the (3D and 2D) binding interactions are depicted in (Figure 13). Compound **136** showed highest binding affinity (-8.0 kcal/mol) among the tested relative to the standard drug followed by **137** (-7.8 kcal/mol). Compound **132** showed similar binding affinity that of Ciprofloxacin (-7.3 kcal/mol). Ciprofloxacin formed hydrogen bonding interactions with Asn-46 and Asp-73. Similarly, the azo nitrogen of compound **134-137** showed H-bonding interactions only with Asn-46 except **134**, in which both azo nitrogen and phenolic hydroxyl groups showed H-bonding with Asn-46. Whereas, the phenolic hydroxyl group of **132** and **133** showed interaction with Asp-73; **135** and **136** with Val-97. The test compounds also showed H-bonding with other amino acids as shown in (Table 5 and Figure 13). Most of the test compounds showed residual interactions with Ile-78, Arg-76, Pro-79, Ile-94.

Table 5: Binding affinity and interaction with the compounds (**132-137**) against *E. coli* DNA gyrase B.

Cpds	Affinity (kcal/mol)	H-bond	Residual Amino acid Interactions	
			Hydrophobic/Pi-Cation/Pi-Anion/ Pi-Alkyl interactions	Van-der Walls interactions
132	-7.3	Asp-73, Thr-165, Gly-77	Glu-50, Ile-78	-
133	-6.9	Asp-73	Glu-50, Ile-78, Arg-76, Asn-46	Ala-47

134	-7.0	Asn-46	Glu-50, Ile-78, Arg-76, Pro-79	-
135	-7.5	Asn-46, Asp-73, Val-97, Thr-165	Ile-78, Ile-94	Ala-47
136	-8.0	Asn-46, Asp-73, Val-97, Thr-165	Ile-78, Ile-94	Ala-47
137	-7.8	Asn-46, Asp-73, Thr-165	Ile-78, Ile-94	Ala-47
CP	-7.3	Asn-46, Asp-73, Asp-49*	Pro-79, Asn-46, Asp-49	Ala-47, Gly-77, Glu-50, Arg-76, Ile-78

*Carbon Hydrogen bond

No.	3D	2D
132	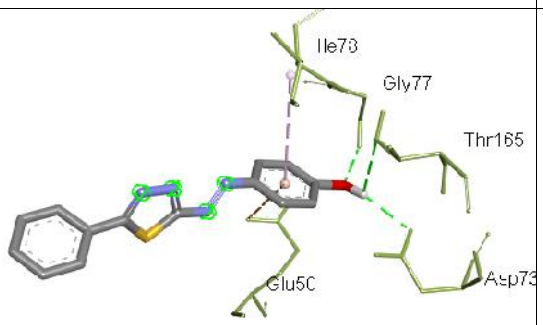	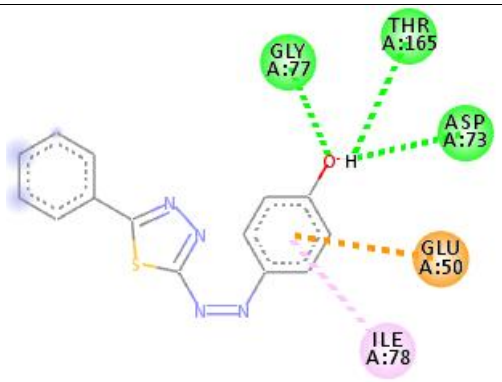
133	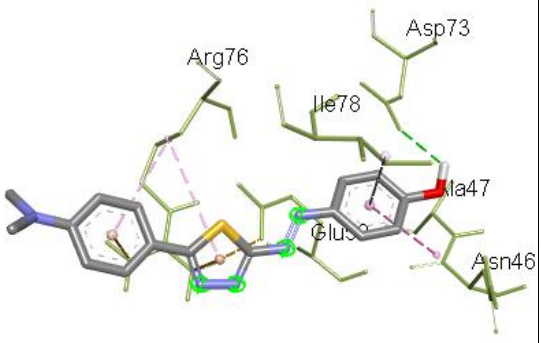	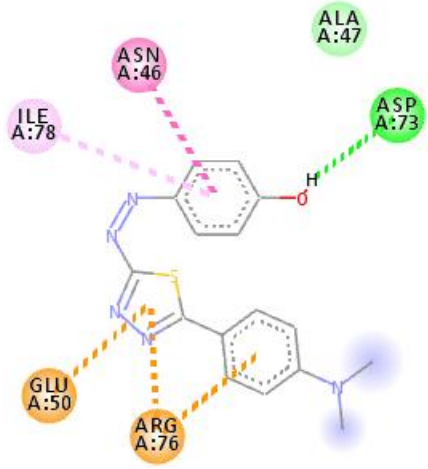

134	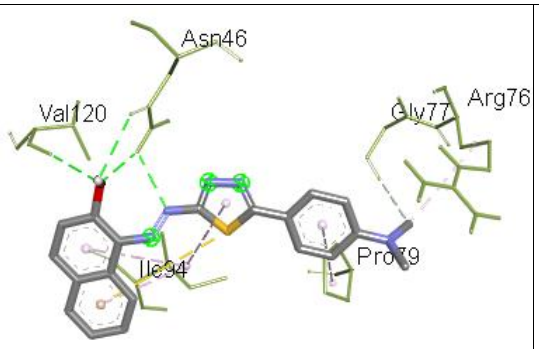	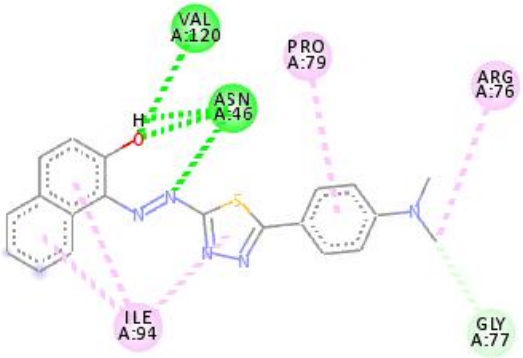
135	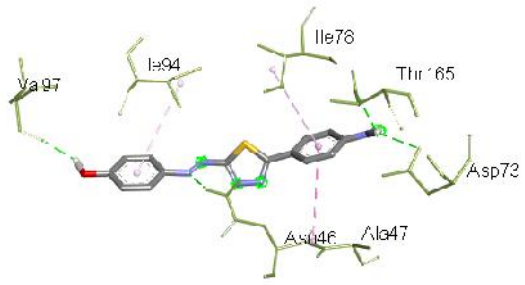	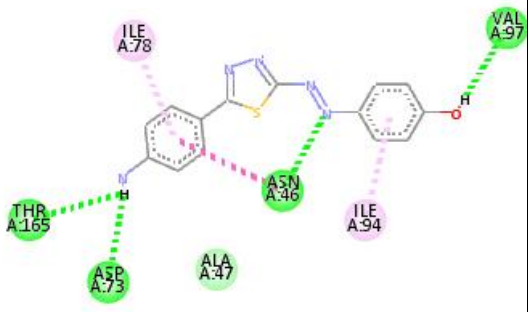
136	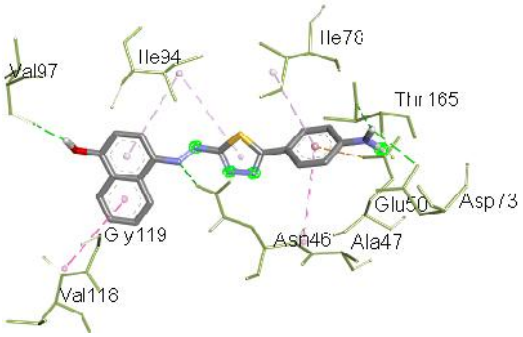	
137	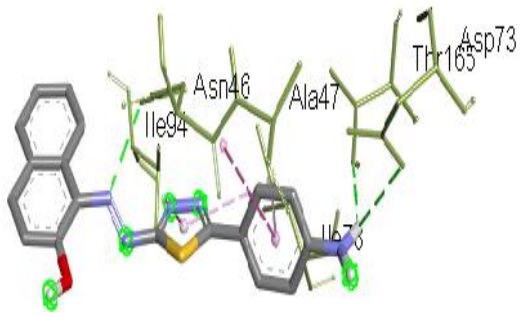	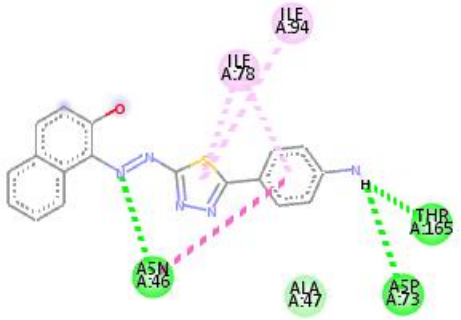

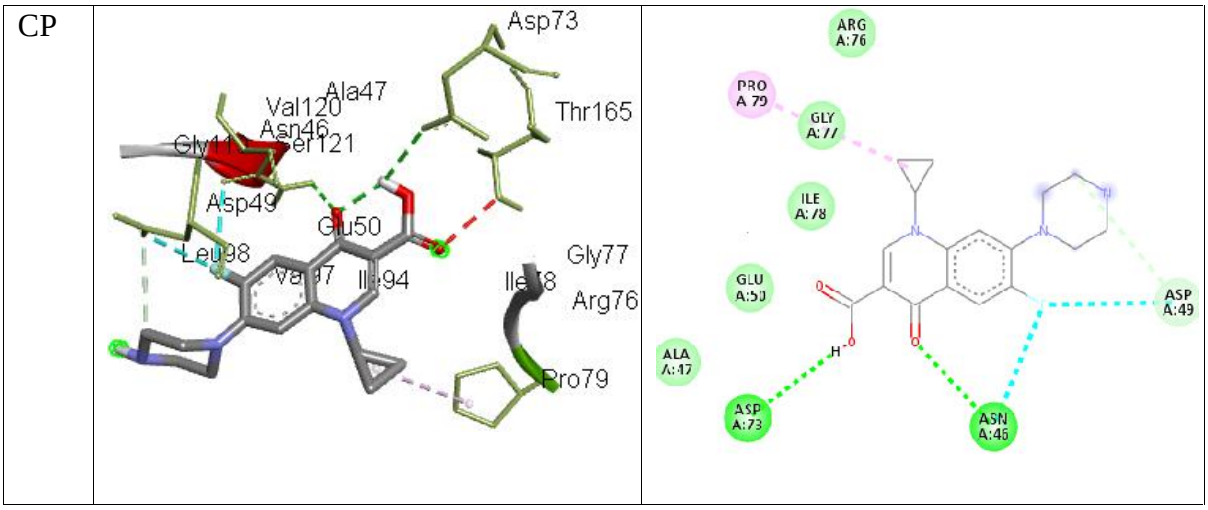

Figure 15: Binding interactions (3D & 2D) of the synthesized and standard compounds against *E. coli* DNA gyrase B.

4.6.2 Molecular Docking with *S. aureus* Pyruvate kinase

Pyruvate kinase (PK) has been identified as a crucial enzyme in staphylococci, and regulates their growth, antibiotic resistance, and biofilm formation (Vasu *et al*., 2015). Furthermore, it was found to be structurally distinct from human homologs, and hence it provides a promising target for novel antimicrobial agents (Akunuri *et al*., 2022). For the docking studies, *S. aureus* PK (PDB ID: 3T07) was used as a target and ciprofloxacin was used as reference drug. Binding affinity and interactions with different amino acids are presented in (Table 6), and the (3D and 2D) binding interactions are depicted in (Figure 14). The highest binding affinity was shown by **134** and **137** (-6.1 kcal/mole) followed by **136** (-5.7 kcal/mole). All the test compounds showed higher binding affinity than the standard ciprofloxacin (-4.9 kcal/mole), which exhibited H-bonding interactions with Ser-362, Thr-366, Asn-369. Similarly, the test compounds showed H-bonding interaction with one or two of these amino acids. In all the tested compounds, nitrogens of the thiadiazole ring and /or phenolic hydroxylic group involved in these H-bonding interaction. The azo nitrogens of **135** involved in the H-bonding interaction with Asn-369. Ciprofloxacin showed residual interaction with Ile-361, while the test compounds had interactions with Ile-361, His-365, along with additional amino acids.

Table 6**:** Binding affinity and interaction of the compounds (**132-137**) with the target *S. aureus* PK.

Compound	Affinity (kcal/mol)	H-bond	Residual Amino acid Interactions	
			Hydrophobic/Pi-	Van-der Walls

			Cation/Pi-Anion/ Pi-Alkyl interactions	interactions
132	-5.2	Ser-362, Thr-366	Ile-361, His-365, Ala-358	-
133	-5.3	Ser-362	Ile-361, His-365	-
144	-6.1	Ser-362, Thr-366	Ile-361, His-365, Ala-358	-
135	-5.1	Ser-362	Ile-361, His-365, Ala-358	Thr-366
136	-5.7	Ser-362	Ile-361, His-365, Ala-358	-
137	-6.1	Ser-362, Thr-366, His-365*	Ile-361, Ala-358	-
CP	-4.9	Ser-362, Thr-366, Asn-369	Ile-361	-

*Carbon Hydrogen bond

No.	3D	2D
132	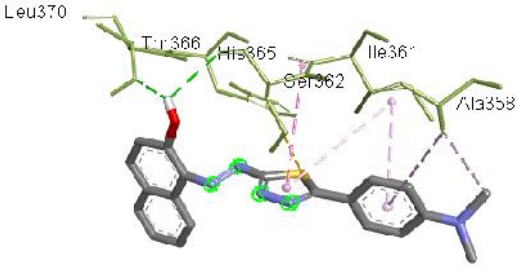	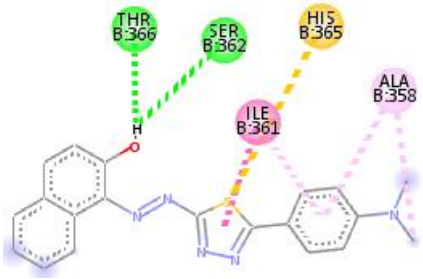
133	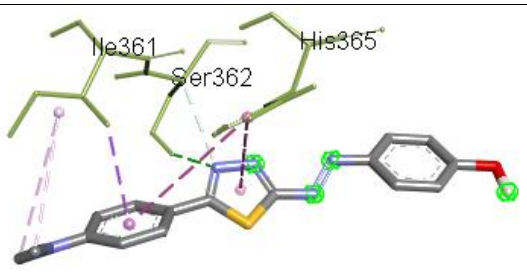	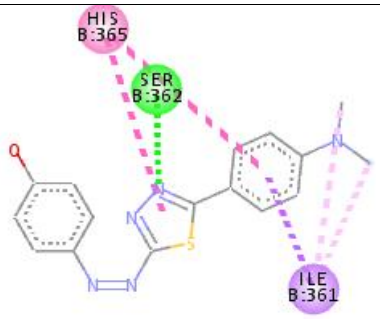

134	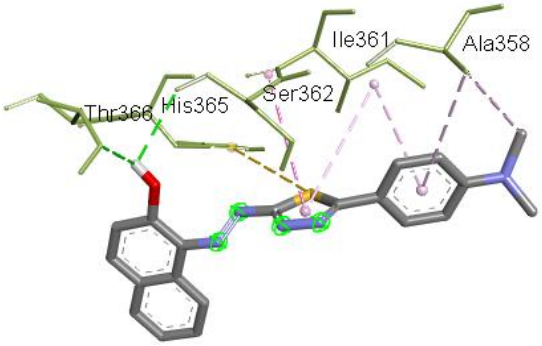	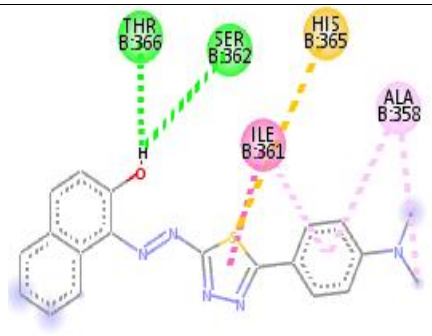
135	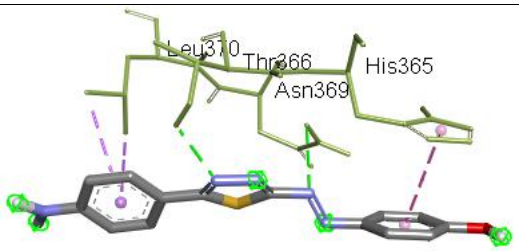	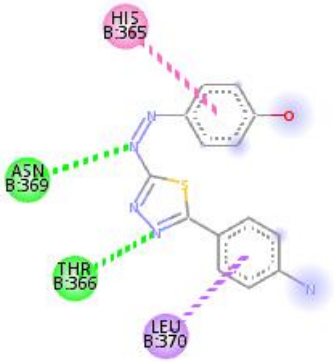
136	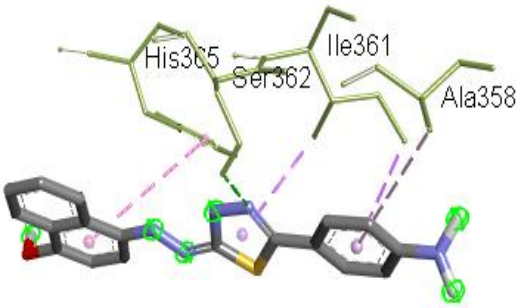	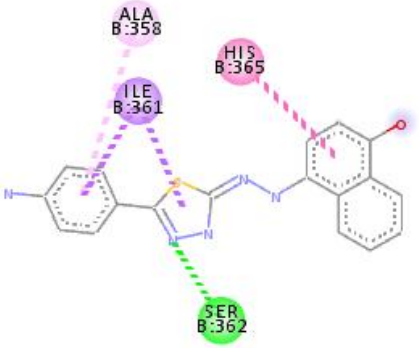
137	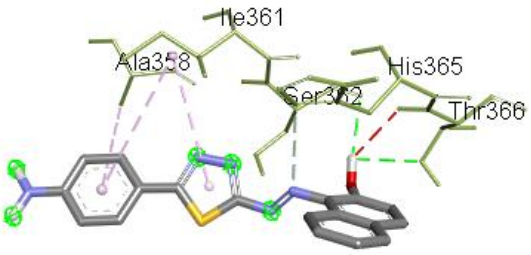	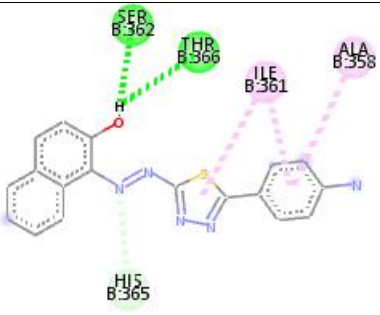

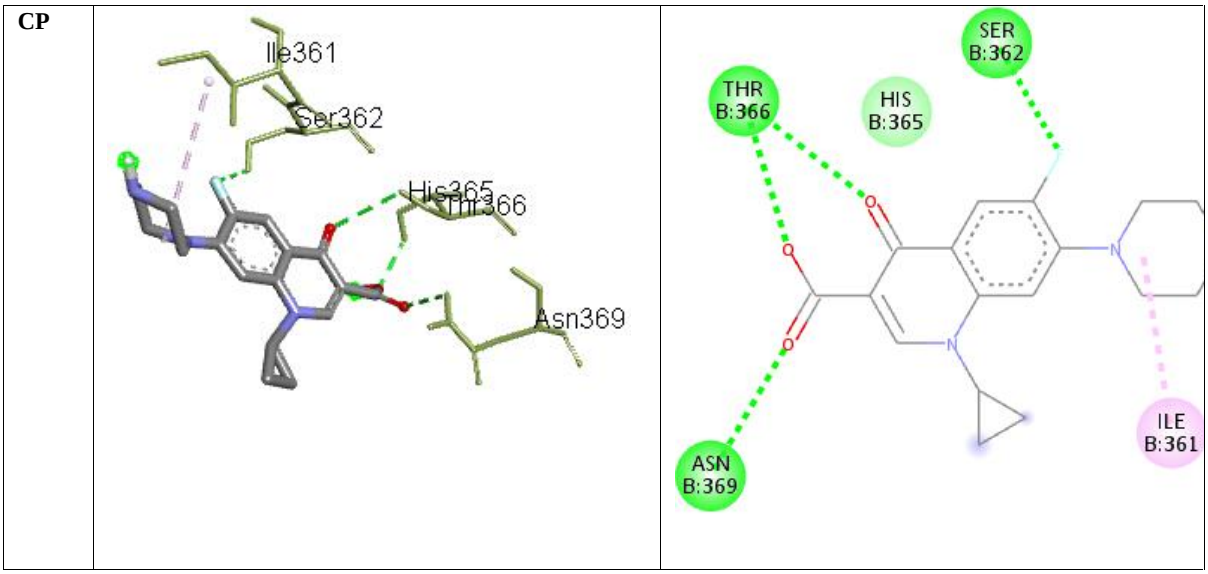

Figure 16: Binding interactions (3D & 2D) of synthesized and standard compounds with *S. aureus* PK.

4.6.3 Molecular docking with *Candida albican* CYP51

Candidiasis is a fungal infection caused by yeast called Candida. Some species of Candida can cause infection in people; the most common is *C. albicans*. Candida normally lives on skin and inside the body, such as the mouth, throat, gut, and vagina, without causing problems. In this study *C. albican* CYP51 (PDB ID: 5V5Z) was used as a target and the ketoconazole (KC) was used as reference control. Binding affinity and interactions with different amino acids are presented in (Table 7), and the (3D and 2D) binding interactions are depicted in (Figure 15). Compound **137** showed highest binding affinity (10.6 kcal/mole,) while, **134** exhibited equal binding affinity that of KC (10.2 kcal/mole). KC exhibited H-bonding interactions with His-377 and Ser-378. Among the test compounds, only **137** showed H-bonding interaction with Ser-378, whereas other compounds interacted with different amino acids in the binding sites. Most of the compounds showed residual interactions with Leu-376, Tyr-118, Met-508.

Table 7: Binding affinity and interaction the compounds (**132-137**) with the target *C. albican* CYP51

Compound	Affinity (kcal/mol)	H-bond	Residual Amino acid Interactions	
			Hydrophobic/Pi-Cation/Pi-Anion/ Pi-Alkyl interactions	Van-der Walls interactions
132	-8.6	Gly-65*	Leu-376, Tyr-118, Met-508, Leu-87	-

133	-8.7	Try-64, Ala-61, His-377*	Leu-376, Tyr-118, Met-508, Phe-380, Phe-233	-
134	-10.2	Tyr-505, Gly-65*, Met-508*	Leu-376, Tyr-118, Met-508, Phe-380, Phe-233, His-377, Pro-230, Ala-61	-
135	-8.4	Tyr-64, His-377*, Ser-378*	Leu-376, Tyr118, Phe-233, Pro-230	-
136	-10.1	Tyr-132	Tyr-118, Phe-380, Phe233, His-377, Pro-230, Tyr-122	-
137	-10.6	Ser-378	Phe-233, Pro-230, His-377, Met-508, Ala-61, Leu-88, Ile-231	-
KC	-10.2	His-377, Ser-378	Phe-233, Phe-380, Tyr-118, Tyr-132, Leu-376	Gly-307, Ile-379, Cys-470, Lys-143, Ile-131, Met-508

*Carbon Hydrogen bond

No.	3D	2D
132	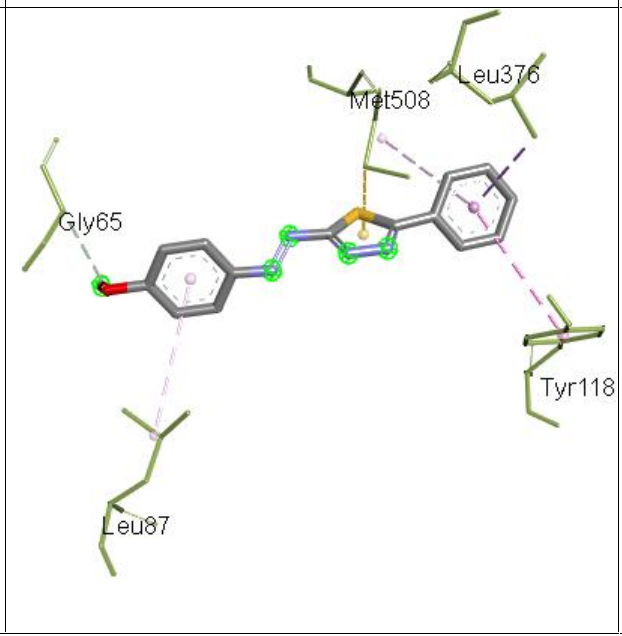	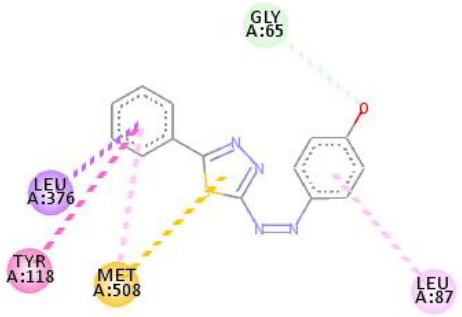

133	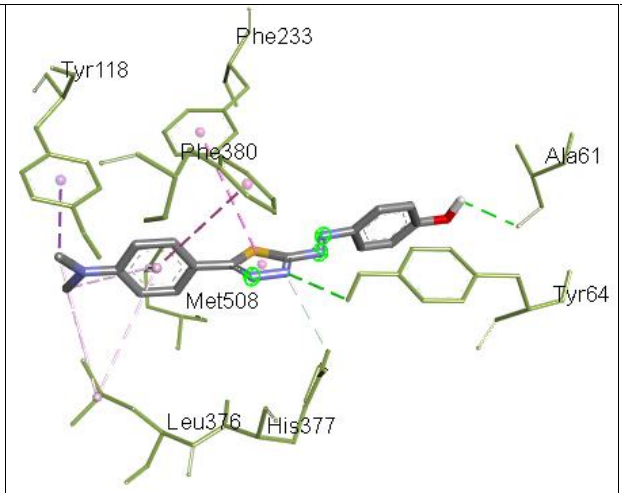 Phe233 Tyr118 Phe380 Ala61 Met508 Tyr64 Leu376 His377	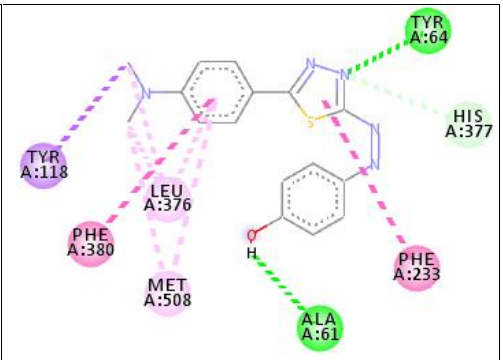 TYR A:64 HIS A:377 TYR A:118 LEU A:376 PHE A:380 PHE A:233 MET A:508 ALA A:61
134	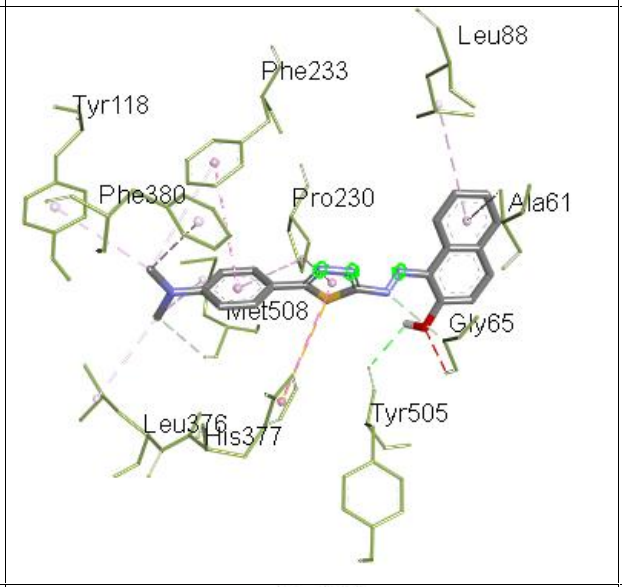 Leu88 Phe233 Tyr118 Phe380 Pro230 Ala61 Met508 Gly65 Leu376 His377 Tyr505	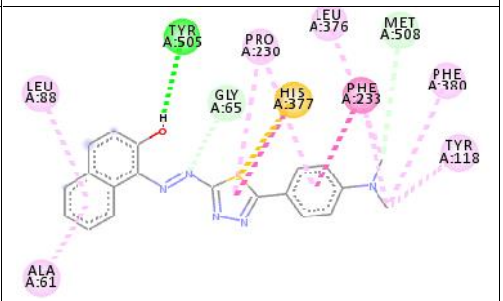 TYR A:505 PRO A:230 LEU A:376 MET A:508 LEU A:88 GLY A:65 HIS A:377 PHE A:233 PHE A:380 TYR A:118 ALA A:61
135	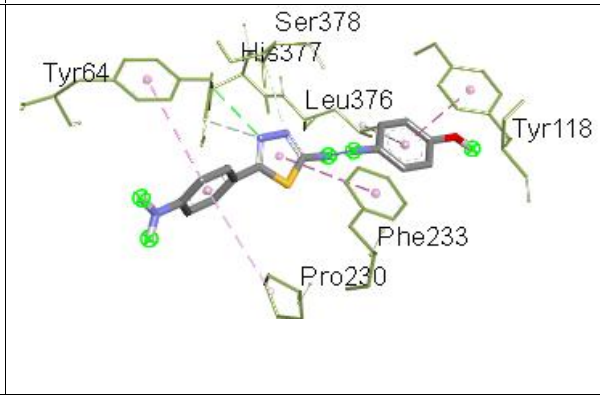 Ser378 His377 Tyr64 Leu376 Tyr118 Phe233 Pro230	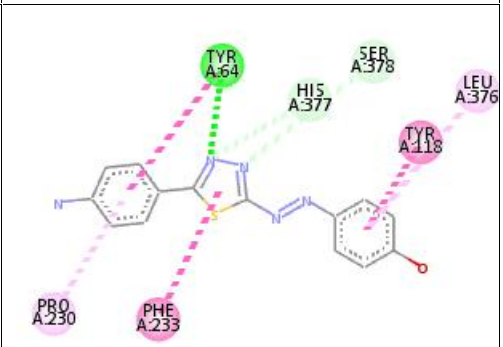 TYR A:64 SER A:378 HIS A:377 LEU A:376 TYR A:118 PRO A:230 PHE A:233

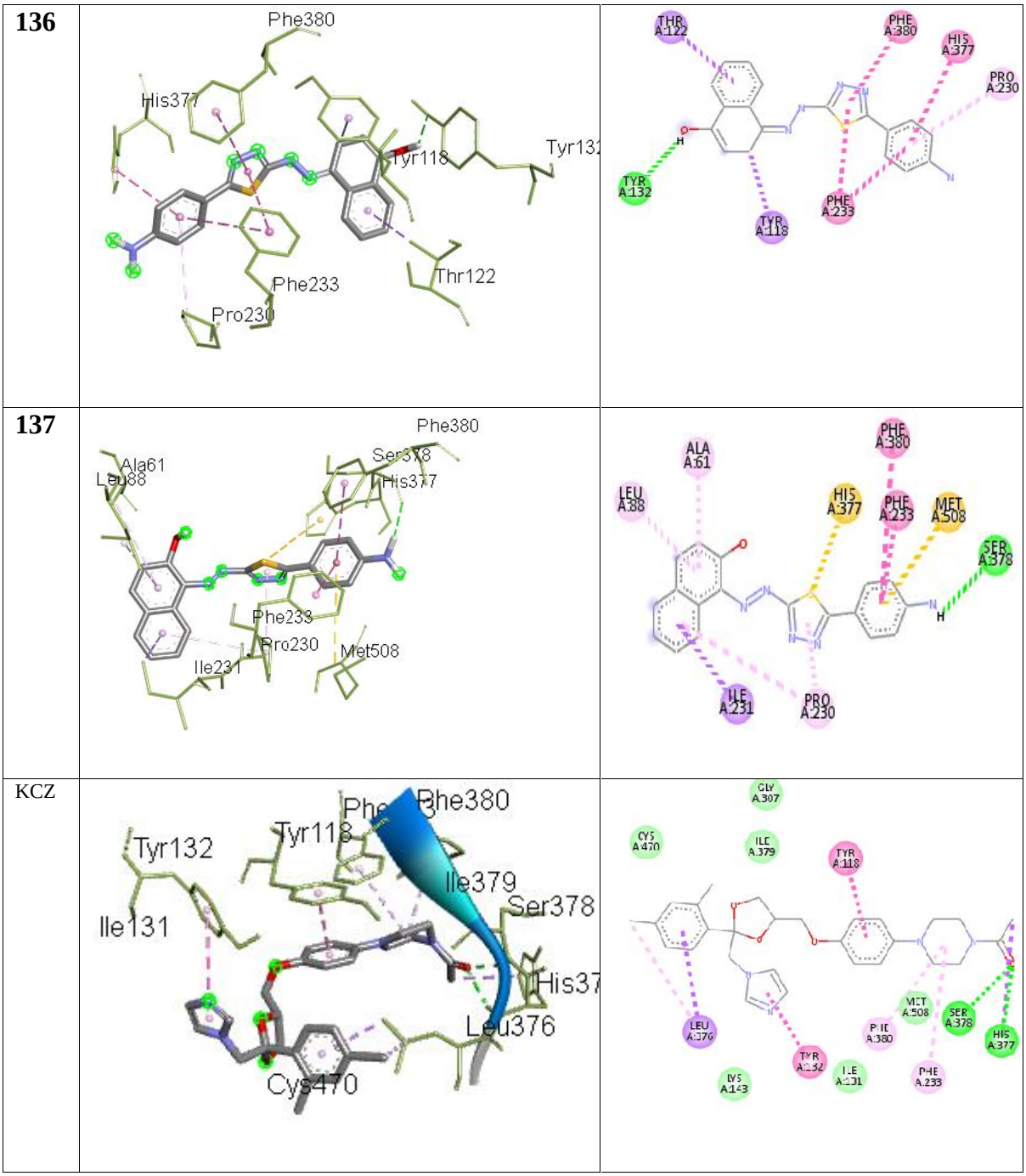

Figure 17: Binding interactions (3D & 2D) of the synthesized and standard compounds with *C. albican* CYP51.

4.6.4 Molecular docking with *Human peroxiredoxins 5*

Human peroxiredoxin 5 (PRDX5) is a member of the peroxiredoxin family of antioxidant enzymes which reduce hydrogen peroxide and alkyl hydroperoxides. The encoded protein interacts with peroxisome receptor 1 and plays an antioxidant protective role in different tissues under normal conditions and during inflammatory processes (Declercq *et al*., 2001). In this present study PRDX5 (PDB ID: 1HD2) enzyme is used as a target and ascorbic acid (AA) was utilized as a reference control for docking. Binding affinity and interactions with

different amino acids are presented in (Table 8), and the (3D and 2D) binding interactions are depicted in (Figure 16). All the test compounds exhibited higher binding affinities than AA (-4.2 kcal/mole). Compound **137** showed highest binding affinity (-5.8 kcal/mol) followed by **134** (-5.7 kcal/mole) and **136** (-5.6 kcal/mole). AA showed H-bonding interactions with Cys-47, Arg-127, Thr-44, and Gly-46; similarly, **132** had interactions with Cys-47, Arg-127, and Thr-44, and **134** had interactions with Cys-47, Thr-44, and Gly-46. Compounds **135** and **137** interacted with Cys-47 and Thr-44, and **136** with Gly-46. Most of the tested compounds showed residual interaction with Pro-45, Phe-120, Arg-127, Leu-149 and Thr-147, whereas AA did not show any residual interactions.

Table 8: Binding affinity and interaction of the compounds (**132-137**) with the target *human peroxidoxins 5*.

Compound	Affinity (kcal/mol)	H-bond	Residual Amino acid Interactions	
			Hydrophobic/Pi-Cation/Pi-Anion/ Pi-Alkyl interactions	Van-der Walls interactions
132	-5.2	Cys-47, Arg-127 Thr-44	Phe-120	-
133	-5.1	Ile-119, Thr147*	Pro-45, Phe-120, Ile119	Arg-127, Gly-148, Leu-149
134	-5.7	Cys-47, Thr-44, Gly-46, Pro-45*	Pro-45, Pro-40, Leu-116	-
135	-5.1	Cys-47, Thr-44	Pro-45, Ile119	-
136	-5.6	Gly-46, Thr-44*	Pro-45, Ile119, Pro-40, Cys-47	-
137	-5.8	Cys-47, Thr-44	Pro-40, Thr-147, Arg-127, Leu-149	-
AA	-4.2	Cys-47, Arg-127 Thr-44, Gly-46	-	-

*Carbon Hydrogen bond

No.	3D	2D
132	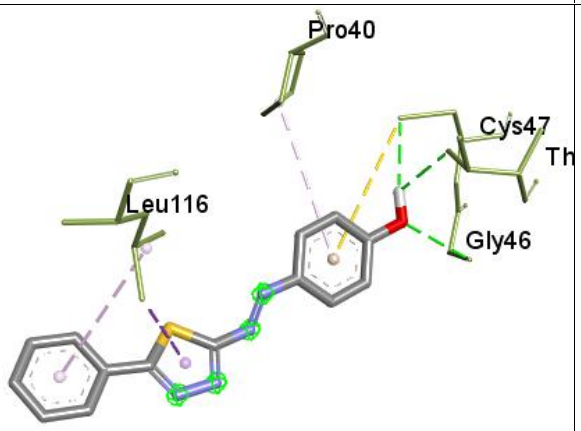	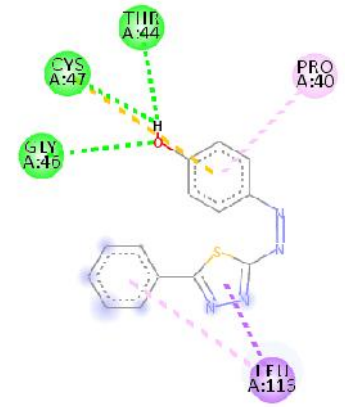
133	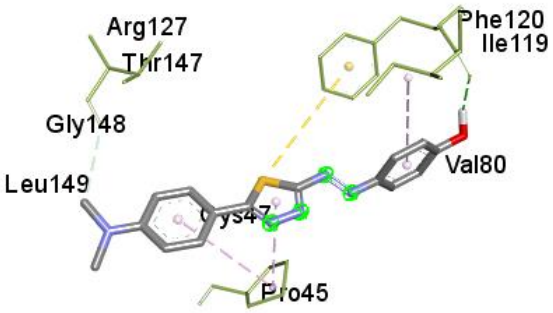	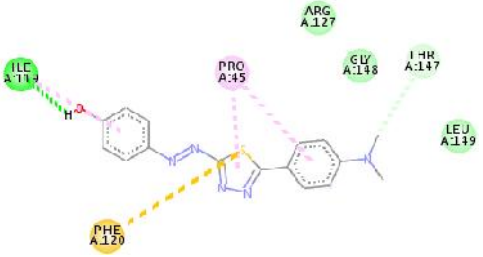
134	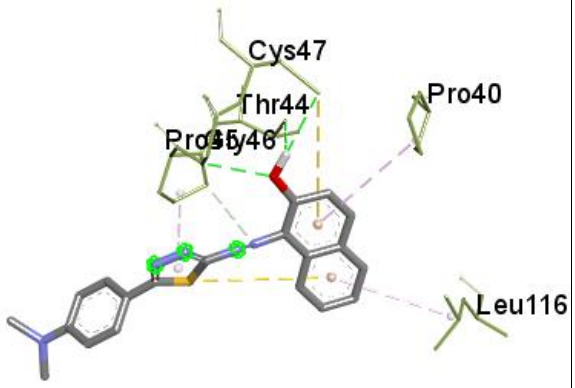	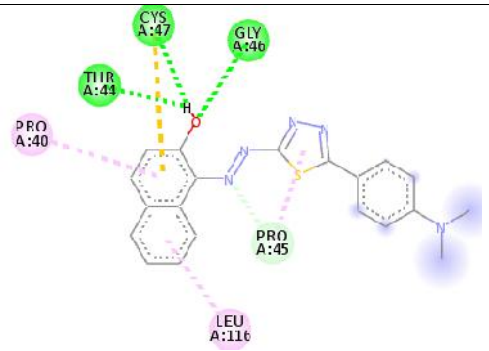
135	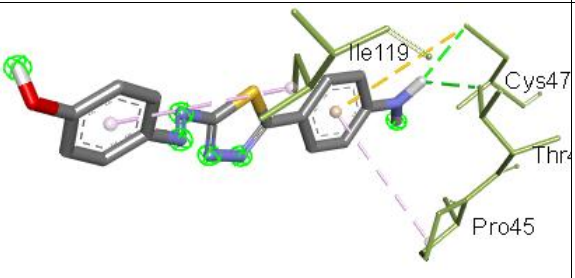	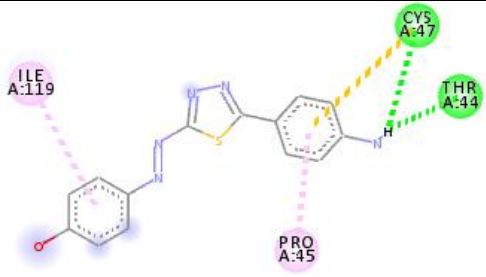

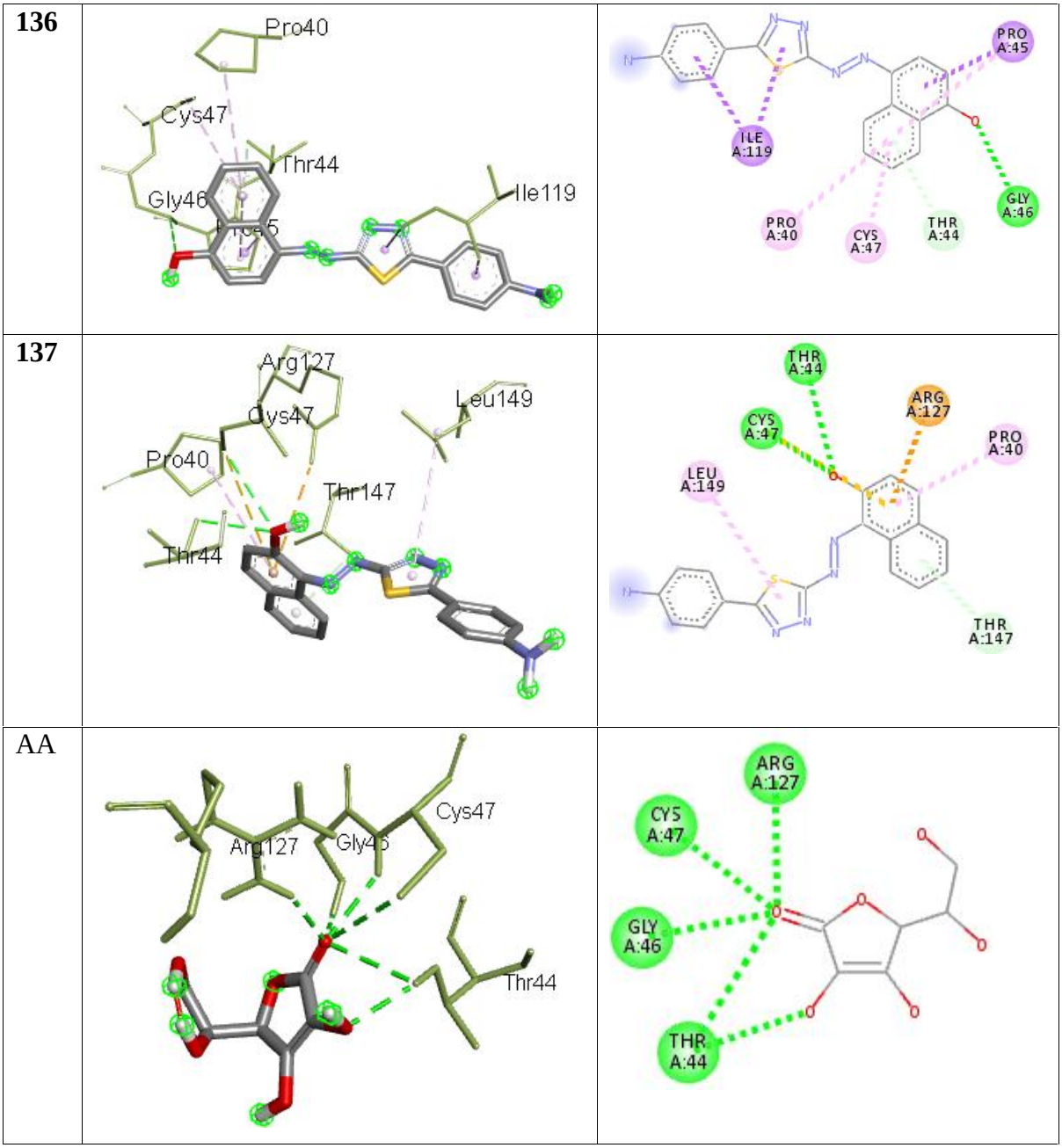

Figure 18: Binding interactions (3D & 2D) of the synthesized and standard compounds with *human peroxidoxins 5*.

4.7 *In silico* ADMET and Drug likeness studies

The physicochemical and pharmacokinetics, properties of the synthesized compounds **132-137** were predicted using a free online tool, SwissADME (http://www.swissadme.ch). The predicted result (Table 9) of the compounds showed that all the compounds satisfy the lipinski's rule of five, since all the synthesized compounds displayed molecular weight (297.34-375.45 g/mol), hydrogen bond donors (1 and 2), hydrogen bond acceptors (5) and the lipophilicity value (3.03-4.53) as described in (Chen *et al*., 2020). Further, the TPSA (Å^2) prediction of the synthesized compounds revealed that except compound **137** (143.92

Å²), all the compounds display good (102.21-124.99 Å²) intestinal absorption. Among the compounds, compound **132** could be a candidate that showed most drug-like properties (Chen *et al*., 2020).

Table 9: The drug-likeness predictions of the compounds (**132-137**) computed by SwissADME.

C-N	Molecular formula	M W (g/mol)	NR B	NHA	NHD	TPSA (Å²)	LogP (cLogP)	Lipinski' s Ro5
132	$C_{16}H_{15}N_5OS$	325.39	4	5	1	102.21	3.61	0
133	$C_{20}H_{17}N_5OS$	375.45	4	5	1	102.21	4.51	0
134	$C_{20}H_{17}N_5OS$	375.45	4	5	1	102.21	4.53	0
135	$C_{14}H_{11}N_5OS$	297.34	3	5	2	124.99	3.03	0
136	$C_{18}H_{13}N_5OS$	347.39	3	5	2	124.99	3.95	0
137	$C_{18}H_{13}N_5OS$	347.39	3	5	2	143.92	3.97	0
CP	$C_{17}H_{18}FN_3O_3$	331.34	3	5	2	74.57	1.10	0

Further, the *in silico* based studies of the pharmacokinetics properties of the synthesized compounds (**132-137**) showed that all the compounds exhibited high GI-absorbation properties other than **136** and **137**. Of all, none of the synthesized compounds exhibited the BBB permeate, and predicated as P-gp-substrate (Table 10). The metabolic properties of the synthesized compounds were predicted by the behaviour of cytochrom P450 and their isoform enzymes, since these enzymes are responsible and essential for metabolizing drugs (Lynch and Neff, 2007). The predicted results showed that all the compounds have no inhibitory activity against CYP3A4; all the synthesized compounds (**132-137**), except **134** showed inhibitory activity against CYP2C19. So, CYP3A4 is an essential enzyme to metabolize all the synthesized compounds, whereas, CYP2D6 metabolize all except **134**.

Table 10: ADME prediction of synthesized compounds was computed by SwissADME and PreADMET.

C-N	Molecular formula	Skin-P (cm/s)	GI-A	BBB-P	P-gp-S	Inhibitor interaction				
						CYP1A2 inhibitor	CYP2C19 inhibitor	CYP2C9 inhibitor	CYP2D6 inhibitor	CYP3A4 inhibitor
132	$C_{16}H_{15}N_5OS$	-5.51	High	No	No	Yes	Yes	Yes	No	No
133	$C_{20}H_{17}N_5OS$	-4.93	High	No	No	No	Yes	Yes	No	No

134	$C_{20}H_{17}N_5OS$	-4.93	High	No	No	No	No	Yes	Yes	No
135	$C_{14}H_{11}N_5OS$	-5.91	High	No	No	Yes	Yes	No	No	No
136	$C_{18}H_{13}N_5OS$	-5.33	Low	No	No	Yes	Yes	No	No	No
137	$C_{18}H_{13}N_5OS$	-5.33	Low	No	No	Yes	Yes	No	No	No
CP	$C_{17}H_{18}FN_3O_3$	-9.09	High	No	Yes	No	No	No	No	No

Table 11: Toxicity prediction of the compounds (**132-137)** computed by Pro-Tox II.

C-N	C-F	LD_{50} (mg/kg)	Toxicity class	Organ toxicity				
				Hepato-toxicity	Carcino-genicity	Immino-toxicity	Muta-genicity	Cyto-toxicity
132	$C_{16}H_{15}N_5OS$	1100	4	Active	Inactive	Active	Inactive	Inactive
133	$C_{20}H_{17}N_5OS$	1100	4	Inactive	Inactive	Inactive	Active	Inactive
134	$C_{20}H_{17}N_5OS$	1100	4	Active	Inactive	Active	Inactive	Inactive
135	$C_{14}H_{11}N_5OS$	1200	4	Active	Active	Inactive	Active	Inactive
136	$C_{18}H_{13}N_5OS$	1200	4	Active	Active	Inactive	Active	Inactive
137	$C_{18}H_{13}N_5OS$	1100	4	Active	Active	Inactive	Active	Inactive
CP	$C_{17}H_{18}FN_3O_3$	2000	4	Inactive	Inactive	Inactive	Active	Inactive

In silico toxicity prediction is the basic method for the investigation of essential bioactive compounds (Goswami *et al*., 2019). All the compounds screen for their *in silico* toxicity risks, such as AMES test (mutagenicity prediction), tumorigenicity carcino-mouse/rat (carcinogenicity) and cytotoxicity effect (Table 11). The predicted result of the synthesized compounds revealed that the LD_{50} of the compounds ranges from 1100-1200 mg/kg leads to the toxicity class 4, infer that they would be harmful, if swallowed ($300LD_{50} \leq 2000$) (Drwal and Preissner, 2014). Among the tested compound, except **132** and **134**, all displayed active mutagenicity behaviour. All the compounds exhibited no possible cytotoxicity effect record. Compounds **132-134** showed the absence of imminotoxicity effect; whereas, the rest compounds display imminotoxicity effect.

4.8. DFT Analysis

4.8.1. Molecular orbital analysis

Frontier molecular orbital theory states that the "Highest Occupied Molecular Orbital (HOMO)" and "Lowest Unoccupied Molecular Orbital (LUMO)" are important indicators

of a molecule's chemical reactivity and stability, respectively. The transition from the ground to the first excited state is related to the electronic absorption, which is mostly stated by a single excited electron from HOMO to LUMO (Aihara *et al*., 1999). Chemical qualities such as chemical hardness and softness, chemical potential, electronegativity, and electrophilicity are all based on the value of the HOMO-LUMO gap. Larger HOMO-LUMO gaps are associated with reduced chemical softness and higher kinetic stability because the transfer of one electron from HOMO to LUMO occurs under energetically unfavourable circumstances. Due to the ease of electron transition, lower HOMO-LUMO gap is linked to the upper chemical softness and lower kinetic stability (Ayers *et al.*, 2007; Azam *et al*., 2018). Among the tested compounds, **134** showed lowest energy gap (0.0906 eV) and the **132** had highest energy gap (0.1191 eV), which is depicted in (Table 11 and Figure 18). The lowest energy gap makes the compound **134** lowermost chemical hardness (0.0453 eV) as well as the uppermost softness (22.0751 eV), whereas, the highest energy gap of **132** contributes the maximum chemical hardness (0.1035 eV) and minimum softness (4.8309 eV) (Table 12).

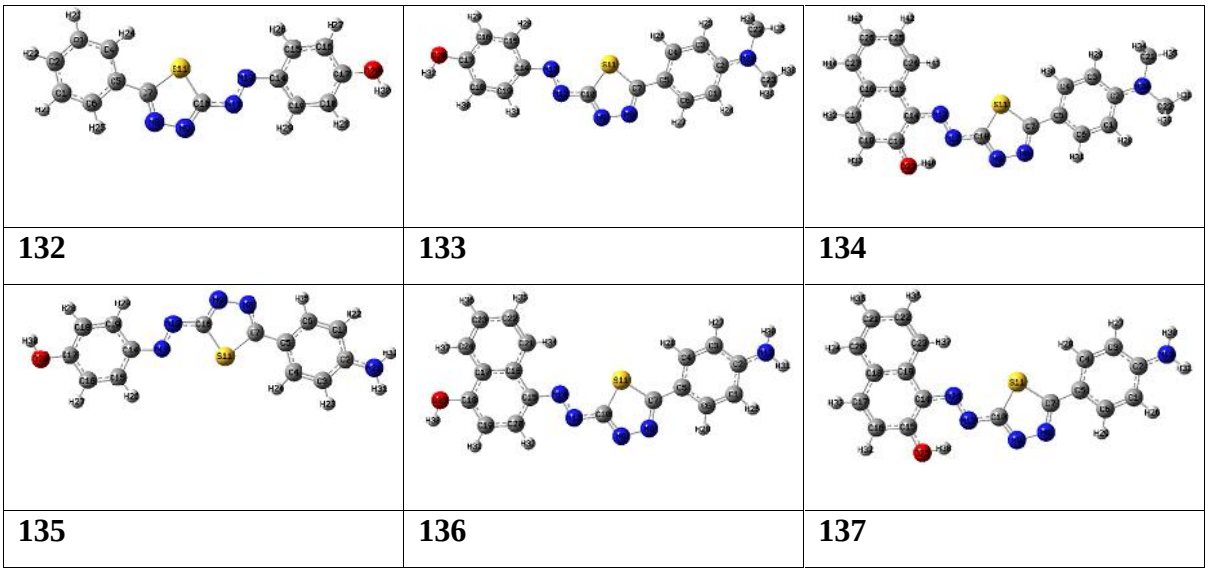

132	**133**	**134**
135	**136**	**137**

Figure 19: Optimized structures of the compounds **132-137**.

Table 12: The quantum chemical parameters of the synthesized compounds.

Cpd	εHOMO	εLUMO	Gap	η	S	μ	χ	ω
132	-0.2211	-0.102	0.1191	0.0596	16.7785	-0.1616	0.1616	0.219
133	-0.1904	-0.091	0.0994	0.0497	20.1207	-0.1407	0.1407	0.2173
134	-0.1911	-0.1005	0.0906	0.0453	22.0751	-0.1458	0.1458	0.2351
135	-0.1957	-0.0917	0.194	0.052	19.2308	-0.1437	0.1437	0.1981
136	-0.1917	-0.0938	0.0979	0.049	20.4082	-0.1428	0.1428	0.2082

137	-0.1957	-0.1014	0.0943	0.0472	21.1864	-0.1486	0.1486	0.2341

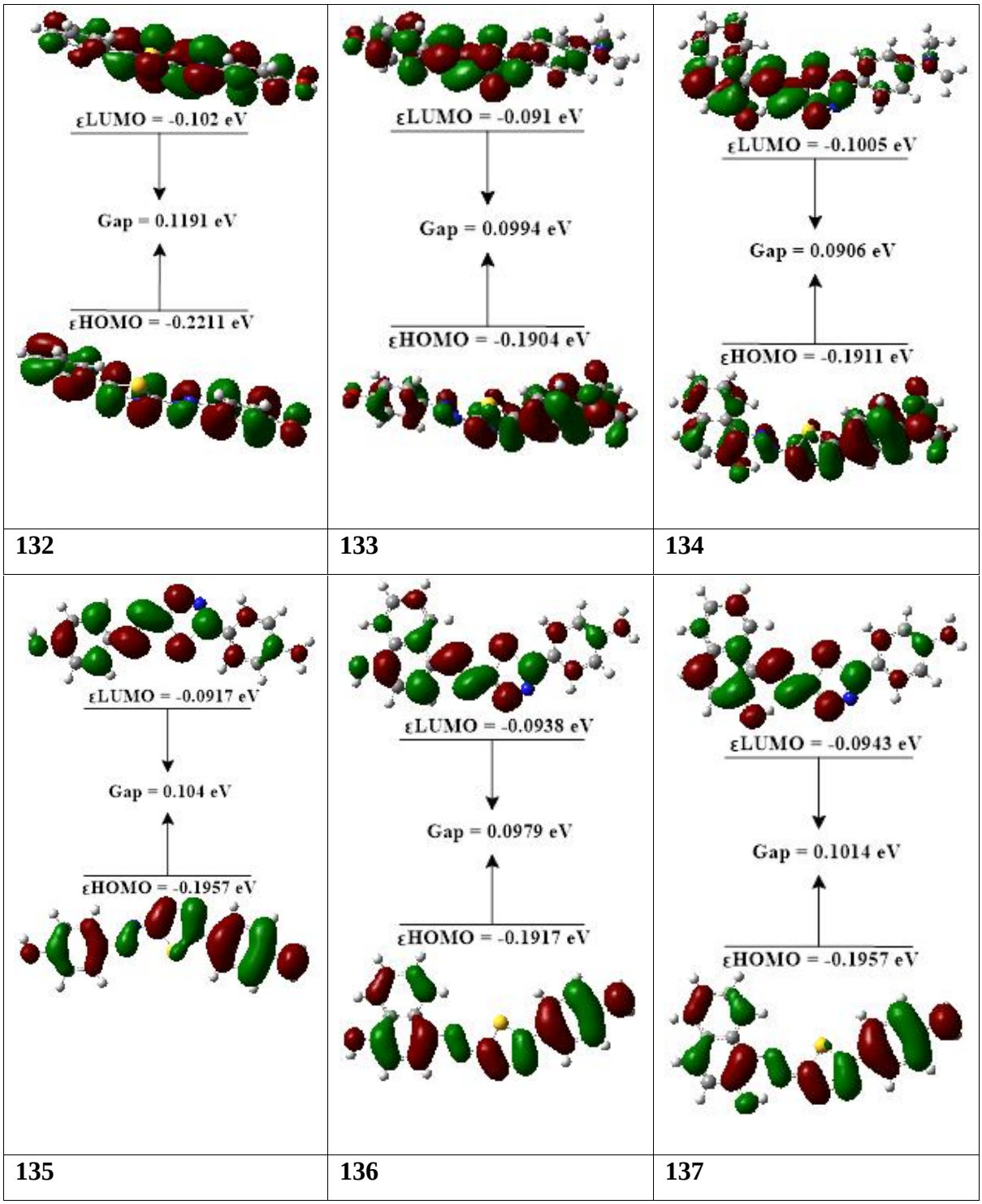

132	**133**	**134**
135	**136**	**137**

Figure 20: The HOMO-LUMO and energy gap of the synthesized compounds.

4.8.2 Molecular electrostatic potential analysis

The total charge of the electrons and nuclei are shown on the molecular electrostatic potential (MEP) map, which also provides some information on the electronegativity, partial charge, dipole moment, and chemical reactivity of the molecule (Borges and

Oliveira, 2022). By using the colors blue and red, it depicts a potential electrophilic and nucleophilic attack. Red color depicts maximum negative regions that are electron rich and have the potential for electrophilic attack (Pahuja and Paularokiadoss, 2022). Because there are fewer electrons present, the deep blue color of the utmost positive region indicates that it may be a target for nucleophilic attack. Furthermore, green color shows zero potential area. When it comes to color grading, MEP simultaneously displays molecule size, shape, and positive, negative, and neutral electrostatic potential portions (Gupta *et al*., 2016). The area with the negative potential is over electronegative atoms (oxygen atoms) on the MEP map (Figure 19), whereas the region with the positive potential is over hydrogen atoms. Compound **132** shows the highest negative potential value (-7.684e-2 a.u., deepest red) and maximum positive potential value (+7.684e-2 a.u., deepest blue). Compound **137** shows the lowest negative potential value (-5.905e-2 a.u.) and minimum positive potential value (+5.905e-2 a.u.).

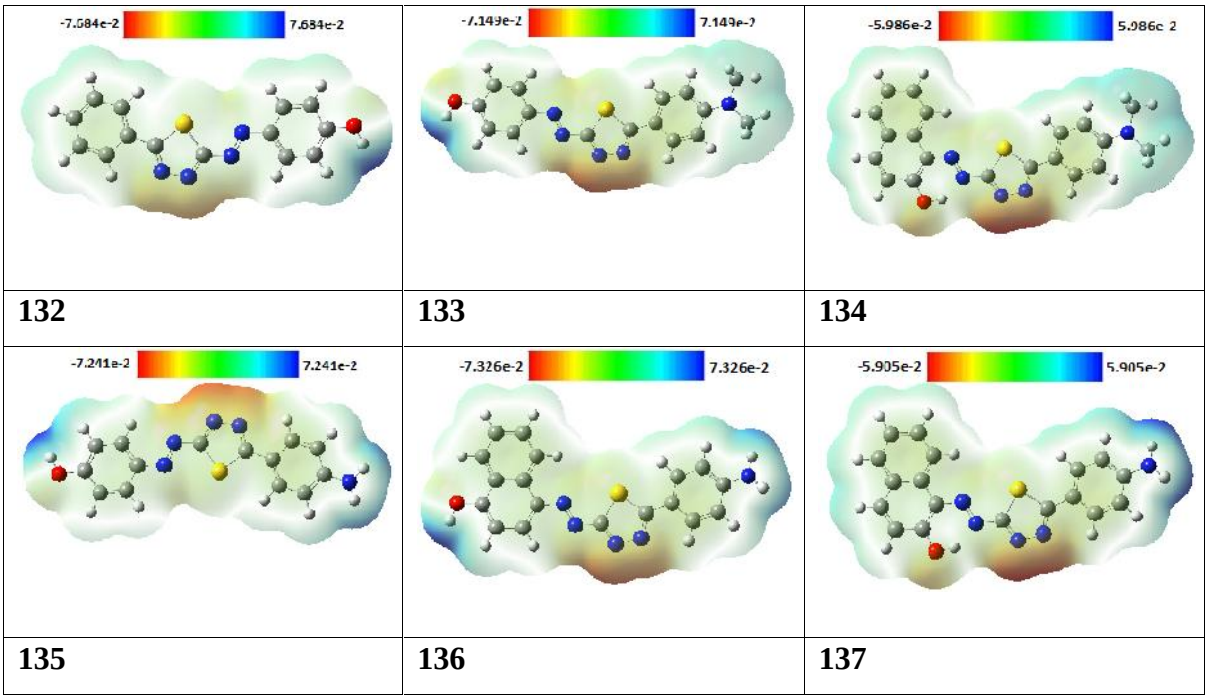

132	**133**	**134**
135	**136**	**137**

Figure 21: Molecular electrostatic potential map of compounds (**132-137)**.

5. Conclusion and Recommendation

Recently, azo dye derivatives incorporated with heterocyclic scaffolds become a research area, since the incorporation of the heterocyclic moiety into the azo dye has enhanced the bioactive properties of the target derivatives. This work focused on the synthesis of azo dye derivatives incorporated 1,3,4-thiadiazole moiety through the conventional diazotization-coupling reaction. Herein, six novel compounds were synthesized and characterized using UV-Visible, FTIR, ^{1}H NMR and ^{13}C NMR. The synthesized compounds were subjected to washing and rubbing fastness test, and compounds **136** and **137** displayed highest washing and rubbing fastness properties which indicate that the compounds have very good coloring performance. Further, *in vitro* antimicrobial activities of the compounds displayed, **137** become the most potent antimicrobial active at (MIC = 0.5 mg/mL) for both bacterial and fungal species. Compound **133**, showed potential radical scavenging activity at IC_{50}= 10.7 µg/mL relative to ascorbic acid IC_{50} = 9.6 µg/mL. *In silico* molecular interaction of the compounds explored that compound **136** has highest binding affinity (-8.0 kcal/mol) to *E.coli* DNA gyrase B than that of ciprofloxacin (-7.3 kcal/mol). Similarly, the highest binding affinity was shown by **134** and **137** (-6.1 kcal/mol) against *S. aureus* PK than the standard ciprofloxacin (-4.9 kcal/mole). Compound **137** showed highest binding affinity (-10.6 kcal/mol) with *C. albican* CYP51 than that of KC (10.2 kcal/mol). Further, compound **137** showed highest binding affinity (--5.8 kcal/mole) with *human peroxidoxins* 5 than that of ascorbic acid (-4.2 kcal/mol). Compound **134** exhibit lowermost chemical hardness (0.0453 eV) as well as the uppermost softness (22.0751 eV), due to lowest energy gap, which indicates highest reactivity of the compound. In general the molecular docking result showed that most of the compounds have promising biological activity; however, the results are not in good agreement with the experimental data.

The synthesized compounds explored poor to good *in vitro* activity combined with promising *in silico* predictions against bacterial and fungal species. The compounds are also active towards free radical scavenging activity. So, these compounds are good candidates for drug development. Thus, this area needs further *in vitro* and *in vivo* studies on antimicrobial and antioxidant activities are recommended. Further tests on the dye performance and properties are also recommended too.

Research Fund Acknowledgment

This research project is funded by Adama Science and Technology University Under the grant number ASTU/SM-R/823/23, Adama, Ethiopia.

Reference

Abou Elmaaty, T., Elsisi, H., Negm, E., Ayad, S., Sofan, M. (2022). Novel nano silica assisted synthesis of azo pyrazole for the sustainable dyeing and antimicrobial finishing of cotton fabrics in supercritical carbon dioxide. *The Journal of Supercritical Fluids, 179*, 105354.

Abu-Melha, S. (2019). Synthesis of novel biologically active thiazole dyes and their applications. *Pigment & Resin Technology, 48*(5), 375-382.

Aihara, J. (1999). Reduced HOMO− LUMO gap as an index of kinetic stability for polycyclic aromatic hydrocarbons. *The Journal of Physical Chemistry A, 103*(37), 7487-7495.

Akunuri, R., Unnissa, T., Vadakattu, M., Bujji, S., Mahammad Ghouse, S., Madhavi Yaddanapudi, V., Nanduri, S. (2022). Bacterial Pyruvate Kinase: A New Potential Target to Combat Drug-Resistant Staphylococcus aureus Infections. *ChemistrySelect, 7*(29), e202201403.

Al-adilee, K. J., Hessoon, H. (2019). Synthesis, Spectral properties and anticancer studies of novel hetrocyclic azo dye ligand derived from 2-Amino-5-methyl thiazole with some transition metal complexes. *Paper presented at the Journal of Physics: Conference Series*, 45(3), 46-53.

Albelwi, F. F., Al-anazi, M., Naqvi, A., Hritani, Z. M., Okasha, R. M., Afifi, T. H., Hagar, M. (2021). Novel oxazolones incorporated azo dye: Design, synthesis photophysical-DFT aspects and antimicrobial assessments with *In-silico* and *In-vitro* surveys. *Journal of Photochemistry and Photobiology, 7*, 100032.

Ali, Y., Hamid, S. A., Rashid, U. (2018). Biomedical applications of aromatic azo compounds. *Mini reviews in medicinal chemistry, 18*(18), 1548-1558.

Almeida, A. K. A., Dias, J. M. M., Santos, D. P., Nogueira, F. A. R., Navarro, M., Tonholo, J., Ribeiro, A. S. (2017). A magenta polypyrrole derivatised with Methyl Red azo dye: synthesis and spectroelectrochemical characterisation. *Electrochimica Acta, 240*, 239-249.

Altıntop, M. D., Sever, B., Ozdemir, A., Ilgın, S., Atlı, O., Turan-Zitouni, G., Kaplancıklı, Z. A. (2018). Synthesis and evaluation of a series of 1, 3, 4-thiadiazole derivatives as potential anticancer agents. *Anti-Cancer Agents in Medicinal Chemistry (Formerly Current Medicinal Chemistry-Anti-Cancer Agents), 18*(11), 1606-1616.

Anthwal, T., Singh, H., Nain, S. (2022). 1, 3, 4-thiadiazole scaffold: Anti-microbial agents. *Pharmaceutical Chemistry Journal, 55*(12), 1345-1358.

Ashfaq, T. T. M., Shahzad, M. I., Tabassum, R. (2020). Antiviral evaluation of bioactive azo derivatives to treat endemic poultry viruses. *Thai J. Vet. Med, 50*(3), 435-443.

Ayers, P. W. (2007). The physical basis of the hard/soft acid/base principle. *Faraday Discussions, 135*, 161-190.

Azam, F., Alabdullah, N. H., Ehmedat, H. M., Abulifa, A. R., Taban, I., Upadhyayula, S. (2018). NSAIDs as potential treatment option for preventing amyloid β toxicity in Alzheimer's disease: An investigation by docking, molecular dynamics, and DFT studies. *Journal of Biomolecular Structure and Dynamics, 36*(8), 2099-2117.

Banpurkar, A. R., Wazalwar, S. S., Perdih, F. (2018). Aqueous phase synthesis, crystal structure and antimicrobial activity of 4-(substituted phenylazo)-3-methyl-4H-isoxazol-5-one azo dyes. *Bulletin of the Chemical Society of Ethiopia, 32*(2), 249-257.

Barros, L. P. C., Del Rio, K. P., Carvalho, T. d. S. C., Pinto, M. d. C. F. R., de Moura, K. C. G., Halicki, P. C. B., da Silva, P. E. A. (2018). Anti-Mycobacterium tuberculosis activity of naphthoimidazoles combined with isoniazid and rifampicin. *Tuberculosis, 111*, 198-201.

Benkhaya, S., M'rabet, S., El Harfi, A. (2020). Classifications, properties, recent synthesis and applications of azo dyes. *Heliyon, 6*(1), e03271.

Borges Jr, I., Oliveira, R. S. S., Oliveira, M. A. S. (2022). Properties of molecular charge distributions affecting the sensitivity of energetic materials. *Theoretical and Computational Chemistry* , 22, 81-105.

Breznik, M., Ge, Y., Bluck, J. P., Briem, H., Hahn, D. F., Christ, C. D., Meier, K. (2023). Prioritizing Small Sets of Molecules for Synthesis through in-silico Tools: A Comparison of Common Ranking Methods. *ChemMedChem, 18*(1), e202200425.

Bruschweiler, B. J., Merlot, C. (2017). Azo dyes in clothing textiles can be cleaved into a series of mutagenic aromatic amines which are not regulated yet. *Regul Toxicol Pharmacol, 88*, 214-226.

Brüschweiler, B. J., Merlot, C. (2017). Azo dyes in clothing textiles can be cleaved into a series of mutagenic aromatic amines which are not regulated yet. *Regulatory Toxicology and Pharmacology, 88*, 214-226.

Canan, K., Uğurlu, E., Ozdamar, E. D., Benay, C.-E. (2017). Synthesis and antioxidant properties of new oxazole-5 (4H)-one derivatives. *Turkish Journal of Pharmaceutical Sciences, 14*(2), 174.

Chakraborty, P., Chatterjee, C. (2017). Does environmental regulation indirectly induce upstream innovation? New evidence from India. *Research Policy, 46*(5), 939-955.

Chen, X., Li, H., Tian, L., Li, Q., Luo, J., Zhang, Y. (2020). Analysis of the physicochemical properties of acaricides based on Lipinski's rule of five. *Journal of computational biology, 27*(9), 1397-1406.

Chung, K.-T. (2016). Azo dyes and human health: A review. *Journal of Environmental Science and Health, Part C, 34*(4), 233-261.

Correia, I., Adao, P., Roy, S., Wahba, M., Matos, C., Maurya, M. R., Avecilla, F. (2014). Hydroxyquinoline derived vanadium (IV and V) and copper (II) complexes as potential anti-tuberculosis and anti-tumor agents. *Journal of inorganic biochemistry, 141*, 83-93.

Crespi, S., Simeth, N. A., Konig, B. (2019). Heteroaryl azo dyes as molecular photoswitches. *Nature Reviews Chemistry, 3*(3), 133-146.

Daina, A., Michielin, O., Zoete, V. (2017). SwissADME: a free web tool to evaluate pharmacokinetics, drug-likeness and medicinal chemistry friendliness of small molecules. *Scientific reports, 7*(1), 42717.

Declercq, J.-P., Evrard, C., Clippe, A., Vander Stricht, D., Bernard, A., Knoops, B. (2001). Crystal structure of human peroxiredoxin 5, a novel type of mammalian peroxiredoxin at 1.5 Å resolution. *Journal of molecular biology, 311*(4), 751-759.

Degu, S., Abebe, A., Gemeda, N., Bitew, A. (2021). Evaluation of antibacterial and acute oral toxicity of Impatiens tinctoria A. Rich root extracts. *Plos one, 16*(8), e0255932.

Demircalı, A., Karcı, F., Avinc, O., Kahrıman, A. U., Gedik, G., Bakan, E. (2019). The synthesis, characterization and investigation of absorption properties of disperse disazo dyes containing pyrazole and isoxazole. *Journal of Molecular Structure, 1181*, 8-13.

Demircalı, A., Karcı, F., Sari, F. (2021). Synthesis and absorption properties of five new heterocyclic disazo dyes containing pyrazole and pyrazolone and their acute toxicities on the freshwater amphipod Gammarus roeseli. *Coloration Technology, 137*(3), 280-291.

Drwal, M. N., Banerjee, P., Dunkel, M., Wettig, M. R., Preissner, R. (2014). ProTox: a web server for the in silico prediction of rodent oral toxicity. *Nucleic acids research, 42*(1), 53-58.

Dyers, S. o., and Colourists. (1990). *Methods of Test for Colour Fastness of Textiles and Leather*: British Standards Institution.

Eloff, J. N. (1998). A sensitive and quick microplate method to determine the minimal inhibitory concentration of plant extracts for bacteria. *Planta medica, 64*(08), 711-713.

Frisch, M., Trucks, G., Schlegel, H., Scuseria, G., Robb, M., Cheeseman, J., Petersson, G. (2009). GAUSSIAN09. Gaussian Inc., Wallingford, CT, USA, 68-87.

Gaffer, H., Khattab, T. (2017). Synthesis and characterization of some azo-heterocycles incorporating pyrazolopyridine moiety as disperse dyes. *Egyptian Journal of Chemistry, 60*(Conference Issue (The 8th International Conference of The Textile Research Division (ICTRD 2017), National Research Centre, Cairo 12622, Egypt.)), 41-47.

Gaffer, H. E. (2019). Antimicrobial sulphonamide azo dyes. *Coloration Technology, 135*(6), 484-500.

Gicevic, A., Hindija, L., Karacic, A. (2019). Toxicity of azo dyes in pharmaceutical industry. *Paper presented at the International Conference on Medical and Biological Engineering*, 32(5), 90-102.

Gicevic, A., Hindija, L., Karacic, A. (2020). Toxicity of azo dyes in pharmaceutical industry. Paper presented at the CMBEBIH 2019: *Proceedings of the International Conference on Medical and Biological Engineering, Banja Luka, Bosnia and Herzegovina*, 16-50.

Gökalp, M., Dede, B., Tilki, T., Atay, C. K. (2020). Triazole based azo molecules as potential antibacterial agents: Synthesis, characterization, DFT, ADME and molecular docking studies. *Journal of Molecular Structure, 1212*, 128140.

Goswami, M. R. (2019). An easy screening throughin silico study for predictive toxicity mechanisms of different phthalate compounds by using online tool (Protox-II webserver). *Journal of Advanced Scientific Research, 10*(04 Suppl 2), 246-253.

Gouda, M. A., Eldien, H. F., Girges, M. M., Berghot, M. A. (2016). Synthesis and antitumor evaluation of thiophene based azo dyes incorporating pyrazolone moiety. *Journal of Saudi Chemical Society*, *20*(2), 151-157.

Govender, T., Govinden, U., Mocktar, C., Kruger, H. G., Veljkovic, J., Cindro, N., Basaric, N. (2016). In vitro investigation of the antimicrobial activity of a series of lipophilic phenols and naphthols. *South African journal of chemistry, 69*, 44-50.

Gupta, V. (2016). Electron density analysis and electrostatic potential. *Principles and Applications of Quantum Chemistry; Elsevier: Amsterdam, The Netherlands*, 195-214.

Gur, M. (2019). Synthesis, Characterization, and Antimicrobial Properties of New 1, 3, 4-Thiadiazoles Derived from Azo Dyes. *Journal of Heterocyclic Chemistry, 56*(3), 980-987.

Gur, M., Sener, N., Kastas, C. A., Ozkan, O. E., Muğlu, H., Elmaswari, M. A. (2017). Synthesis and Characterization of Some New Heteroaromatic Compounds Having Chirality Adjacent to a 1, 3, 4-Thiadiazole Moiety and Their Antimicrobial Activities. *Journal of Heterocyclic Chemistry, 54*(6), 3578-3590.

Hamidian, H., Tagizadeh, R., Fozooni, S., Abbasalipour, V., Taheri, A., Namjou, M. (2013). Synthesis of novel azo compounds containing 5 (4H)-oxazolone ring as potent tyrosinase inhibitors. *Bioorganic and medicinal chemistry, 21*(7), 2088-2092.

Harisha, S., Keshavayya, J., Prasanna, S., Hoskeri, H. J. (2020). Synthesis, characterization, pharmacological evaluation and molecular docking studies of benzothiazole azo derivatives. *Journal of Molecular Structure, 1218*, 128477.

Hu, Y., Li, C.-Y., Wang, X.-M., Yang, Y.-H., Zhu, H.-L. (2014). 1, 3, 4-Thiadiazole: synthesis, reactions, and applications in medicinal, agricultural, and materials chemistry. *Chemical reviews, 114*(10), 5572-5610.

Humphries, R., Bobenchik, A. M., Hindler, J. A., Schuetz, A. N. (2021). Overview of changes to the clinical and laboratory standards institute performance standards for antimicrobial susceptibility testing, M100. *Journal of clinical microbiology, 59*(12), e00213-00221.

Jadhav, I., Vasniwal, R., Shrivastav, D., Jadhav, K. (2016). Microorganism-Based Treatment of Azo Dyes. *Journal of Environmental Science and Technology, 9*(2), 188-197.

Janupally, R., Medepi, B., Brindha Devi, P., Suryadevara, P., Jeankumar, V. U., Kulkarni, P., Sriram, D. (2015). Design and Biological Evaluation of Furan/ Pyrrole/ Thiophene-2-carboxamide Derivatives as Efficient DNA GyraseB Inhibitors of Staphylococcus aureus. *Chemical Biology and Drug Design*, *86*(4), 918-925.

Karabacak Atay, C., Gokalp, M., Tuncer, B. O., Tilki, T. (2017). Antimicrobial activities and absorption properties of disazo dyes containing imidazole and pyrazole moieties. *Journal of Macromolecular Science, Part A, 54*(4), 236-242.

Karaburun, A. C., Acar Cevik, U., Osmaniye, D., Saglık, B. N., Kaya Cavusoglu, B., Levent, S., Kaplancıklı, Z. A. (2018). Synthesis and evaluation of new 1, 3, 4-thiadiazole derivatives as potent antifungal agents. *Molecules, 23*(12), 3129.

Keerthi Kumar, C. T., Keshavayya, J., Rajesh, T. N., Peethambar, S. K., Shoukat Ali, A. R. (2013). Synthesis, characterization, and biological activity of 5-phenyl-1, 3, 4-thiadiazole-2-amine incorporated azo dye derivatives. *Organic Chemistry International, 2013*.

Keshavayya, J., Pushpavathi, I., Keerthikumar, C., Maliyappa, M., Ravi, B. (2020). Synthesis, characterization, computational and biological studies of nitrothiazole incorporated heterocyclic azo dyes. *Structural Chemistry, 31*(4), 1317-1329.

Khattab, T., Rehan, M. (2018). A review on synthesis of nitrogen-containing heterocyclic dyes for textile fibers - Part 1: Five and six-membered heterocycles. *Egyptian Journal of Chemistry, 8*(2), 20-28.

Kudelko, A., Olesiejuk, M., Luczynski, M., Swiatkowski, M., Sieranski, T., Kruszynski, R. (2020). 1, 3, 4-Thiadiazole-containing azo dyes: Synthesis, spectroscopic properties and molecular structure. *Molecules, 25*(12), 2822.

Li, Y., Geng, J., Liu, Y., Yu, S., Zhao, G. (2013). Thiadiazole—A promising structure in medicinal chemistry. *ChemMedChem, 8*(1), 27-41.

Lynch, T., and Neff, A. P. (2007). The effect of cytochrome P450 metabolism on drug response, interactions, and adverse effects. *American family physician, 76*(3), 391-396.

Mahmoodi, N. O., Rahimi, S., Pasandideh Nadamani, M. (2017). Microwave-assisted synthesis and photochromic properties of new azo-imidazoles. *Dyes and Pigments, 143*, 387-392.

Maliyappa, M., Keshavayya, J., Mahanthappa, M., Shivaraj, Y., Basavarajappa, K. (2020). 6-Substituted benzothiazole based dispersed azo dyes having pyrazole moiety: synthesis, characterization, electrochemical and DFT studies. *Journal of Molecular Structure, 1199*, 126959.

Maliyappa, M., Keshavayya, J., Mallikarjuna, N., Pushpavathi, I. (2020). Novel substituted aniline based heterocyclic dispersed azo dyes coupling with 5-methyl-2-(6-methyl-1,3-benzothiazol-2-yl)-2, 4-dihydro-3*H*-pyrazol-3-one: synthesis, structural,

computational and biological studies. *Journal of Molecular Structure, 1205*, 127576.

Maliyappa, M., Keshavayya, J., Sudhanva, M., Pushpavathi, I. (2022). Heterocyclic azo dyes derived from 2-(6-chloro-1, 3-benzothiazol-2-yl)-5-methyl-2, 4-dihydro-3H-pyrazol-3-one having benzothiazole skeleton: synthesis, structural, computational and biological studies. *Journal of Molecular Structure, 1247*, 131321.

Mallikarjuna, N., Keshavayya, J. (2020). Synthesis, spectroscopic characterization and pharmacological studies on novel sulfamethaxazole based azo dyes. *Journal of King Saud University-Science, 32*(1), 251-259.

Manjunatha, B., Bodke, Y. D. (2021). Novel isoxazolone based azo dyes: synthesis, characterization, computational, solvatochromic UV-Vis absorption and biological studies. *Journal of Molecular Structure, 1244*, 130933.

Manjunatha, B., Bodke, Y. D., Nagaraja, O., Nagaraju, G., Sridhar, M. (2021). Coumarin-benzothiazole based azo dyes: synthesis, characterization, computational, photophysical and biological studies. *Journal of Molecular Structure, 1246*, 131-170.

Maruszewska, A., Podsiadły, R. (2016). Dyes based on the azo-1*H*-pyrrole moiety – synthesis, spectroscopic and electrochemical properties, and adsorption on TiO_2. *Coloration Technology, 132*(1), 92-97.

Matada, M. N., Jathi, K., Rangappa, M. M., Geoffry, K., Kumar, S. R., Nagarajappa, R. B., Zahara, F. N. (2020). A new sulphur containing heterocycles having azo linkage: Synthesis, structural characterization and biological evaluation. *Journal of King Saud University-Science, 32*(8), 3313-3320.

Mohamed, H. A., Abdel-Wahab, B. F., Fahmy, H. M. (2021). Thiazole azodyes containing sulfonamide moiety for UV protection and antimicrobial of cotton fabrics. *Polycyclic Aromatic Compounds, 42*(1), 195-203.

Mohammadi, A., Khalili, B., Tahavor, M. (2015). Novel push–pull heterocyclic azo disperse dyes containing piperazine moiety: Synthesis, spectral properties, antioxidant activity and dyeing performance on polyester fibers. *Spectrochimica Acta Part A: Molecular and Biomolecular Spectroscopy, 150*, 799-805.

Nagasundaram, N., Govindhan, C., Sumitha, S., Sedhu, N., Raguvaran, K., Santhosh, S., and Lalitha, A. (2022). Synthesis, characterization and biological evaluation of novel azo fused 2, 3-dihydro-1H-perimidine derivatives: In vitro antibacterial,

antibiofilm, anti-quorum sensing, DFT, in silico ADME and Molecular docking studies. *Journal of Molecular Structure, 1248*, 131437.

Narramore, S., Stevenson, C. E., Maxwell, A., Lawson, D. M., Fishwick, C. W. (2019). New insights into the binding mode of pyridine-3-carboxamide inhibitors of E. coli DNA gyrase. *Bioorganic and medicinal chemistry, 27*(16), 3546-3550.

Naz, A., Iqtadar, R., Siddiqui, F. A., Ul-Haq, Z. (2020). Degradation kinetics of fluvoxamine in buffer solutions: In silico ADMET profiling and identification of degradation products by LC-MS/ESI. *Arabian Journal of Chemistry, 13*(2), 4134-4146.

Nguyen, N. T., Nguyen, T. H., Pham, T. N. H., Huy, N. T., Bay, M. V., Pham, M. Q., Ngo, S. T. (2019). Autodock vina adopts more accurate binding poses but autodock4 forms better binding affinity. *Journal of Chemical Information and Modeling, 60*(1), 204-211.

Olomola, T., Akinboye, A., Olasunkanmi, O., Olasunkanmi, L. (2018). Synthesis, antimicrobial activities and computational studies of some oxazolone derivatives. *Ife Journal of Science, 20*(1), 1-14.

Pahuja, A., Jeyakumar, T. C., Paularokiadoss, F. (2022). Structural analysis and chemical descriptors analysis of 4-aminopyridine adsorbed on M4 (M= Co, Ni, Cu) clusters: A DFT study. *Vietnam Journal of Chemistry, 60*(3), 376-388.

Pawar, S. S., Rohane, S. H. (2021). Review on discovery studio: An important tool for molecular docking, 128-136.

Prakash, S., Somiya, G., Elavarasan, N., Subashini, K., Kanaga, S., Dhandapani, R., Sujatha, V. (2021). Synthesis and characterization of novel bioactive azo compounds fused with benzothiazole and their versatile biological applications. *Journal of Molecular Structure, 1224*, 129016.

Ramachandran, V. P., Rajappan, R. (2022). Anxiolytic-like activity of serotonin-3 receptor antagonist: In-silico molecular modeling, drug-likeness and evaluation of anxiolytic activity. *Songklanakarin Journal of Science and Technology, 44*(3), 50-56.

Raman, N., Sakthivel, A., Pravin, N. (2014). Exploring DNA binding and nucleolytic activity of few 4-aminoantipyrine based amino acid Schiff base complexes: A comparative approach. *Spectrochimica Acta Part A: Molecular and Biomolecular Spectroscopy, 125*, 404-413.

Ramprasad, J., Nayak, N., Dalimba, U., Yogeeswari, P., Sriram, D., Peethambar, S., Kumar, H. S. (2015). Synthesis and biological evaluation of new imidazo [2, 1-

b][1, 3, 4] thiadiazole-benzimidazole derivatives. *European Journal of Medicinal Chemistry, 95*, 49-63.

Ravi, B., Keshavayya, J., Mallikarjuna, N., Kumar, V., Zahara, F. N. (2021). Synthesis, spectral characterization, anticancer and cyclic voltammetric studies of azo colorants containing thiazole structure. *Chemical Data Collections, 33*, 100686.

Ravi, B., Keshavayya, J., Mallikarjuna, N., Santhosh, H. (2020). Synthesis, characterization, cyclic voltammetric and cytotoxic studies of azo dyes containing thiazole moiety. *Chemical Data Collections, 25*, 100334.

Rezaei-Seresht, E., Salimi, A., Mahdavi, B. (2018). Synthesis, antioxidant and antibacterial activity of azo dye-stilbene hybrid compounds. *Pigment & Resin Technology*.

Rizk, H. F., Ibrahim, S. A., El-Borai, M. A. (2015). Synthesis, fastness properties, color assessment and antimicrobial activity of some azo reactive dyes having pyrazole moiety. *Dyes and Pigments, 112*, 86-92.

Rufchahi, E. M., Pouramir, H., Yazdanbakhsh, M., Yousefi, H., Bagheri, M., Rassa, M. (2013). Novel azo dyes derived from 8-methyl-4-hydroxyl-2-quinolone: Synthesis, UV–vis studies and biological activity. *Chinese Chemical Letters*, *24*(5), 425-428.

Sahu, R. K., Kar, M., Routray, R. (2013). DPPH free radical scavenging activity of some leafy vegetables used by tribals of Odisha, India. *J Med Plants*, *1*(4), 21-27.

Serban, G., Stanasel, O., Serban, E., Bota, S. (2018). 2-Amino-1, 3, 4-thiadiazole as a potential scaffold for promising antimicrobial agents. *Drug design, development and therapy*, 1545-1566.

Shah, K. (2014). Biodegradation of azo dye compounds. *International Research Journal of Biochemistry and Biotechnology*, *1*(2), 5-13.

Shinde, S., Sekar, N. (2019). Synthesis, spectroscopic characteristics, dyeing performance and TD-DFT study of quinolone based red emitting acid azo dyes. *Dyes and Pigments, 168*, 12-27.

Shridhar, A., Keshavayya, J., Peethambar, S., Hoskeri, H. J. (2016). Synthesis and biological activities of Bis alkyl 1, 3, 4-oxadiazole incorporated azo dye derivatives. *Arabian Journal of Chemistry*, *9*, 1643-1648.

Song, X., Hou, A., Xie, K., Hu, T. (2020). Synthesis and Dyeing Properties of New Bi-heterocyclic Disperse Dyes Containing Pyridone Group for Polyester Fabrics. *Fibers and Polymers, 21*(8), 1743-1749.

Talebi Bezmin Abadi, A., Rizvanov, A. A., Haertle, T., Blatt, N. L. (2019). World Health Organization report: current crisis of antibiotic resistance. *BioNanoScience, 9*, 778-788.

Tropp, J., Ihde, M. H., Crater, E. R., Bell, N. C., Bhatta, R., Johnson, I. C., Azoulay, J. D. (2020). A sensor array for the nanomolar detection of azo dyes in water. *ACS sensors, 5*(6), 1541-1547.

Trott, O., Olson, A. J. (2010). AutoDock Vina: improving the speed and accuracy of docking with a new scoring function, efficient optimization, and multithreading. *Journal of computational chemistry, 31*(2), 455-461.

Unnisa, A., Abouzied, A. S., Baratam, A., Lakshmi, K. C., Hussain, T., Kunduru, R. D., Selvarajan, K. K. (2020). Design, synthesis, characterization, computational study and in-vitro antioxidant and anti-inflammatory activities of few novel 6-aryl substituted pyrimidine azo dyes. *Arabian Journal of Chemistry*, *13*(12), 8638-8649.

Uzzaman, M., Hasan, M. K., Mahmud, S., Yousuf, A., Islam, S., Uddin, M. N., Barua, A. (2021). Physicochemical, spectral, molecular docking and ADMET studies of Bisphenol analogues; A computational approach. *Informatics in Medicine Unlocked, 25*, 100706.

Vasu, D., Sunitha, M., Srikanth, L., Swarupa, V., Prasad, U. V., Sireesha, K., Chaudhary, A. (2015). In Staphylococcus aureus the regulation of pyruvate kinase activity by serine/threonine protein kinase favors biofilm formation. *3 Biotech, 5*, 505-512.

Veber, D. F., Johnson, S. R., Cheng, H.-Y., Smith, B. R., Ward, K. W., Kopple, K. D. (2002). Molecular properties that influence the oral bioavailability of drug candidates. *Journal of medicinal chemistry, 45*(12), 2615-2623.

Wu, Z., Shi, J., Chen, J., Hu, D., Song, B. (2021). Design, synthesis, antibacterial activity, and mechanisms of novel 1, 3, 4-thiadiazole derivatives containing an amide moiety. *Journal of Agricultural and Food Chemistry, 69*(31), 8660-8670.

Xu, D., Li, Z., Peng, Y.-X., Geng, J., Qian, H.-F., Huang, W. (2016). Post-modification of 2-formylthiophene based heterocyclic azo dyes. *Dyes and Pigments, 133*, 143-152.

Yousefi, H., Yahyazadeh, A., Rufchahi, E. M., Rassa, M. (2013). Synthesis, spectral properties, biological activity and application of new 4-(benzyloxy) phenol derived azo dyes for polyester fiber dyeing. *Journal of Molecular Liquids, 180*, 51-58.

Zeb, A. (2020). Concept, mechanism, and applications of phenolic antioxidants in foods. *J Food Biochem, 44*(9), e13394.

Zhao, X.-L., Geng, J., Qian, H.-F., Huang, W. (2017). pH-induced azo-keto and azo-enol tautomerism for 6-(3-methoxypropylamino)pyridin-2-one based thiophene azo dyes. *Dyes and Pigments, 147,* 318-326.

LIST OF APPENDIX

Appendix 1: FTIR [(KBr) υ_{max}/cm^{-1}] spectrum of compound **131a**.

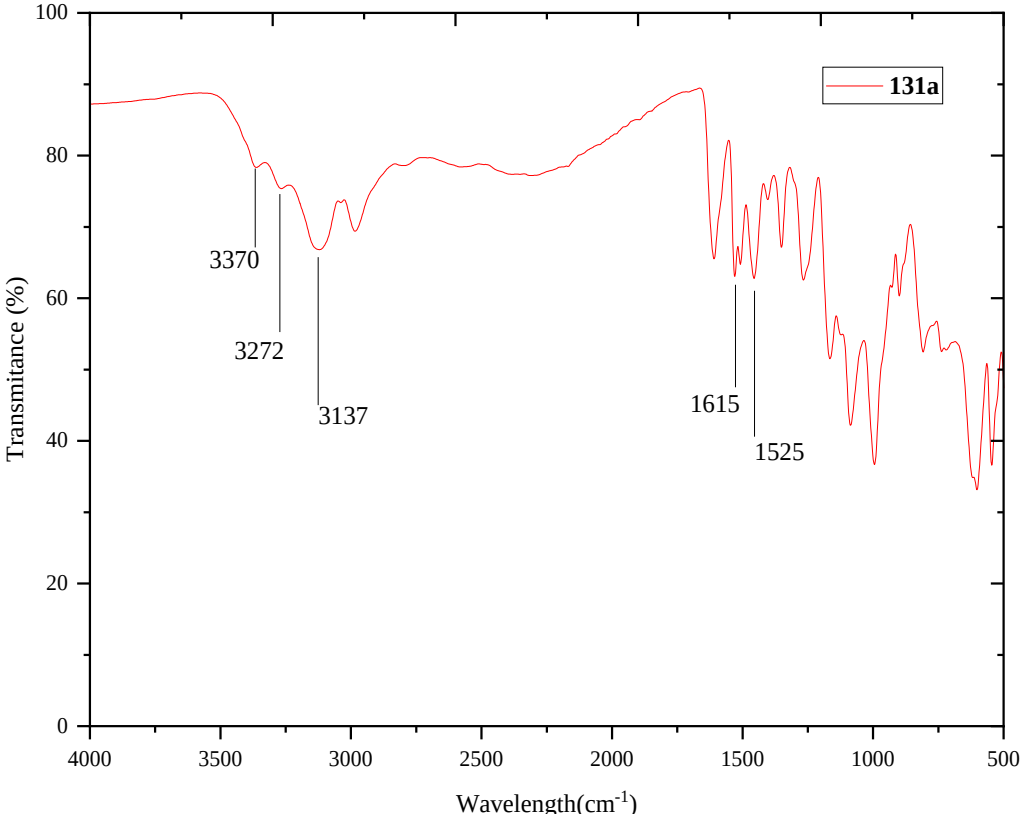

Appendix 2: ^{1}H-NMR (400 MHz, DMSO-d_6) spectrum of compound **131a**.

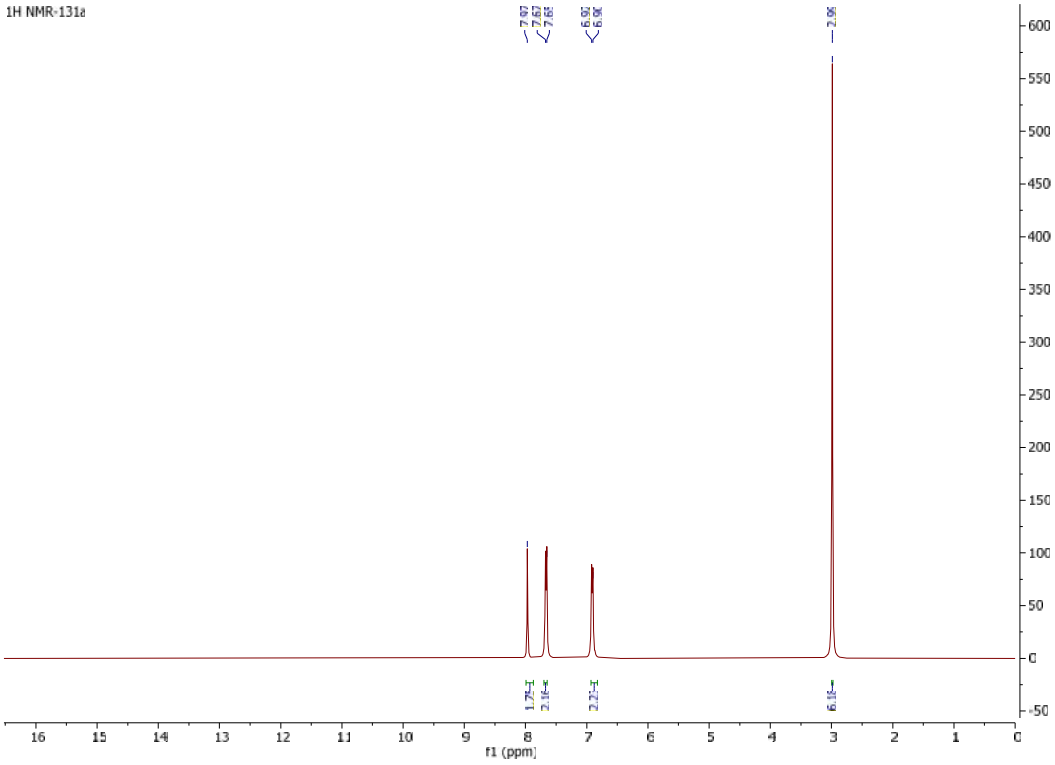

Appendix 3: ^{13}C-NMR (100 MHz, DMSO-d_6) spectrum of compound **131a**.

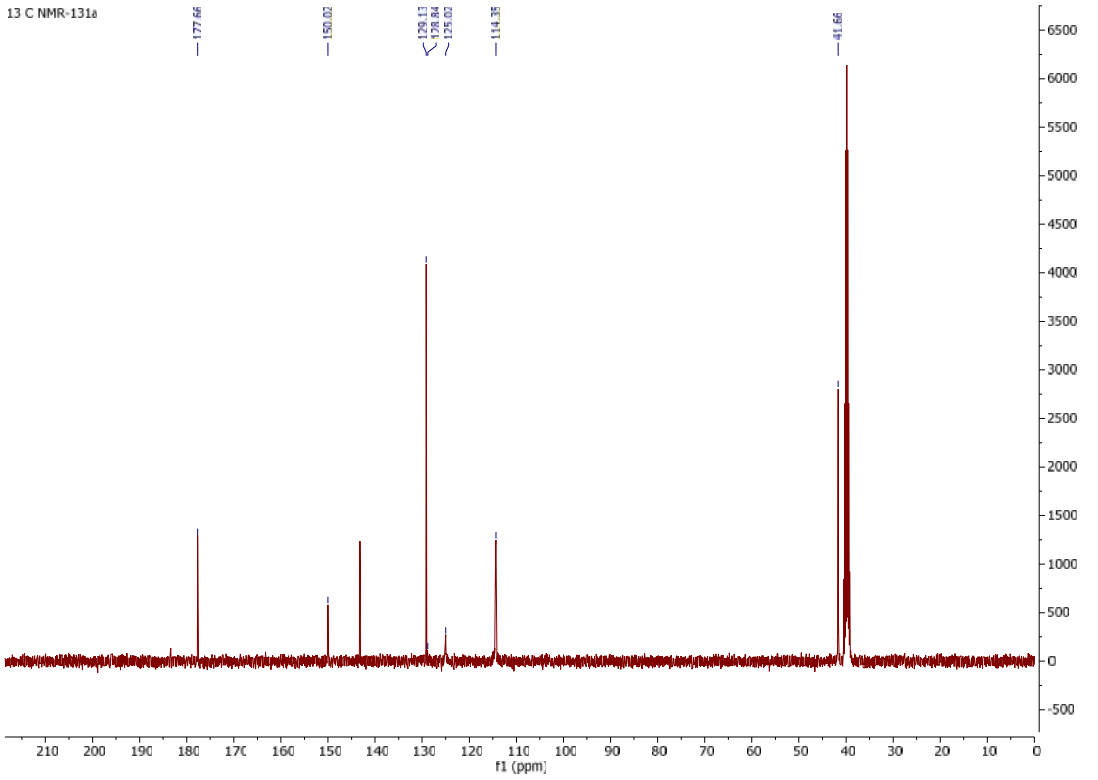

Appendix 4: DEPT-135 (100 MHz, DMSO-d_6) spectrum of compound **131a**.

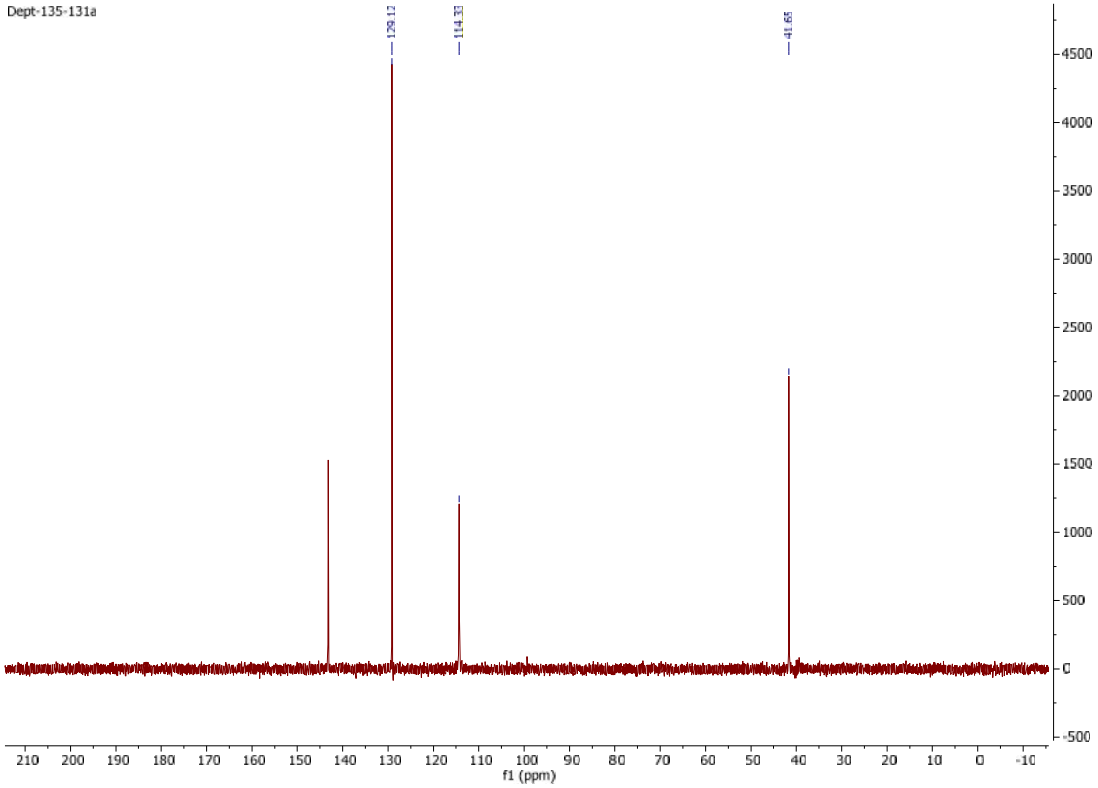

Appendix 5: FTIR [(KBr) υ_{max}/cm^{-1}] spectrum of compound **131b**.

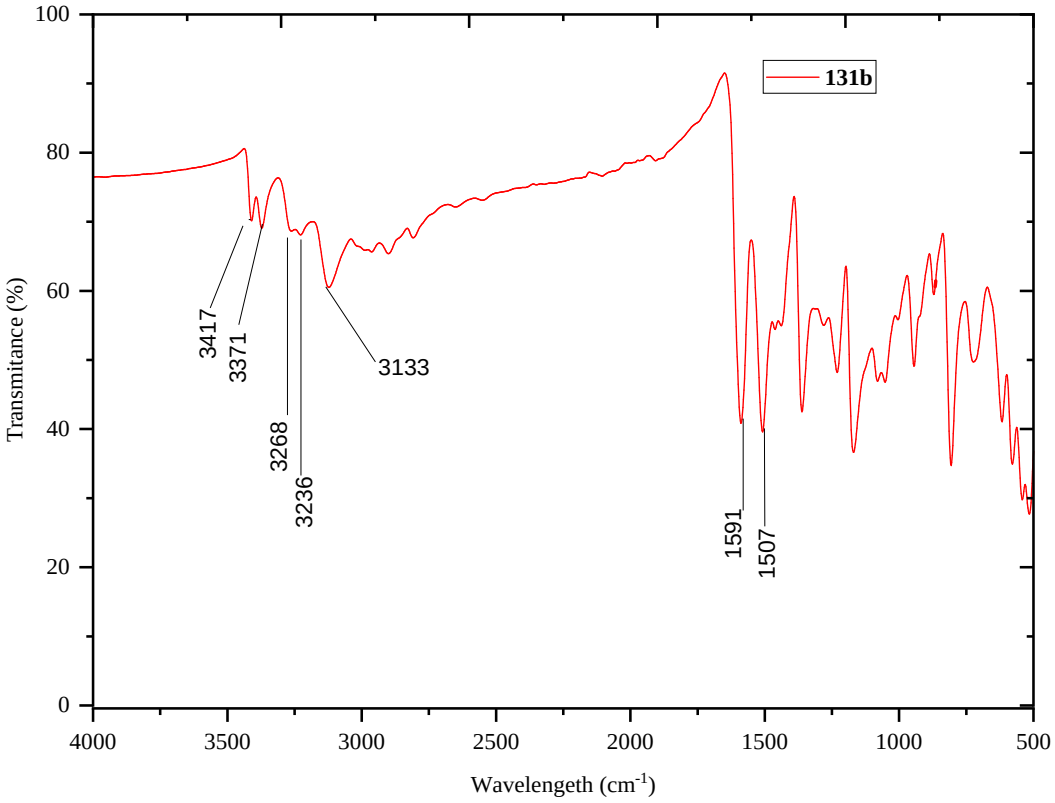

Appendix 6: ^{1}H-NMR (600 MHz, DMSO-d_6) spectrum of compound **131b**.

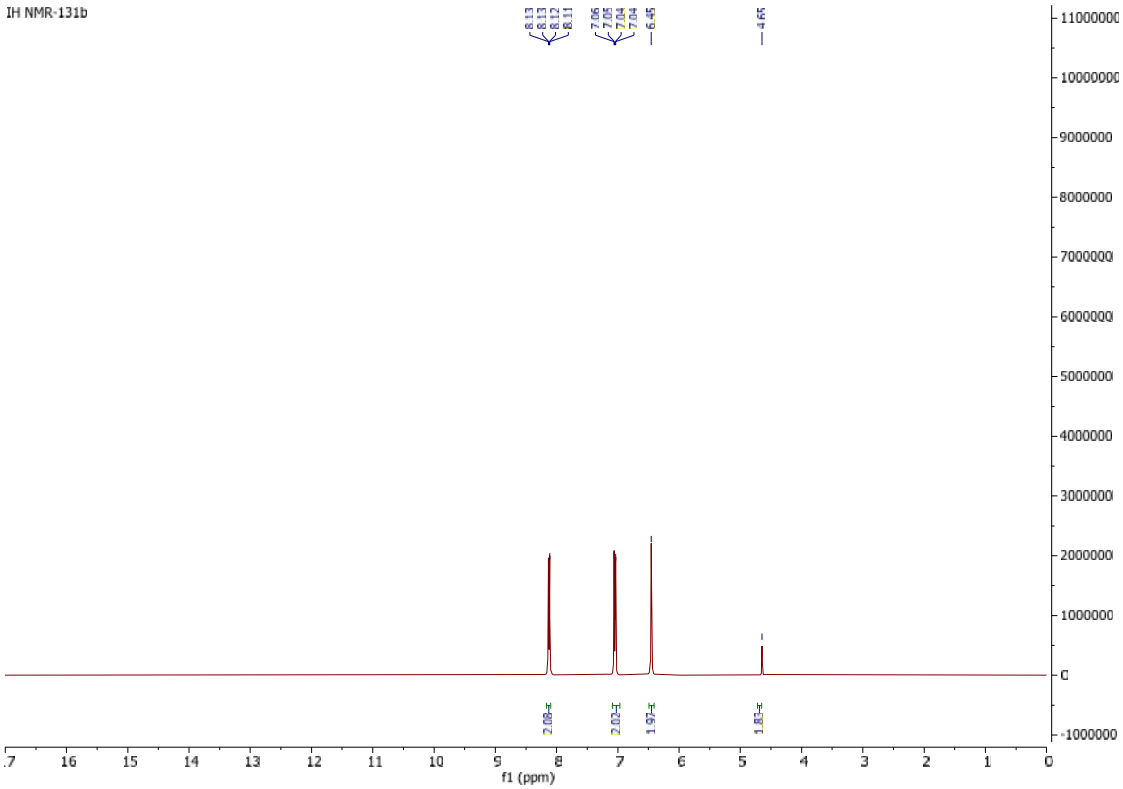

Appendix 7: ^{13}C-NMR (100 MHz, DMSO-d_6) spectrum of compound **131b**.

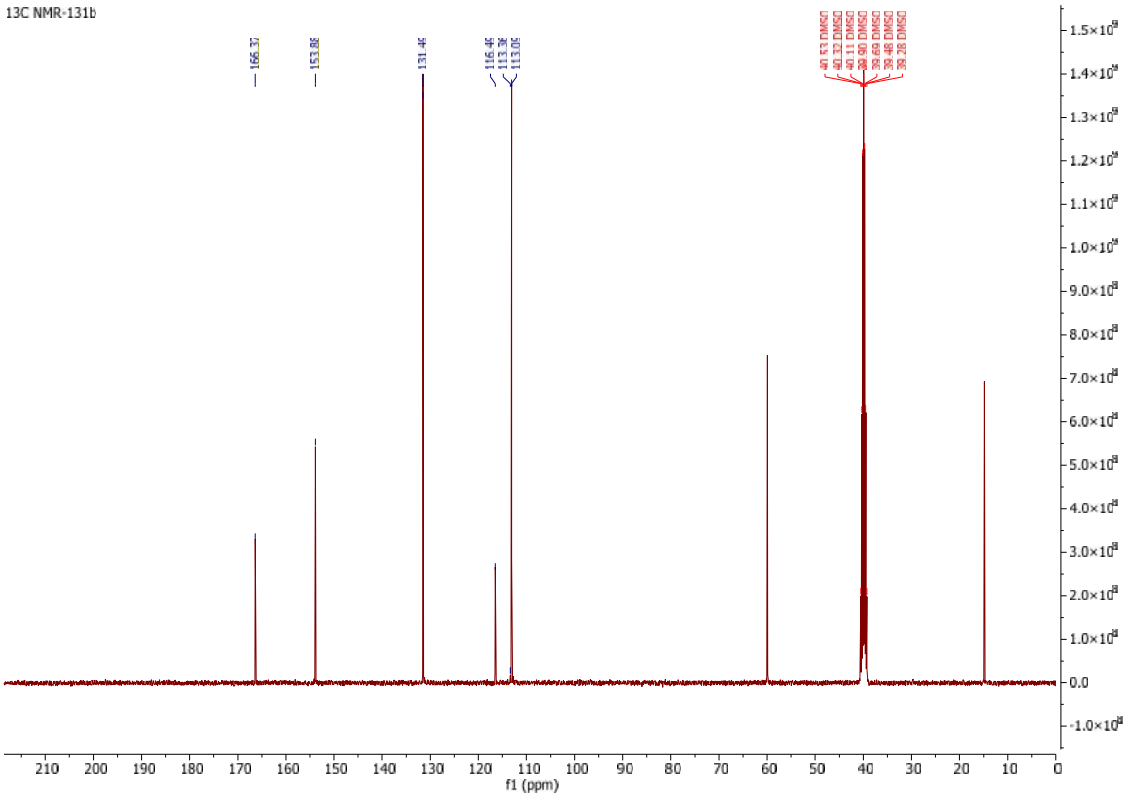

Appendix 8: DEPT-135 (400 MHz, DMSO-d_6) spectrum of compound **131b**.

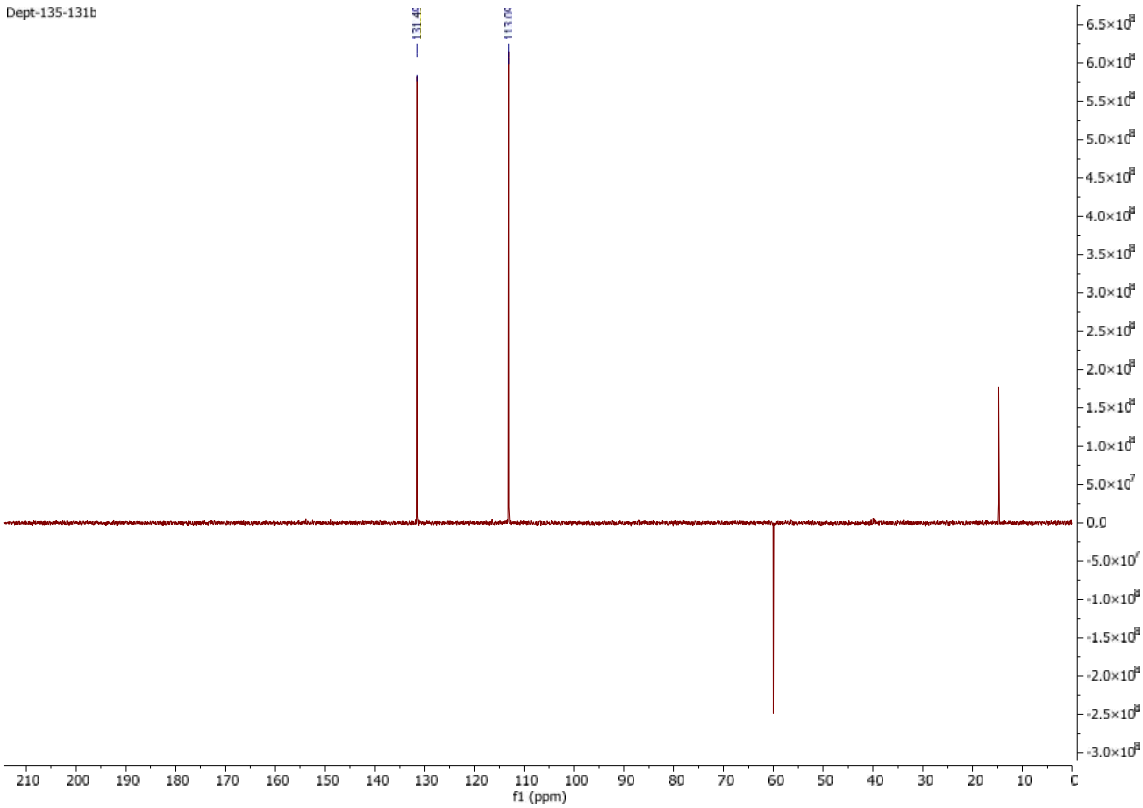

Appendix 9: UV-Vis spectra of the synthesized compound **132**.

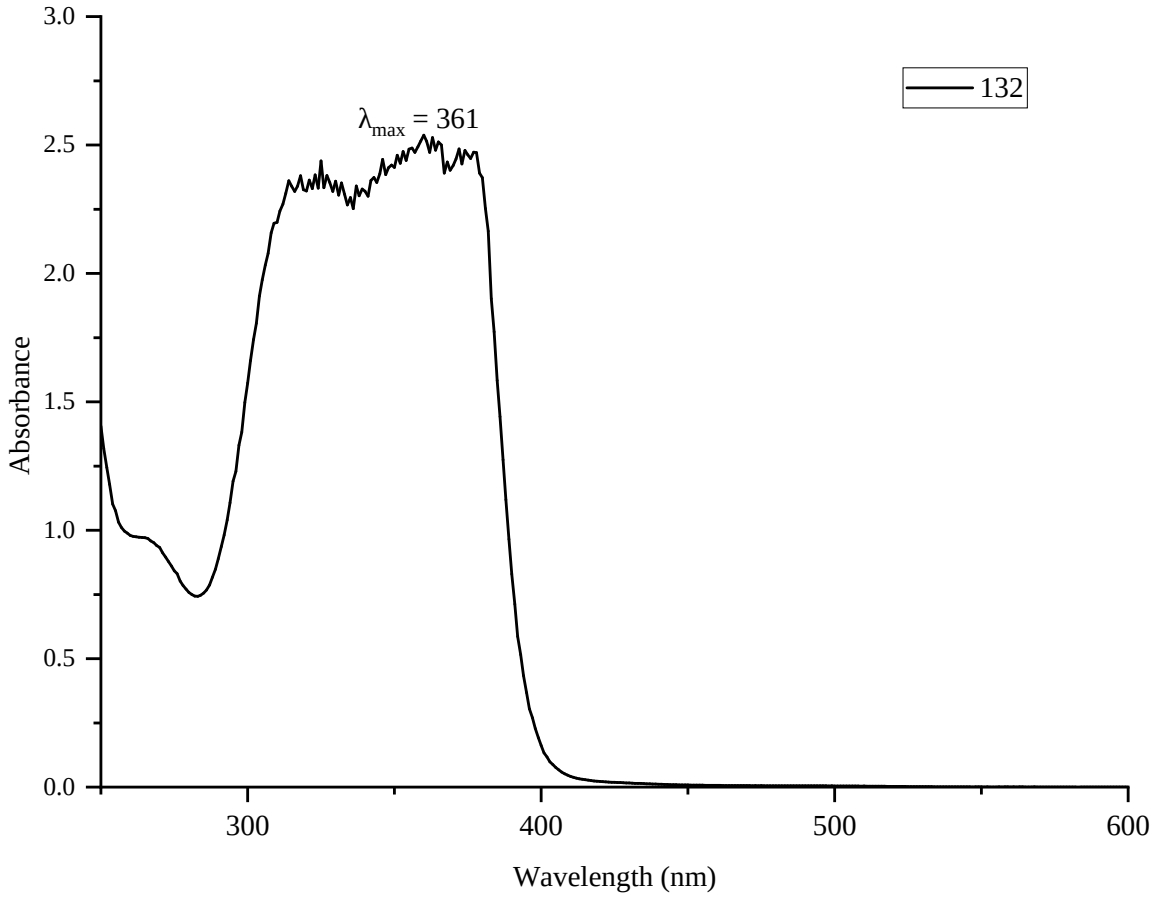

Appendix 10: ^{1}H-NMR (400 MHz, DMSO-d_6) spectrum of compound **132.**

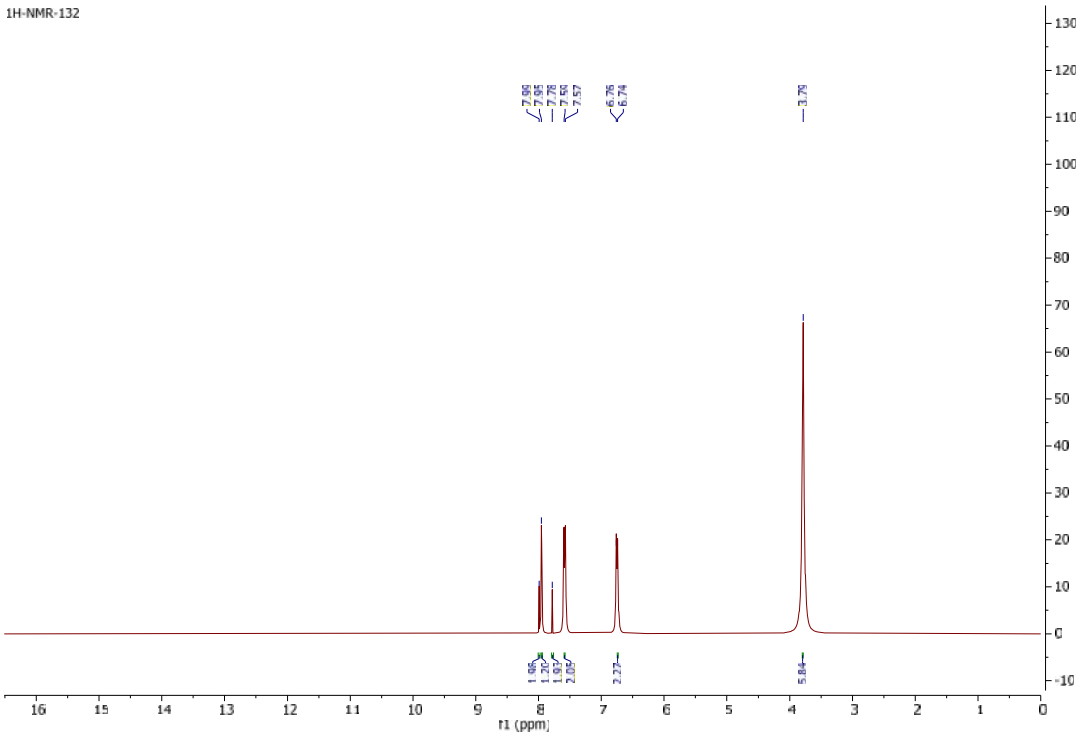

Appendix 11: ^{1}C-NMR (100 MHz, DMSO-d_6) spectrum of compound **132.**

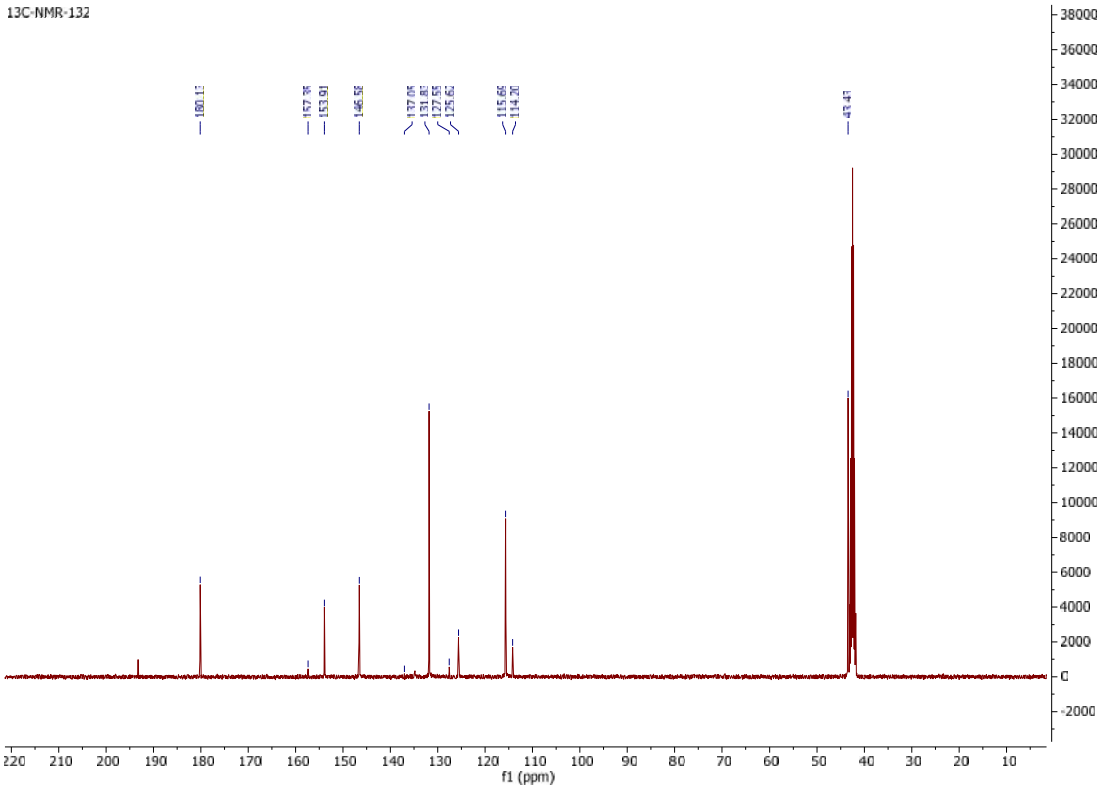

Appendix 12: DEPT-135 (100 MHz, DMSO-d_6) spectrum of compound **132.**

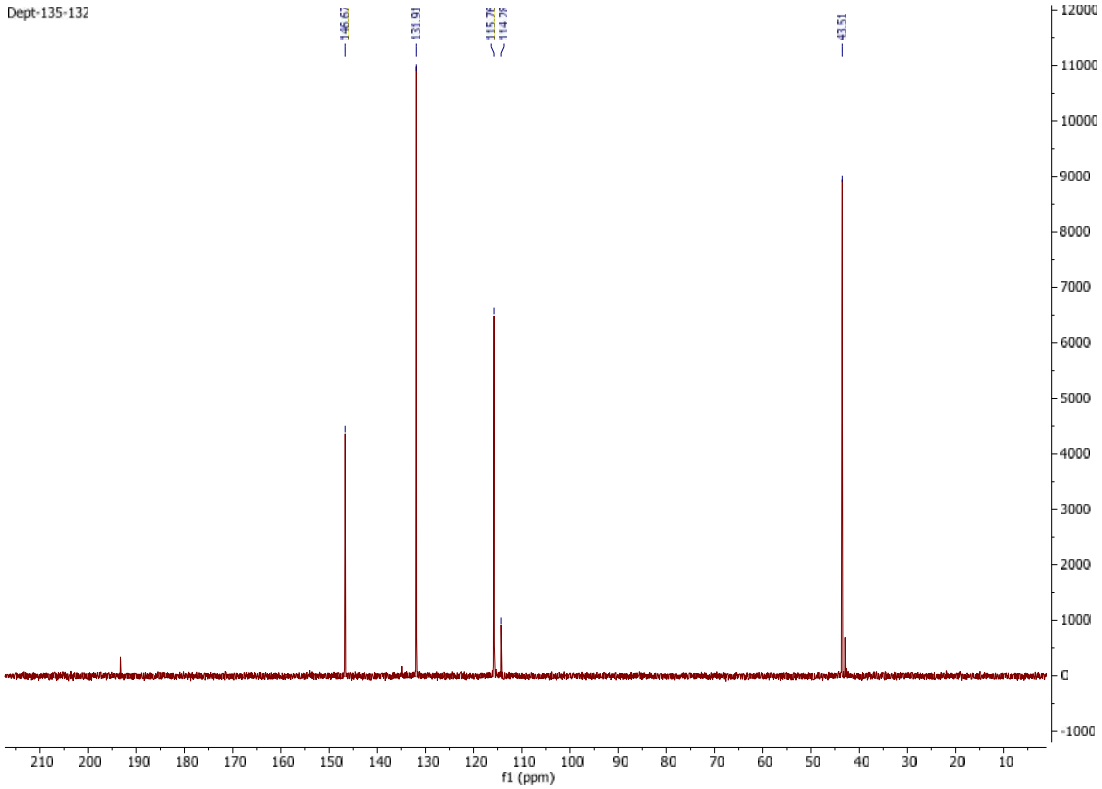

Appendix 13: Appendix 9: UV-Vis spectra of the synthesized compound **133**.

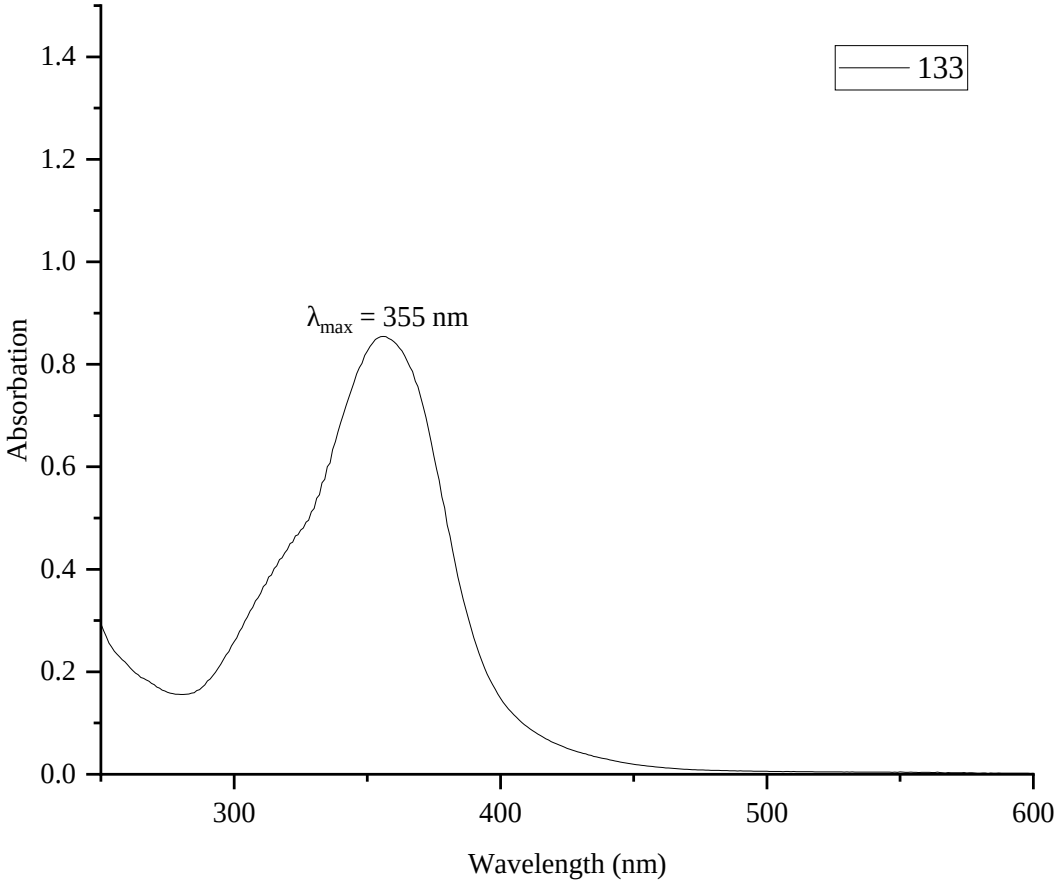

Appendix 14: [1]H-NMR (400 MHz, DMSO-d_6) spectrum of compound **133.**

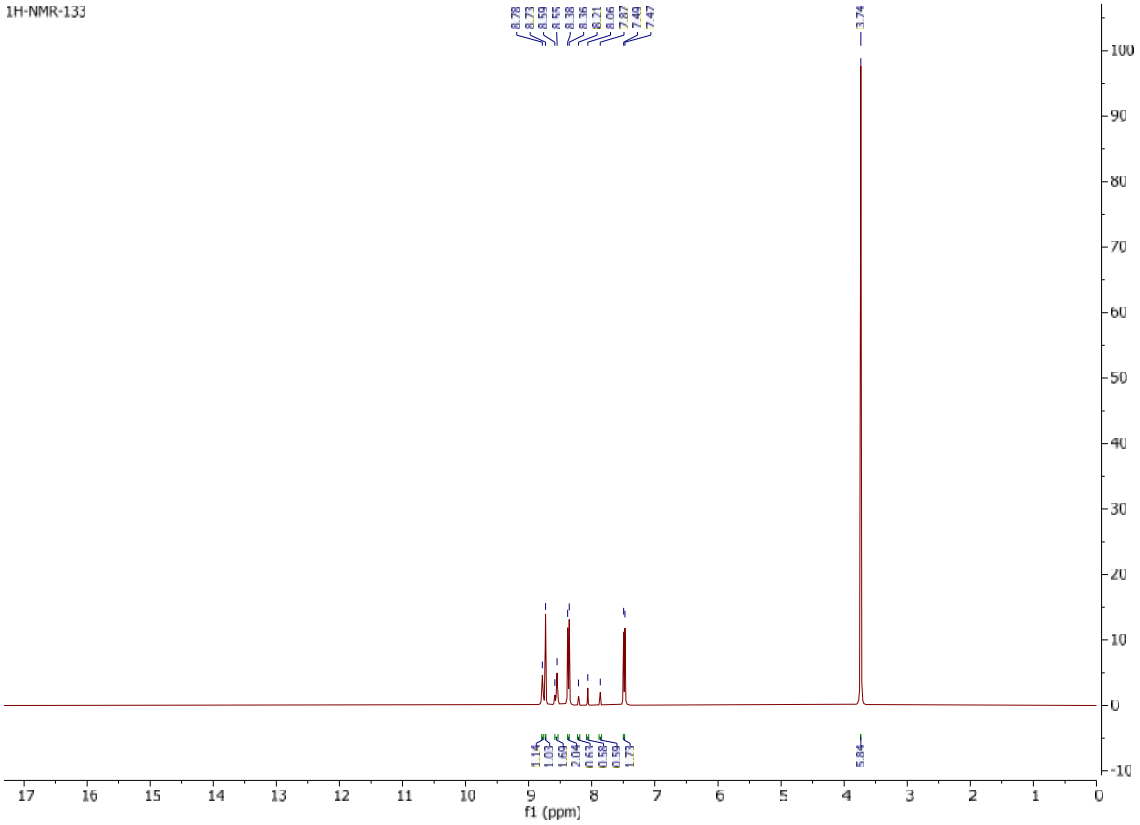

Appendix 15: [13] C-NMR (100 MHz, DMSO-d_6) spectrum of compound **133.**

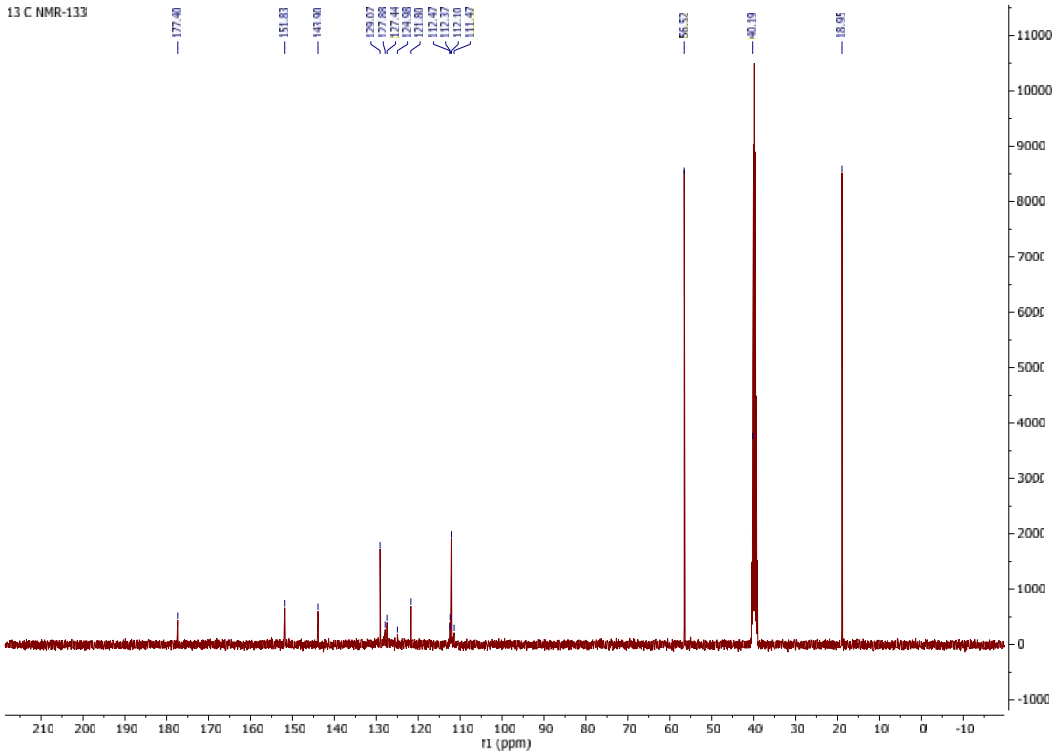

Appendix 16: Dept-135 (100 MHz, DMSO-d_6) spectrum of compound **133.**

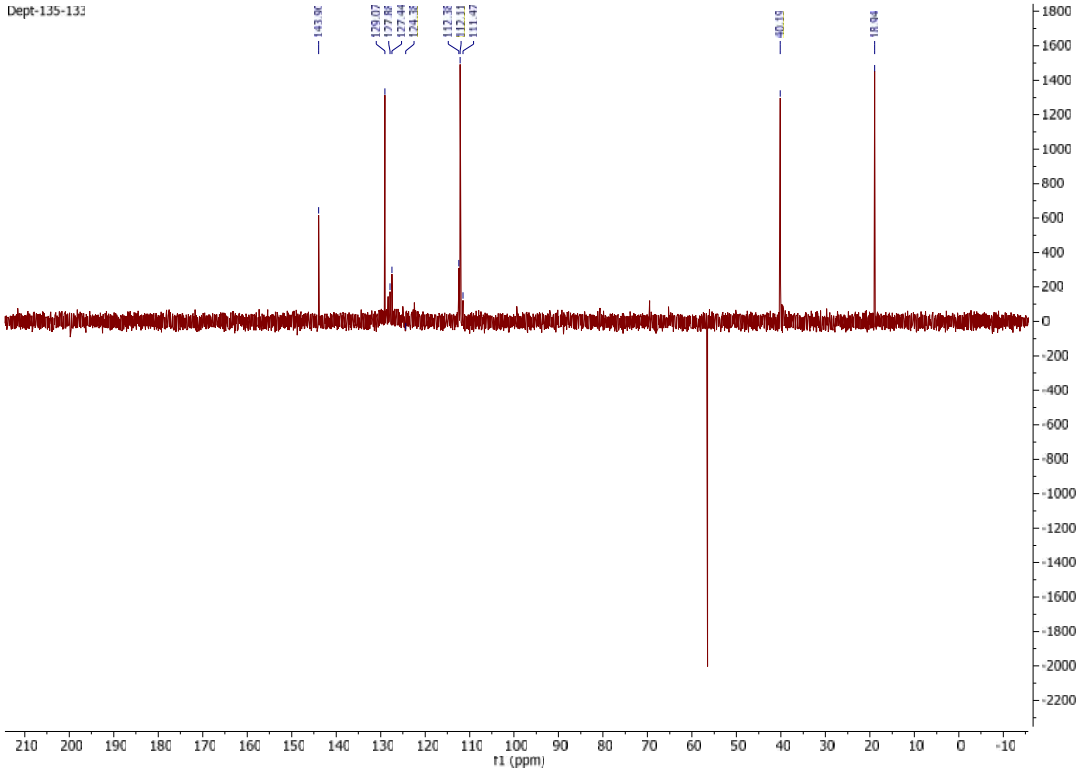

Appendix 17: UV-Vis spectra of the synthesized compound **134**.

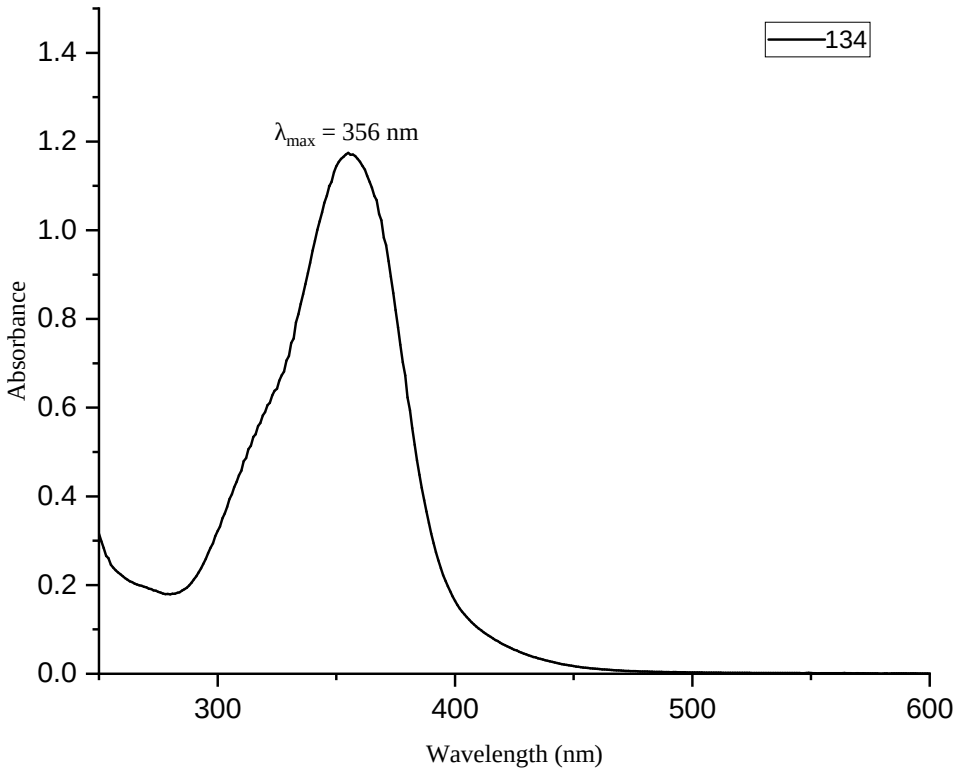

Appendix 18: ^{1}H-NMR (400 MHz, DMSO-d_6) spectrum of compound **134.**

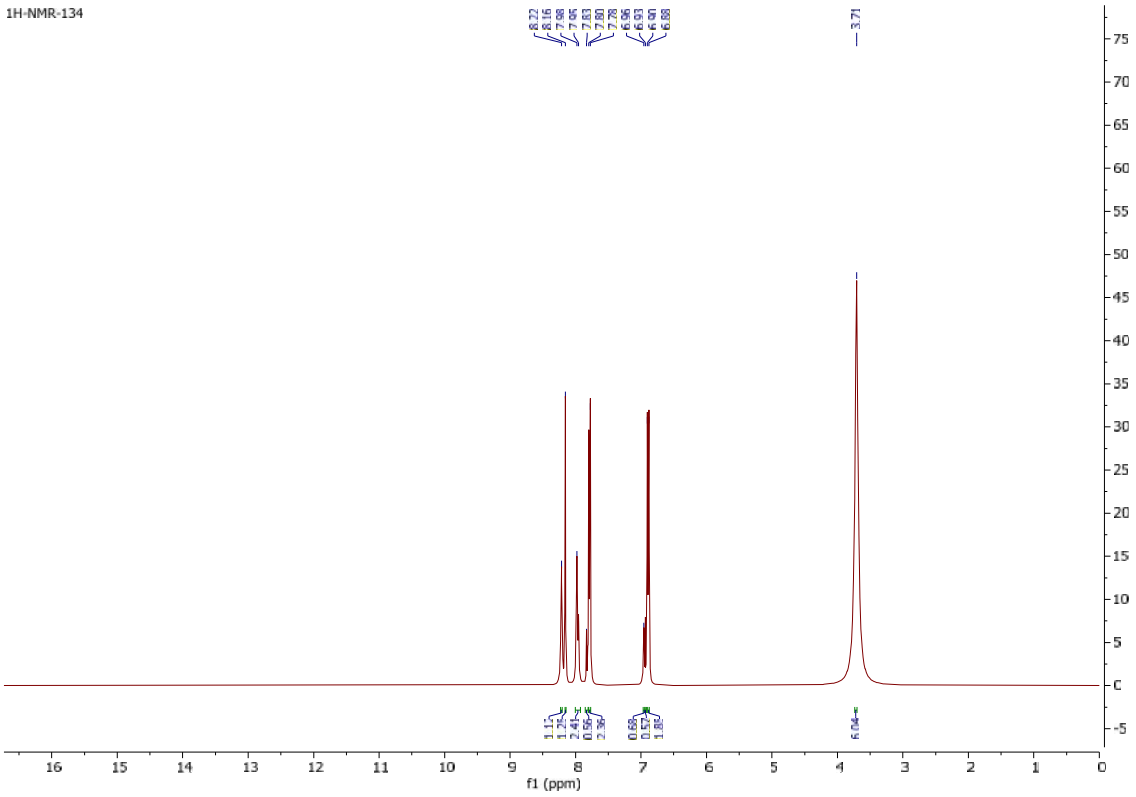

Appendix 19: ^{13}C NMR (100 MHz, DMSO-d_6) spectrum of compound **134.**

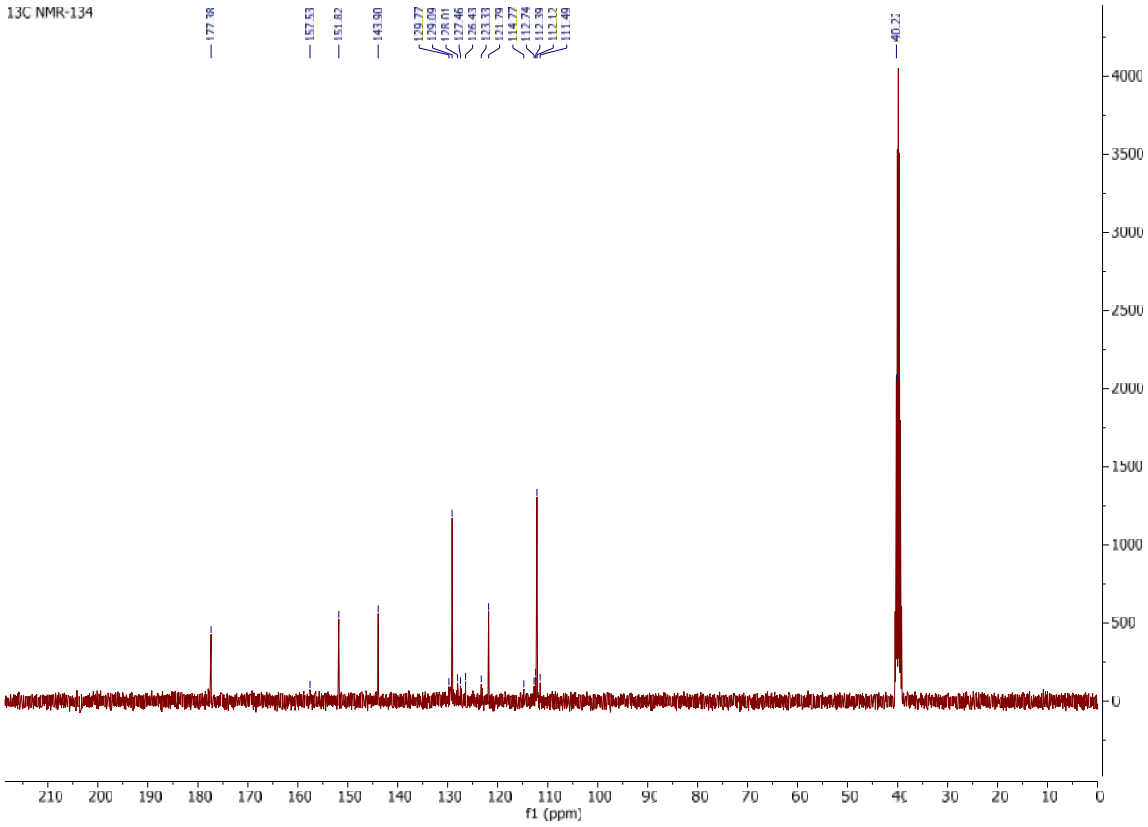

Appendix 20: Dept-135 (100 MHz, DMSO-d_6) spectrum of compound **134.**

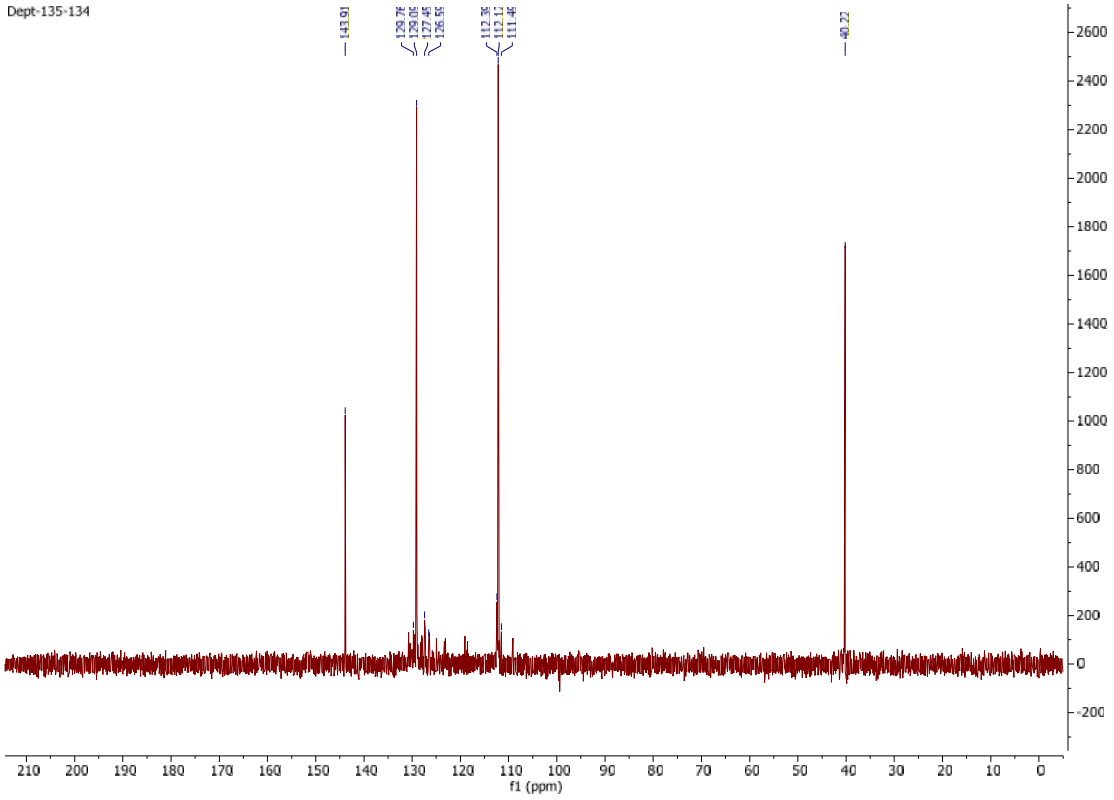

Appendix 21: UV-Vis spectra of the synthesized compound **135**.

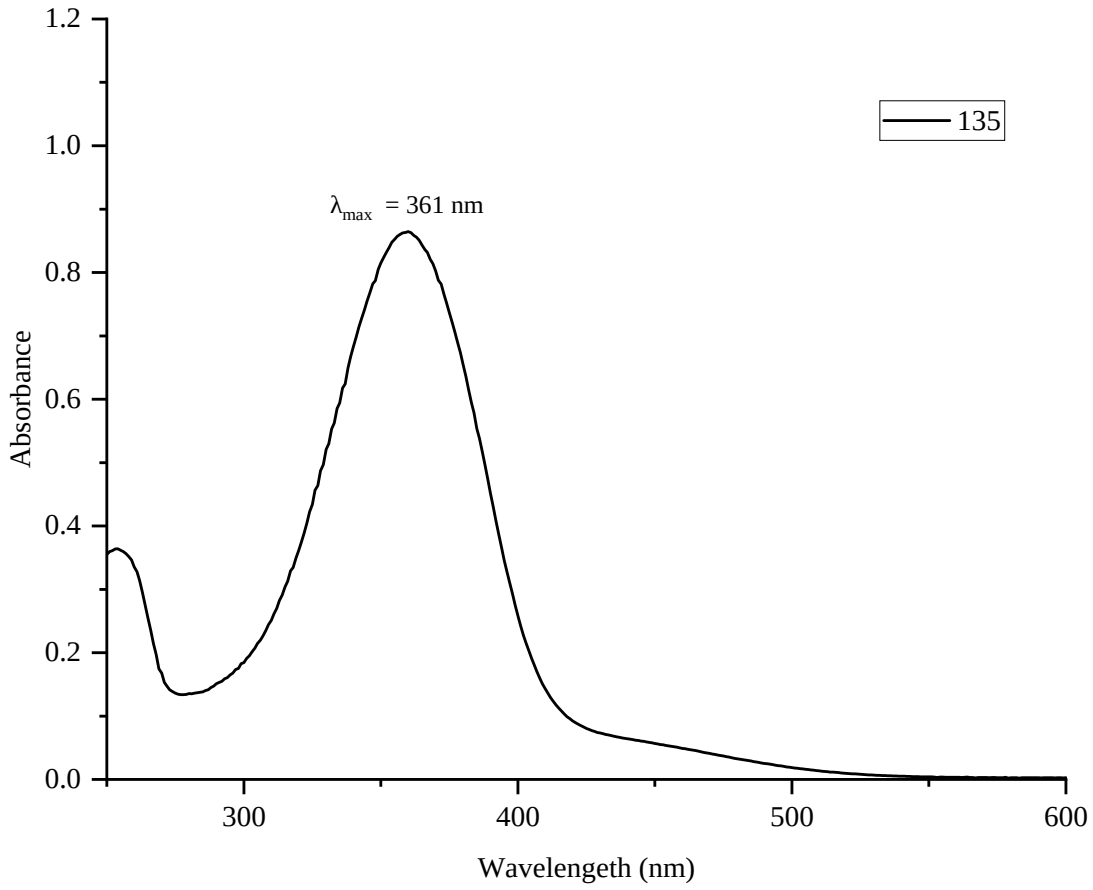

Appendix 22: ^{1}H-NMR ($CDCl_3$, 400 MHz) spectrum of compound **135.**

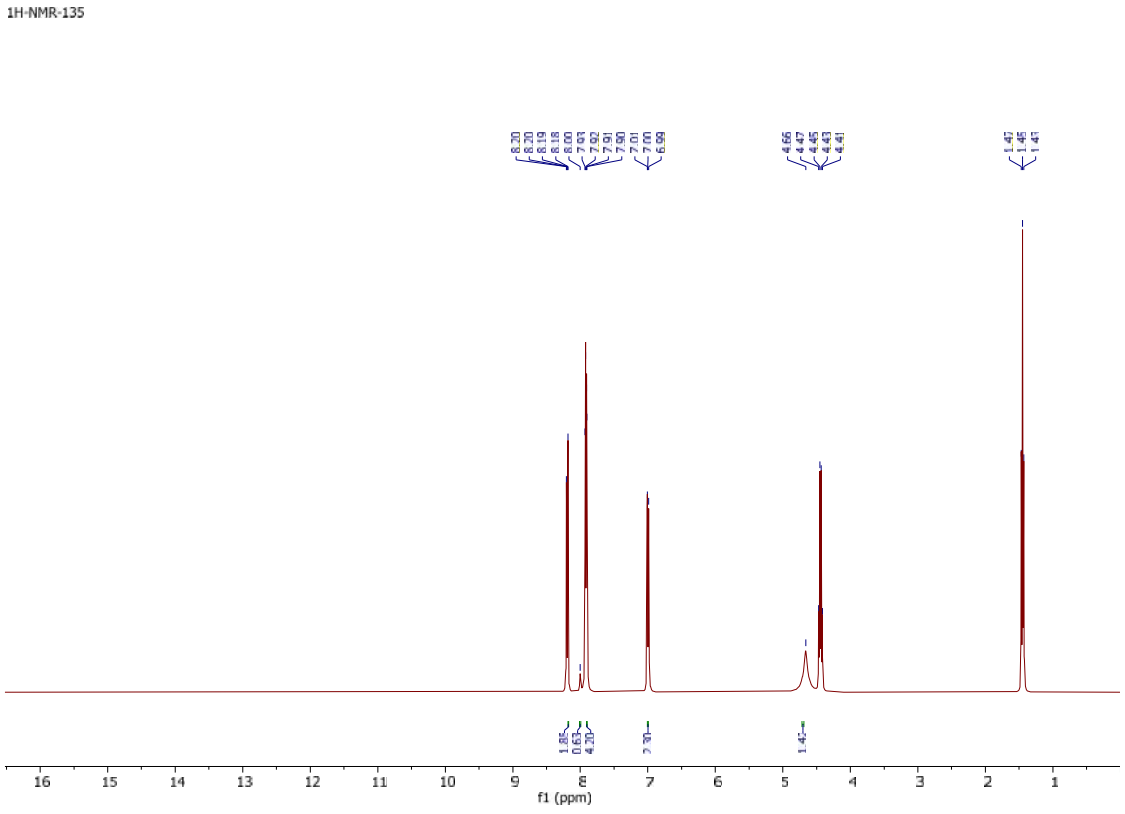

Appendix 23: ^{13}C-NMR ($CDCl_3$, 101 MHz) spectrum of compound **135.**

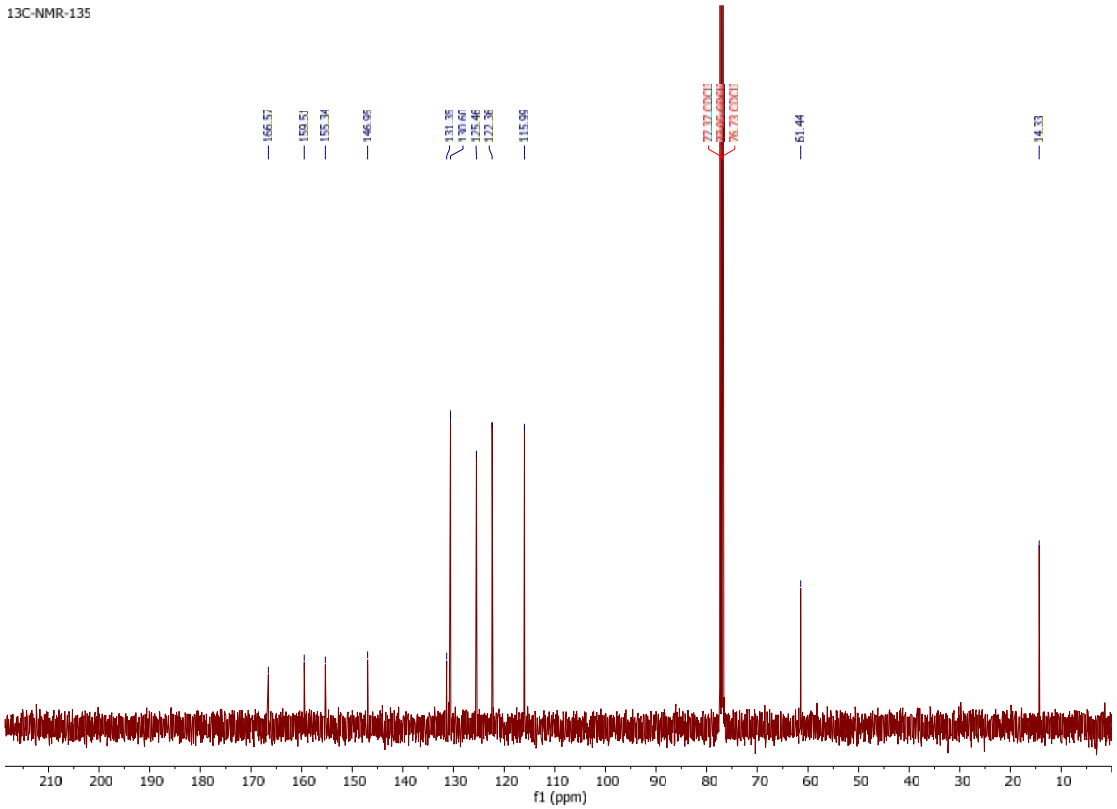

Appendix 24: DEPT-135 ($CDCl_3$, 101 MHz) spectrum of compound **135.**

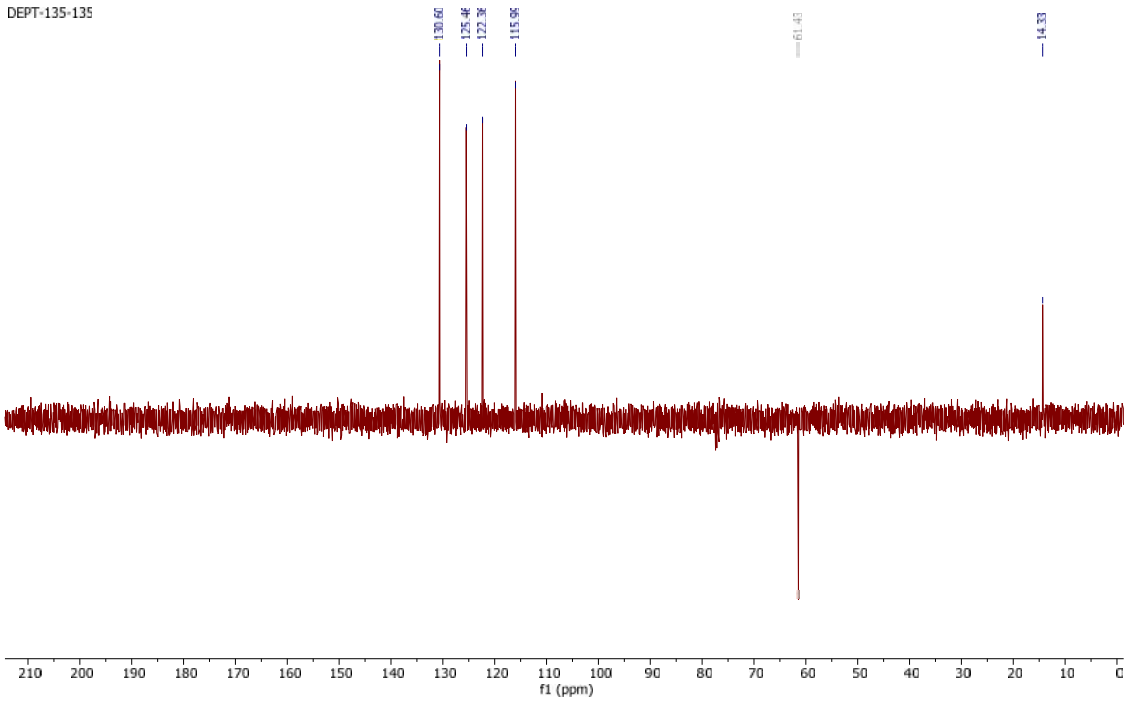

Appendix 25: UV-Vis spectra of the synthesized compound **136**.

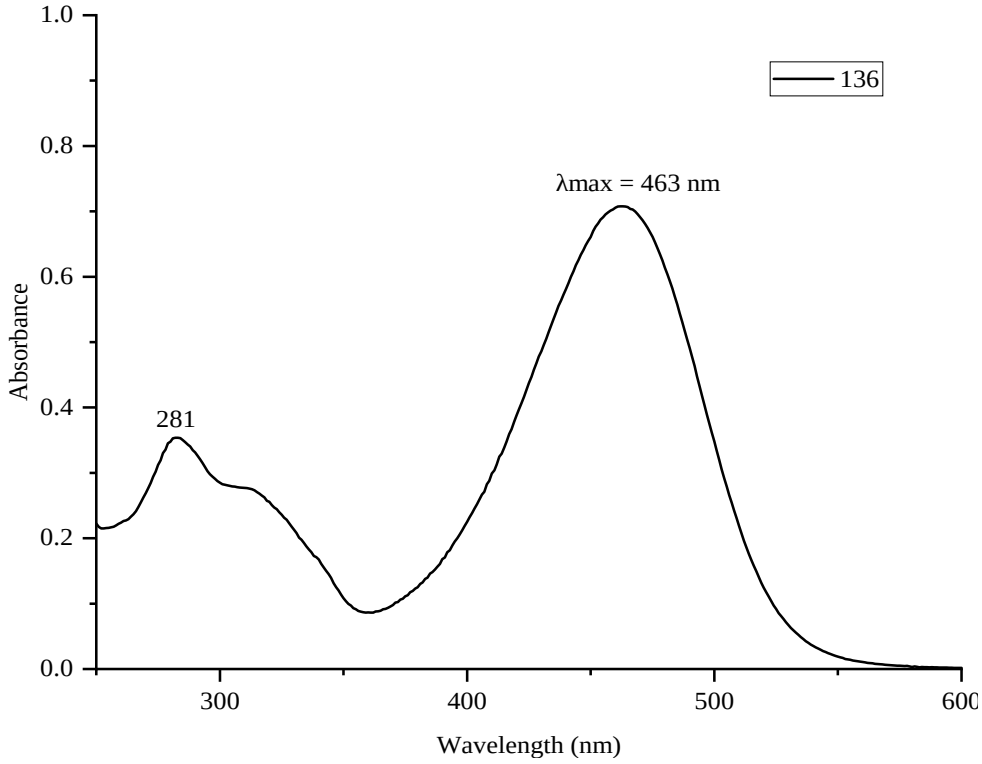

Appendix 26: ^{1}H-NMR ($CDCl_3$, 400 MHz) spectrum of compound **136**

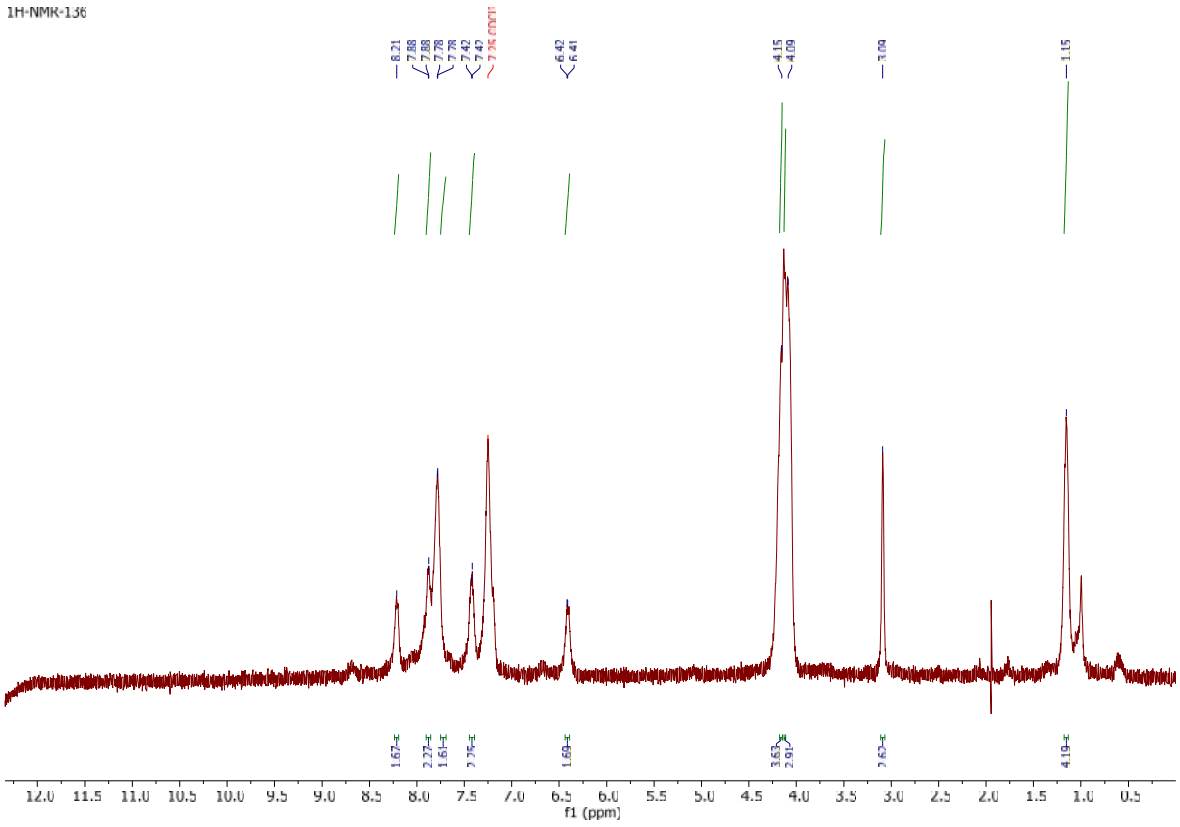

Appendix 27: UV-Vis spectra of compound **137**.

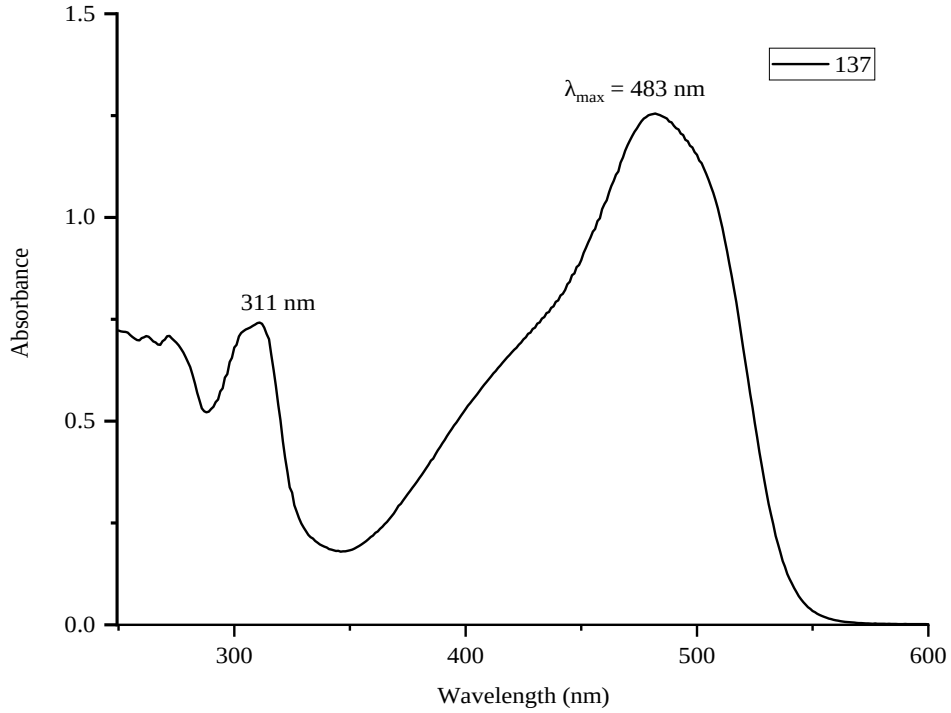

Appendix 28: 1H-NMR ($CDCl_3$, 400 MHz) spectra of compound **137**.

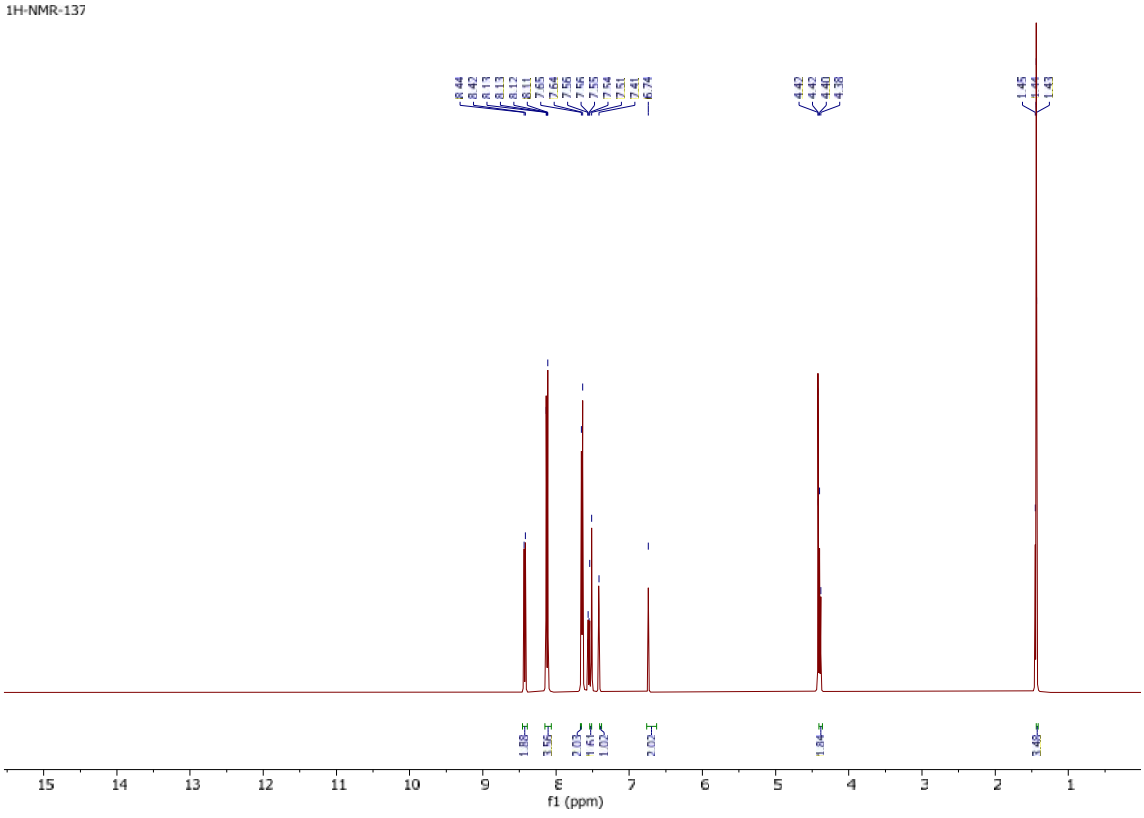

Appendix 29: 13C-NMR ($CDCl_3$, 101 MHz) spectrum of compound **137**.

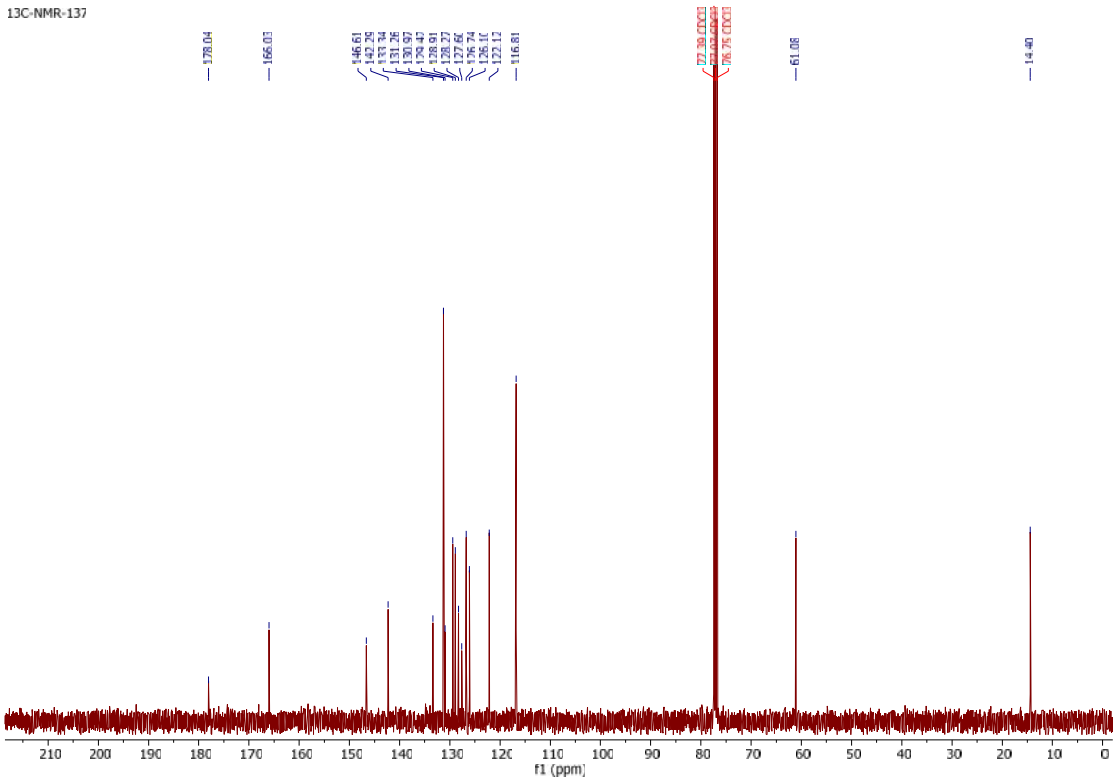

Appendix 30: DEPT-135 ($CDCl_3$, 101 MHz) spectrum of compounds **137**.